Cell Cycle-Specific Functions and Regulation of the DNA Nuclease SNM1B

by

Jordann Alyse Smak

A dissertation submitted in partial fulfillment
of the requirements for the degree of
Doctor of Philosophy
(Cellular and Molecular Biology)
in the University of Michigan
2019

Doctoral Committee:

Associate Professor JoAnn Sekiguchi, Chair
Associate Professor Christine Canman
Professor Thomas Glover
Professor Mats Ljungman

Jordann Alyse Smak

jsmak@umich.edu

ORCID iD: 0000-0002-5143-0196

Dedication

This dissertation is dedicated to my parents,
Joseph and Pamela Smak

Acknowledgements

This dissertation could not have been completed without the support and assistance from several individuals. I would first like to thank my advisor, JoAnn Sekiguchi, for her patience, kindness, and optimism throughout my graduate career. Her dedicated mentorship helped me grow as a scientist, and I truly appreciate her confidence in allowing me to pursue my independent ideas. I would also like to thank Dave Ferguson and my thesis committee members, Christine Canman, Thomas Glover, and Mats Ljungman, for their scientific guidance and valuable feedback on my project. Additionally, I could not have successfully navigated through this training process without aid from the Cellular and Molecular Biology Program and my funding.

When I was searching for a lab to join, I knew that I wanted a collaborative and friendly work environment. I couldn't have asked for a better group of colleagues than the ones I found in the Sekiguchi and Ferguson labs. I would specifically like to thank Kayla Capper, Ishita Das, Mary Morgan, Andrea Hartlerode, Hilary Moale, William Lu, Todd Festerling, and Jean Crilly for making my time in the lab fun and memorable. I would also like to thank my good friends Rachel Stephenson, Torey Arnold, Olivia McGovern, and Liz Umbrino for providing the laughter to help keep me in good spirits. I am extremely grateful to Julian Bahr who stood by my side throughout this entire process and was always there to listen and cheer me on. His encouragement was a boon to my growth as a more grounded and confident person. Finally, I could not have succeeded without the love and support of my amazing family. I am fortunate to have such caring parents whose guidance, inspiration, and friendship I will always value.

Table of Contents

List of Figures

List of Abbreviations

53BP1	p53-binding protein 1
9-1-1	RAD9-RAD1-HUS1
βCASP	β-CPSF-Artemis-SNM1/PSO2
APC	Anaphase-promoting complex
Aph	Aphidicolin
ATM	Ataxia telangiectasia-mutated
ATR	Ataxia telangiectasia and Rad3-related
ATRIP	ATR-interacting protein
BIR	Break-induced replication
BLM	Bloom syndrome helicase
BRCA1	Breast cancer 1
BRCA2	Breast cancer 2
BrdU	5-bromo-2'-deoxyuridine
CDK	Cyclin-dependent kinase
CFS	Common fragile site
CHFR	Checkpoint with FHA and ring finger domains
CHK1	Checkpoint kinase 1
CHK2	Checkpoint kinase 2
CldU	Chloro-deoxyuridine
CMG	CDC45-MCM-GINS
CNV	Copy number variant
CPSF73	Cleavage and polyadenylation specificity factor 73
CPT	Camptothecin
CtIP	C-terminal binding protein interacting protein
DDR	DNA damage response
DDT	DNA damage tolerance
DNA-PKcs	DNA-dependent protein kinase catalytic subunit
DNA2	DNA replication ATP-dependent helicase-nuclease 2
DSB	Double-strand break
dsDNA	Double-stranded DNA
ELAC2	ElaC ribonuclease Z 2
ETP	Etoposide
EXO1	Exonuclease 1
FA	Fanconi anemia
FAAP	Fanconi anemia core complex-associated protein
FACS	Fluorescence-activated cell sorting

FAN1	Fanconi-associated nuclease 1
FANC	Fanconi anemia complementation group
FBH1	F-box DNA helicase 1
GFP	Green fluorescent protein
HLTF	Helicase-like transcription factor
HR	Homologous recombination
HSP	Heat shock protein
HU	Hydroxyurea
ICL	Interstrand crosslink
IdU	Iodo-deoxyuridine
IR	Ionizing radiation
JNK	c-Jun N-terminal kinase
LTGC	Long-tract gene conversion
MAPK	Mitogen-activated protein kinase
MBL	Metallo-β-lactamase
MCM	Minichromosome maintenance
MEF	Mouse embryonic fibroblast
mES	Mouse embryonic stem cell
MiDAS	Mitotic DNA synthesis
MMC	Mitomycin C
MMS	Methyl methanesulfonate
MPS1	Monopolar spindle 1 kinase
MRE11	Meiotic recombination 11
MRN	MRE11/RAD50/NBS1
MTI	Microtubule inhibition
MUS81	MMS and UV sensitive 81
NEK2	NIMA related kinase 2
NHEJ	Non-homologous end-joining
NS	Non-silencing
ORC	Origin-recognition complex
PAR	Poly(ADP-ribose)
PARP	Poly(ADP-ribose) polymerase
PCNA	Proliferating cell nuclear antigen
PICH	Polo-like kinase 1 interacting checkpoint helicase
PIKK	Phosphatidylinositol 3-kinase-related kinase
PLK1	Polo-like kinase 1
POT1	Protection of telomeres protein 1
PPase	Phosphatase
Pre-RC	Pre-replication complex
PSF2	Partner of Sld Five 2
PSO	Sensitivity to psoralen
PTM	Post-translational modification
RFP	Red fluorescent protein
RNR	Ribonucleotide reductase
ROS	Reactive oxygen species
RPA	Replication protein A

SAC	Spindle assembly checkpoint
SDSA	Synthesis-dependent strand annealing
SERBP1	Serpine mRNA binding protein 1
SMARCAL1	SWI/SNF-related matrix-associated actin-dependent regulator of chromatin subfamily A-like protein 1
SNM1	Sensitivity to nitrogen mustard
SNP	Single nucleotide polymorphism
SSB	Single-strand break
ssDNA	Single-stranded DNA
STGC	Short-tract gene conversion
SUMO	Small ubiquitin-like modifier
TAP	Tandem affinity purification
TD	Tandem duplication
Ter	Terminator sequence
TIF	Telomere dysfunction-induced foci
TLS	Translesion synthesis
TOPBP1	DNA Topoisomerase II binding protein 1
TOPI	Topoisomerase I
TOPII	Topoisomerase II
TRF2	Telomere repeat binding factor 2
Tus	Terminus utilization substance
UFB	Ultra-fine bridge
UV	Ultraviolet
WRN	Werner syndrome ATP-dependent helicase
ZRANB3	Zinc finger RANBP2-type containing 3

Abstract

DNA replication is a fundamental cellular process that ensures the accurate duplication and transmission of genetic information. The replication machinery is frequently challenged by endogenous and exogenous sources of DNA lesions or barriers, which can interfere with replication fork progression. If stalled replication forks are not properly stabilized and restarted, they can collapse, resulting in the generation of DNA double-strand breaks (DSBs). Mis-repaired breaks lead to increased genome instability in the form of chromosomal deletions, amplifications, and aberrant rearrangements. These detrimental alterations characterize many human diseases and can contribute to malignant transformation and the progression of cancer. Therefore, the cell has evolved intricate mechanisms to promote the efficient resolution of replication stress.

The repair of stalled or collapsed replication forks requires precise nucleolytic processing of DNA intermediate structures. However, the molecular details of these processing events are not well defined. We describe a critical role for the DNA nuclease, SNM1B, in the resolution of replication stress and uncover potential mechanisms for its regulation. We found that SNM1B is dispensable for the detection of stalled forks, as it localizes independently to sites of stress after early-response proteins. DNA fiber analyses and immunofluorescence assays also revealed that SNM1B is important for efficient replication restart and for preventing the accumulation of single-stranded DNA intermediates and DSBs at stalled forks. Using a chromosomally integrated substrate that induces site-specific replication fork arrest in mammalian cells, we showed that SNM1B is required for the recombination-mediated repair of DSBs after fork collapse. Together, these findings highlight the importance of

SNM1B in accurately processing DNA intermediates and in preserving genomic integrity during DNA replication.

DNA repair pathways are tightly controlled and coordinated within the cell cycle to safeguard genetic information. The regulation of nucleases is especially important as inappropriate DNA resection can lead to fragile DNA structures or mis-repaired substrates. Little is known about the regulation of the SNM1B nuclease; thus, we sought to identify the mechanisms underlying the control of its functions and stability within the cell cycle. We found that SNM1B protein levels are stabilized during S-phase in response to agents that induce replication stress and that SNM1B is phosphorylated on its C-terminus in G2-phase and mitosis. Investigations using non-phosphorylatable mutants demonstrated that SNM1B phosphorylation is dispensable for its localization to stalled forks, but may promote protein stability by preventing polyubiquitination during mitosis. Overall, these studies define a novel role for SNM1B in resolving stalled replication forks and provide insight into the regulatory mechanisms necessary for the prevention of replication-associated DNA damage.

Chapter 1

Introduction

Eukaryotic DNA Replication

The faithful transmission of genetic information depends on accurate DNA replication and chromosome segregation. These processes occur during the cell cycle, a carefully orchestrated series of events that allows for the proper duplication and division of genomic DNA into two daughter cells. The prototypical cell cycle in eukaryotes is divided into four phases. In the synthesis phase (S-phase), the nuclear DNA is replicated, which is then separated and equally distributed to the newly forming daughter cells in mitosis (M-phase). S-phase and mitosis are separated by two gap phases, G1- and G2-phase, which prepare the cells for DNA replication and division, respectively [1].

The initiation of eukaryotic DNA replication occurs in a two-step process: origin licensing and origin firing. Origin licensing occurs during late mitosis or G1-phase of the cell cycle, when the origin-recognition complex (ORC) binds to defined replication origins throughout the genome and recruits a set of licensing factors. Together, these factors load the minichromosome maintenance (MCM) helicase around DNA at each origin to form the inactive pre-replication complex (pre-RC). In S-phase, the pre-RC is converted into the active CMG helicase comprised of MCM, CDC45, and the tetrameric GINS complex, which together initiate bidirectional origin firing. The leading-strand polymerase, Pol ε, and the lagging-strand polymerases, Pol δ and Pol α, associate with the CMG complex to concomitantly replicate DNA [2–4].

Sources of Replication Stress

In order for successful completion of DNA synthesis, ongoing replication forks must advance in a timely and efficient manner. When the progression of replication forks is slowed, blocked, or stalled, this results in what is referred to as replication stress. Replication stress can be caused by a variety of endogenous and exogenous sources, and if not properly resolved, can lead to deleterious effects on genome stability (Figure 1.1) [5,6]. One of the most common types of replication stress is unrepaired DNA lesions, which can occur at a rate of up to 10^5 per day [7]. These spontaneous alterations result from dNTP misincorporation, DNA base modifications, or DNA deamination or depurination [8]. By-products of cellular metabolism, such as reactive aldehydes and reactive oxygen species (ROS), are endogenous sources of DNA lesions that block replication fork progression [9,10].

Collisions between the replication fork and DNA-protein complexes are an additional barrier to the progression of DNA synthesis. One DNA-protein complex that the fork may encounter is the transcription machinery. Although DNA replication and transcription are coordinated processes that are spatially and temporally separated, there are circumstances in which the two machineries can converge [11–13]. The consequences of this collision include increases in topological stress and/or the formation of DNA-RNA structures called R-loops, which can result in DNA damage if left unresolved [12,13]. Additionally, replication forks stall if there is improper control of replication initiation or if resources required for this process are limited. For example, excessive origin firing can result in depletion of the nucleotide pools while the firing of too few origins can lead to under-replication and loss of genomic information [14,15].

Replication forks also encounter specific DNA sequences or genomic loci that are difficult to replicate. Trinucleotide repeats and GC-rich DNA can form secondary structures, such as hairpins or G-quadruplexes, that can block or slow fork progression [16,17]. Additionally, common fragile sites (CFSs) are regions within the genome that are sensitive to replication stress. CFSs are found in all individuals and exhibit instability in the form of gaps and breaks in metaphase chromosomes after mild inhibition of DNA synthesis [18–21]. The mechanism of CFS instability is not fully understood, but there are several characteristics of CFSs that may make them sensitive to replicative damage.

CFSs are enriched within large genes that span hundreds of kilobases and require more than one cell cycle to transcribe. Active transcription of these genes could therefore increase the probability of collisions between the replication fork and the transcription machinery [22–24]. CFSs also have the potential to form secondary DNA structures, are late replicating, and are located in regions that contain fewer origins, making them more susceptible to incomplete DNA replication [25–27].

Overexpression or activation of oncogenes is an additional source of replication stress. Oncogenes, such as HRAS, C-MYC, and Cyclin E, can cause premature entry into S-phase and promote mis-regulated replication initiation and origin firing [28]. This leads to a decrease in nucleotide pools and an increase in replication-transcription collisions [28]. Although the precise mechanism of oncogene-induced replication stress is still being uncovered, it is clear that it can contribute to genome instability and tumorigenesis.

Exogenous sources of replication stress also exist and are frequently used in the laboratory to examine the effects of replication fork stalling. The most common extrinsic sources are ultraviolet (UV) radiation and genotoxic chemical compounds that can generate a broad spectrum of replication-blocking DNA lesions [29]. Exposure to UV radiation induces the formation of pyrimidine dimers that uncouple leading- and lagging-strand replication [30]. Chemical compounds can also cause bulky DNA lesions or DNA crosslinks, which occur when nucleotides are covalently linked within a single DNA strand (intrastrand crosslink) or between the two opposite strands of the DNA double-helix (interstrand crosslink – ICL) [31]. These lesions are induced by the chemotherapeutic agents, cisplatin or mitomycin C (MMC). ICLs act as a replication barrier because they prevent strand separation and must be properly unhooked, bypassed, and repaired before the replication fork can progress [32,33]. DNA lesions are also produced by the alkylating agent, methyl methanesulfonate (MMS), which blocks replication forks by attaching alkyl groups to DNA [34].

Other agents that induce replication stress do not damage the DNA directly, but instead interfere with replication-associated enzymes [29]. Hydroxyurea (HU) interferes with the ribonucleotide reductase (RNR), which consequently disrupts the metabolism of dNTPs. This perturbs the incorporation of nucleotides into the replicating DNA and

halts synthesis [35,36]. Camptothecin (CPT) and etoposide (ETP) target topoisomerase I (TOPI) and topoisomerase II (TOPII), respectively, which act beyond the replication fork to relax supercoiled DNA. Stabilization of these cleavage complexes by CPT and ETP results in collisions with the replication machinery [37,38]. Aphidicolin (Aph) induces replication stress by inhibiting the DNA polymerases α, δ, and ε. This forces the uncoupling of the polymerase and helicase activities, resulting in long stretches of single-stranded DNA (ssDNA) that are vulnerable to breakage [39–41].

Pathways for Resolving Replication Stress

Cells have evolved complex surveillance mechanisms to detect and respond to DNA damage and replication stress. The DNA damage response (DDR) is coordinated by three major proteins of the phosphatidylinositol 3-kinase-related kinase (PIKK) family – ATM, ATR, and DNA-PKcs [42,43]. Ataxia telangiectasia-mutated (ATM) and DNA-dependent protein kinase (DNA-PKcs) are primarily involved in DNA double-strand break (DSB) repair and signaling, whereas ATM- and Rad3-related (ATR) responds to a broader spectrum of DNA damage, specifically those associated with DNA replication [44–46]. All three DDR kinases act by sensing the DNA damage through protein-protein interactions and by initiating a cellular signaling cascade of phosphorylation events to promote repair and activation of cell cycle checkpoints.

ATR is the key responder to genotoxic stress associated with stalled replication forks. Although replication stress is triggered by a variety of sources, it usually results in the formation of long stretches of ssDNA [47]. This often occurs from helicase-polymerase uncoupling or from the nucleolytic processing events at stalled forks [48]. When ssDNA is generated, it is rapidly coated by the ssDNA-binding protein complex, replication protein A (RPA). This constitutes the signal for recruiting ATR via its binding partner, ATRIP [49]. Another regulator of ATR is the RAD9-RAD1-HUS1 (9-1-1) complex, which loads onto DNA at RPA-coated ssDNA-dsDNA junctions. DNA topoisomerase II binding protein 1 (TOPBP1) interacts with ATR-ATRIP and the RAD9 subunit of the 9-1-1 complex to fully activate ATR [50,51]. Once activated, ATR can initiate a signaling cascade by phosphorylating downstream targets, such as the

effector kinase CHK1 and members of the Fanconi anemia (FA) pathway or the FA/BRCA network.

The FA pathway is comprised of at least 21 known genes (*FANCA*-*FANCV*). Inactivation of any one of these genes causes Fanconi anemia, an inherited genome instability disorder characterized by bone marrow failure, developmental defects, and a predisposition to cancer [52]. The most well-defined function of the FA pathway is in the repair of ICLs, as FA patient cells are hypersensitive to agents that induce this type of lesion, but additional evidence has demonstrated roles for FA proteins in other repair processes and in the stabilization of stalled replication forks [53]. In response to replication stress, the ATR kinase activates the FA core complex (FANCA, B, C, E, F, G, L, M, T, FAAP100, MHF1, MHF2, FAAP20 and FAAP24), which then loads onto chromatin at sites of damage [54–56]. This complex monoubiquitinates the FANCD2-I heterodimer through its ubiquitin ligase subunit, FANCL, and the ubiquitin conjugating enzyme, UBE2T (FANCT) [57]. Monoubiquitinated FANCD2-I can localize to chromatin and recruit downstream factors of the FA/BRCA network, including BRCA2 (FANCD1), RAD51 (FANCR), FANCJ (BRIP1), FANCN (PALB2), and SLX4 (FANCP) [58–60]. These proteins have important functions in stabilizing stalled forks and in recombination-mediated repair following fork collapse.

Unlike ICLs that illicit repair through the FA/BRCA network, some lesions can stall the replicating polymerases without physically blocking the unwinding helicase. In the case of unrepaired lesions or base modifications on the leading-strand, the replisome can bypass these obstructions via DNA damage tolerance (DDT) mechanisms. The replication machinery can reprime or reinitiate DNA synthesis downstream of the lesion, leaving behind a ssDNA gap. This gap is filled in by specialized translesion synthesis (TLS) polymerases that replicate through the damaged template or by recombination-mediated repair involving template switching to the newly synthesized sister chromatid [61]. If left unrepaired, the ssDNA gap can be converted into a DSB and promote genome instability.

Despite the diversity of replication fork impediments, ssDNA accumulation is a common feature of all stalled forks [47]. The ssDNA is often generated through polymerase-helicase uncoupling, but this uncoupling event is not feasible when physical

blocks, such as ICLs or DNA-protein complexes, block progression of the helicase. Therefore, the blocked replication forks must be processed in a way that generates stretches of ssDNA for proper signaling and repair. One method of processing is through replication fork reversal, which is a global response to various types of genotoxic stress [47]. During fork reversal, the parental DNA strands reanneal and the complementary nascent leading- and lagging-strands anneal to form a four-way junction [62–64]. This junction produces a fourth regressed arm at the fork and is often referred to as a "chicken foot" structure. Several DNA translocases and helicases have been implicated in initiating fork regression, including FANCM, SMARCAL1, HLTF, FBH1, ZRANB3, BLM, and WRN [65–71]. Another required component for fork reversal is the recombinase RAD51, which promotes homologous pairing and strand exchange of ssDNA. RAD51 has been proposed to either bind to the parental ssDNA to drive reversal or to the ssDNA of the regressed arm to capture the reversed fork [72].

After the replication fork is regressed, it must be processed or remodeled to allow for replication restart (Figure 1.2). The RecQ family of helicases have been described to facilitate fork restart after reversal. The RECQ1 helicase promotes branch migration of the reversed fork and is regulated by poly(ADP-ribose) polymerase 1 (PARP1), which suppresses the activity of RECQ1 until the replication stress is relieved [73]. RECQ1 binding can also inhibit a second pathway of fork restart mediated by the Werner syndrome ATP-dependent helicase (WRN) and the DNA replication ATP-dependent helicase-nuclease (DNA2). WRN and DNA2 can restart forks by unwinding and resecting the regressed arm with a 5' to 3' polarity [74]. The resulting 3' overhang could recruit another motor protein to drive branch migration or it could activate recombination-mediated restart by invading donor sequences ahead of the reversed fork [75,76].

Additional nucleases have been implicated in processing stalled replication forks to promote restart, but the specific DNA structures that they act upon are not fully established [76]. The Fanconi-associated nuclease 1 (FAN1) and the C-terminal binding protein interacting protein (CtIP) both cooperate with FANCD2 to aid in fork recovery [77,78]. Additionally, PARP1 has been shown to recruit the meiotic recombination 11 (MRE11) nuclease to stalled forks to promote DNA resection for recombinational repair

and restart [79]. MRE11 has also been implicated in generating ssDNA gaps at stalled replication forks, which may enable RAD51 filament formation to facilitate fork reversal or template switching [80,81]. Exonuclease 1 (EXO1) has been described to perform a similar function in yeast, although the structure of the fork in this scenario is unknown and DNA degradation by EXO1 may counteract fork reversal [82].

The nucleolytic processing of nascent DNA at stalled forks is an integral step for replication restart, but dysregulated nuclease activity can lead to uncontrolled degradation and genome instability. Therefore, the cell has evolved mechanisms to monitor and protect the fork from excessive DNA end resection. Members of the FA/BRCA network play key roles in stabilizing stalled forks and preventing extensive degradation by the nucleases EXO1 and MRE11 [83–86]. Fork protection is dependent on the stabilization of RAD51 filaments, which is facilitated by BRCA1, BRCA2, and FANCD2 [80,83,84].

If stalled replication forks remain unstable and fail to restart, they may collapse and generate DNA DSBs. These breaks can form by endonucleolytic cleavage of irresolvable fork structures or vulnerable ssDNA regions. The endonuclease MUS81 has been implicated in these cleavage events at reversed forks, and once generated, the DSBs are repaired via homologous recombination (HR) [87]. DNA end resection by the coordinated activities of MRE11, CtIP, EXO1, and DNA2 produces the 3' overhangs necessary for initiating recombination [88–92]. These overhangs are coated by the ssDNA-binding protein RPA, which is then displaced by the RAD51 recombinase. The RAD51 filaments coordinate homology search and strand invasion to initiate DNA synthesis using a homologous template [93]. The downstream factors of the FA/BRCA network, such as BRCA1 and BRCA2, aid in this process independently of their protective roles at stalled replication forks.

Consequences of Unresolved Replication Stress

The DNA intermediates that form in response to replication stress play an integral role in the repair process, but if not properly resolved, they can result in pathological consequences. Defects in the signaling events or mis-repair at stalled forks can lead to genome instability and disease. For example, loss of the ATR kinase

or mutations in its binding partner ATRIP can cause Seckel syndrome, a disorder characterized by developmental delay and microcephaly [94–96]. Similarly, helicases that aid in fork remodeling and stabilization are also associated with disease. The RecQ helicases, BLM and WRN, are mutated in patients with Bloom syndrome and Werner syndrome, respectively, which are both characterized by premature aging, growth retardation, and cancer predisposition [97]. A disease with clinically overlapping symptoms with Bloom and Werner syndrome is Fanconi anemia. Inherited mutations in any one of the known FA genes can cause this heterogeneous autosomal recessive disorder, with the exception of the X-linked gene *FANCB* or the rare dominant negative mutations of *RAD51* (*FANCR*). Patients with FA display skeletal abnormalities, developmental delays, growth retardation, and bone marrow failure [59]. Interestingly, monoallelic inactivation of genes within the BRCA portion of the FA/BRCA network, including *BRCA1* (*FANCS*), *BRCA2* (*FANCD1*), *FANCN*, and *FANCJ*, can cause an increased predisposition to breast and ovarian cancer [98]. Additionally, somatic FA gene mutations have also been identified in sporadic cancers of individuals without FA [99].

Processes associated with genome maintenance, such as DNA replication and repair, bear an intrinsic risk of mutagenesis. Errors during replication have the potential to induce deleterious copy number variants (CNVs), which are defined as deletions or duplications of genomic regions ranging from 50 base pairs to megabases in length [100]. CNVs have been associated with genetic and neurodevelopmental disorders, including autism and schizophrenia, and they arise frequently in cancer [101,102]. A large proportion of pathogenic CNVs are nonrecurrent and contain breakpoint microhomologies, indicative of aberrant template switching at stalled replication forks. In these models of CNV formation, stalled forks can utilize another active fork as a template to resume replication, or one-ended DSBs at collapsed forks can undergo template switching into regions of microhomology in an attempt to repair the break [103,104]. Intriguingly, CNV hotspots occur in the same genomic loci as CFSs, which as described previously, are regions prone to breakage from replication stress. These loci associate with late-replicating, large, active transcription units that can stall replication due to R-loop formation and/or collisions between the transcription and replication machinery. The two most frequent CFSs, FRA3B and FRA16D, map within the large tumor suppressor

genes, *FHIT* and *WWOX*, respectively [105,106]. These genes were found to be sites of recurrent deletions in various cancers, and the loss of gene expression is associated with tumor progression and decreased survival [107–109]. Therefore, replication errors at CFSs can lead to genome instability and promote tumorigenesis.

Cell Cycle Control of DNA Repair Processes

Genome maintenance and DNA repair processes are tightly linked to the cell cycle. When a cell is exposed to genotoxic stress, the repair pathway choice often depends on the type of damage encountered and on the cell cycle phase [110,111]. The most prominent example of this modulation is in the periodic inhibition of DSB repair. The two main pathways of DSB repair include non-homologous end-joining (NHEJ) and HR. NHEJ functions by directly ligating broken DNA ends together, whereas HR repairs DSBs through extensive end processing and DNA synthesis using a homologous template [88,112]. Because HR requires a homologous sequence, such as a duplicated sister chromatid, this pathway functions primarily during S- and G2-phase when replicated DNA is present. Alternatively, DSBs that form during G1-phase are predominantly repaired by NHEJ. This is due to the absence of sister chromatids and to the high compaction of DNA at this stage.

The regulation of DSB repair by the cell cycle is partially dictated by the extent of DNA end resection. The cyclin-dependent serine/threonine kinases (CDKs), which partner with cyclins to drive cell cycle progression, also play a role in mediating end resection [113]. CDK activity levels rise during S- and G2-phase, leading to the phosphorylation and stimulation of CtIP, EXO1, and DNA2, which are all nucleases involved in the DNA processing events associated with HR [114–116]. Alternatively, p53-binding protein 1 (53BP1) promotes NHEJ in G1-phase by blocking resection and opposing HR [117–119]. The interplay between these events is an important factor in determining DSB repair pathway choice in different phases of the cell cycle.

The primary goal of mitosis is the successful segregation of sister chromatids; however, unresolved DNA replication intermediates can result in linked chromatids that fail to separate during anaphase. Therefore, components of the HR pathway remain active in early mitosis to process these intermediates. CDK-dependent phosphorylation

promotes the formation of the MUS81-EME1-SLX1-SLX4 nuclease complex, which resolves the joint DNA structures [120]. Incomplete replication at loci such as CFSs also poses a problem for chromatid segregation, and the endonuclease MUS81-EME1 has been implicated in cleaving the branched structures at CFSs [121,122]. Studies have shown that MUS81-EME1 can also promote POLD3-dependent DNA replication at these loci in a process called mitotic DNA synthesis (MiDAS) [123]. MiDAS may help minimize chromosome mis-segregation through a microhomology-mediated repair mechanism independent of the canonical HR proteins, BRCA2 and RAD51 [124]. If DNA is not properly processed at CFSs, the chromatids remain linked, forming anaphase or ultra-fine bridges (UFBs) [125]. Additional repair factors, such as BLM and FANCD2, localize to UFBs in an attempt to facilitate disjunction, and defects in this process can lead to micronucleation [126,127].

Most of the DNA damage that is repaired during mitosis is propagated from S- or G2-phase, but there is evidence that DSBs can occur in mitotic cells. Mitotic cells sense the DSBs and initiate a signaling cascade, but they do not repair the breaks after late prophase or prevent the progression of cell division [128]. The early signaling events in the pathway are unaffected, but modifications of downstream effectors interrupt their canonical repair functions. Specifically, phosphorylation of 53BP1 disrupts its accumulation on damaged chromatin, thereby preventing efficient NHEJ [129–132]. This disruption is particularly evident at mitotic telomeres, where NHEJ is blocked to allow for telomere uncapping and to prohibit end-to-end chromosome fusions [130]. Because the initial signaling cascade is intact, DSBs that occur in mitosis are “marked” for repair in the following G1-phase when the chromatin environment is more favorable [129].

Regulation of DNA Repair

The regulation of DNA repair throughout the cell cycle relies heavily on post-translational modifications (PTMs). PTMs are important for the complex DNA damage response because they allow for the rapid and precise control of protein function by altering protein activity, localization, and interactions. The most common PTMs that regulate the DDR include phosphorylation, ubiquitination, SUMOylation, and PARylation.

Protein phosphorylation is a key event in most signaling cascades, especially during the DDR. The protein kinases ATM, ATR, and DNA-PKcs are activated by autophosphorylation and they initiate the cellular responses to DNA damage by phosphorylating an extensive network of substrates [43]. One major role of these phosphorylation events is the activation of cell cycle checkpoints, which provide the cells with additional time to repair DNA damage or resolve replication stress before proceeding with cell division. Phosphorylation can also modulate the functions of specific proteins that act in multiple pathways of repair. For example, the DNA helicase BLM is phosphorylated by ATR to aid in replication fork recovery, whereas in mitosis, it is phosphorylated by MPS1 to facilitate checkpoints that ensure faithful chromosome segregation [133,134].

Ubiquitination is another PTM that is important for maintaining genome integrity and regulating DNA repair. Ubiquitin is a small peptide that is covalently attached to lysine residues, either as a single modification (monoubiquitination) or as a linked chain (polyubiquitination). Polyubiquitination on defined lysines, specifically K48 or K29, targets proteins for degradation by the proteasome, whereas monoubiquitination or K63 polyubiquitination can regulate DNA repair processes [135,136]. One major example of this type of modification is FANCD2 monoubiquitination, which is important for localization of FANCD2 to sites of replication stress [52]. Proliferating cell nuclear antigen (PCNA), which is an essential replication factor, is also ubiquitinated during cellular responses to DNA damage. PCNA is mono- and polyubiquitinated to recruit DNA polymerases for translesion synthesis or to promote an alternative pathway of error-free lesion bypass, respectively [110,137]. Another mechanism for regulating DNA repair is through alterations in protein levels and stability. K48 polyubiquitination can facilitate this process by targeting proteins for degradation by the proteasome. For example, BLM is polyubiquitinated and degraded to modulate its levels throughout the cell cycle [138,139]. The FA member, FANCM, is also polyubiquitinated in mitosis to ensure its removal from chromatin when it is no longer required for replication fork repair [140].

Similar to ubiquitin, small ubiquitin-like modifier (SUMO) is covalently attached to other proteins to modify their cellular functions. SUMOylation of PCNA on multiple sites is predicted to help prevent replication fork collapse and DSB formation [141]. SUMO

modification of BLM is also required at stalled forks to efficiently recruit BRCA2 and prevent excessive ssDNA accumulation [142]. Poly(ADP-ribosyl)ation (PARylation) is a PTM catalyzed by the poly(ADP-ribose) polymerase (PARP) family of enzymes. It is comprised of both linear and branched polymers of poly(ADP-ribose) (PAR) on multiple amino acid residues. PARylation plays a pivotal role in DNA damage repair, as demonstrated by the hypersensitivity of *Parp1* knockout mice to various genotoxic agents [143]. PARP1 localizes to single-strand breaks (SSBs) and DSBs to facilitate the recruitment of DDR proteins, such as MRE11 and ATM, potentially through PARylation of other targets [144–146].

Several DNA repair proteins have roles in multiple pathways or respond to diverse forms of DNA damage. Therefore, PTMs provide a practical mechanism for fine-tuning protein functions within different pathways or throughout various stages of the cell cycle. DNA nucleases have been implicated in the resolution and repair of numerous types of DNA damage and studies have demonstrated that their nucleolytic activities must be tightly controlled to prevent genome instability. However, the precise mechanisms of their regulation are not well characterized. One exonuclease that has been described to function in the resolution of replication stress and in the DDR is SNM1B. This thesis is focused on elucidating the role of SNM1B in replication repair and on its regulation by PTMs throughout cell cycle.

Identification of SNM1B

The *SNM1* (sensitivity to nitrogen mustard) gene family was first discovered in genetic screens in *Saccharomyces cerevisiae* for hypersensitivity to the ICL-inducing agents, nitrogen mustard and psoralen [147,148]. These screens identified the founding member of this family, *SNM1* or *PSO2* (sensitivity to psoralen), which has five putative homologs in mammals: SNM1A, SNM1B/Apollo, SNM1C/Artemis, CPSF73, and ELAC2 [149–153]. These proteins are characterized by a common metallo-β-lactamase (MBL) fold and an appended βCASP domain (β-CPSF-Artemis-SNM1/PSO2), which together provide nucleolytic function. The canonical MBL fold contains five conserved sequence motifs that participate in metal ion coordination and hydrolysis of various substrates [154]. Motif 2 contains the highly conserved HxHxDH sequence, which serves as the active

site for this class of enzymes [154,155]. Mutation of the aspartic acid (D) in motif 2 has been shown to disrupt the nuclease activity of both Artemis and SNM1B [156–158]. The βCASP domain is unique to the SNM1 members of the MBL superfamily and contributes to their nucleic acid binding capabilities. An analysis of the amino acid sequences revealed a set of three conserved residues within the βCASP domain, which are all located at the end of predicted β-strands [154]. A valine within the last motif is characteristic of DNA processing enzymes, such as SNM1A, SNM1B, and Artemis, whereas a histidine is characteristic of the RNA processing enzymes, CPSF73 and ELAC2 [154]. Therefore, the residue within this motif appears to be responsible for distinguishing between RNA and DNA specificity within the metallo-β-lactamase/βCASP family, although the importance of the histidine residue in nucleolytic activity has been disputed [159].

The metallo-β-lactamase/βCASP domain is the region of highest conservation between SNM1A, SNM1B, and SNM1C/Artemis, with the remaining sequences being distinct to each protein (Figure 1.3). Although the members of this family share a similar catalytic domain, the specificity of their nucleolytic activities differ. SNM1A and SNM1B both possess 5′ to 3’ exonuclease activity, whereas Artemis functions mainly as a structure-specific endonuclease [156,160,161]. Both SNM1A and SNM1B can digest short double-stranded and single-stranded DNA substrates with similar catalytic efficiency, but SNM1A becomes more processive on higher molecular weight DNA oligonucleotides [159]. They can both also digest past an ICL, but with SNM1A functioning at a higher capacity through this type of lesion [159,162]. The nucleolytic activity of SNM1A supports the findings that it functions in ICL repair, and recent evidence suggests that it may also possess endonuclease activity to aid in this process [151,163]. Artemis is a structure-specific nuclease that can act on 5’ and 3’ overhangs and on DNA hairpin substrates during V(D)J recombination and NHEJ [156,164,165]. Artemis has 5’ to 3’ exonuclease activity on its own, but its endonuclease activity is dependent on an interaction with DNA-PKcs. It has been proposed that autophosphorylation of DNA-PKcs activates Artemis through phosphorylation of its inhibitory C-terminus, thereby promoting the dissociation of this region from the N-terminal catalytic domain [164–167]. Finally, SNM1B and its 5’ to 3’ exonuclease activity have known roles in ICL repair, the

DNA damage response, and telomere maintenance, which will be discussed in the next few sections.

Roles of SNM1B in the Response to Stalled Replication Forks

Studies characterizing the role of SNM1B in DNA repair revealed that SNM1B-deficient cells are sensitive to agents that induce ICLs, such as MMC or cisplatin, but not to UV [168–172]. Additionally, there is conflicting evidence on whether SNM1B-depleted cells are sensitive to IR [168–170,172]. These experiments were all done using different cell types, both human and chicken, so these discrepancies may be attributed to differences in species or cell line tested. SNM1B-deficient cells also display an increase in chromosomal gaps, breaks, and radial structures after exposure to ICL-inducing agents, further highlighting a role for SNM1B in the repair of ICLs [168,170,171].

Because SNM1B is involved in the cellular response to ICLs, its link to the FA pathway was investigated. SNM1B is not required for the monoubiquitination of FANCD2 after MMC treatment, but is important for the efficient localization of FANCD2, BRCA1, and RAD51 to sites of ICL damage [171]. SNM1B was also shown to function epistatically with FANCD2 and FANCP/SLX4 in the response to ICL-induced replication stress and to suppress chromosomal aberrations [171,172]. The FA pathway not only responds to ICL damage, but is also essential for stabilizing and repairing stalled or collapsed replication forks. SNM1B functions with the FA/BRCA network in the cellular response to stalled forks induced by the polymerase inhibitor, aphidicolin. SNM1B-deficient cells are hypersensitive to aphidicolin treatment and display a decrease in FANCD2 and BRCA1 localization to sites of replication stress [173]. Additionally, SNM1B depletion results in elevated levels of spontaneous and aphidicolin-induced chromosomal gaps and breaks, including breaks at common fragile sites [173]. Together, these data reveal an important function of SNM1B in the response to replication stress.

Roles of SNM1B in Cell Cycle Checkpoints

The ATM and ATR protein kinases play central roles in initiating the signaling events of cell cycle checkpoints during S-phase. Several studies have investigated the role of SNM1B in these signaling events after DNA damage or replication stress. In

response to ICL-inducing agents, SNM1B depletion results in no change in ATR-signaling events, but a decrease in ATM-mediated signaling [170]. Localization and phosphorylation of ATR substrates was also unaffected by SNM1B knockdown in cells treated with the DNA polymerase inhibitor, aphidicolin [173]. This suggests that SNM1B is not involved in the early ATR-signaling events in response to aphidicolin or ICL-induced damage. However, the decrease in ATM-mediated signaling during ICL repair could be due to DSB formation that occurs from processing this type of lesion. The ATM-signaling events in SNM1B-deficient cells were also examined after IR treatment [168,170]. These studies found conflicting results, which could be attributed to differences in the IR doses and timepoints examined.

In addition to checkpoint signaling during S-phase, the role of SNM1B has also been examined in mitotic checkpoints. SNM1B was shown to function in an early prophase checkpoint, which prevents DNA condensation and nuclear envelope breakdown when conditions are unfavorable for cell division [174]. Similar findings have also been reported for the MBL/βCASP family member, SNM1A [175]. The precise role of SNM1B in this prophase checkpoint is still unknown, but it suggests that SNM1B may promote successful cell cycle progression.

Roles of SNM1B in Telomere Maintenance

Telomeres are the structures at the end of linear chromosomes, which consist of a G-rich repeat DNA sequence, the shelterin complex, and shelterin accessory factors [176]. The shelterin complex binds to telomeric DNA to prevent the recognition of these ends as DSBs and to protect them from aberrant repair [177,178]. The shelterin complex associates with several accessory factors, which are distinguished from the core shelterin components by their lower abundance at telomeres or their transient association with the complex [177]. In mass spectrometry experiments, SNM1B was identified as a shelterin accessory factor that associates with the shelterin proteins, RAP1 and telomere repeat binding factor 2 (TRF2) [179]. Multiple groups have described the interaction between SNM1B and TRF2 using co-immunoprecipitation, yeast two-hybrid screens, GST pulldown assays, co-immunofluorescence, and even isothermal titration calorimetry [161,179–182]. The last 37 amino acids (496-532) of SNM1B are

necessary and sufficient for binding to the TRF homology (TRFH) domain of TRF2, and this association is important for SNM1B localization to the telomere [161,179,180].

In addition to being capped by the shelterin complex, telomeres also form T-loops as a mechanism to protect against DSB recognition. T-loops are generated by 3' overhangs that insert back into the double-stranded portion of the telomeric tract. The 5' to 3' exonuclease activity of SNM1B has been implicated in initiating the formation of the 3' overhangs at leading-strand telomeres, and this resection is limited by the shelterin component, POT1b (Figure 1.4) [157,183,184]. SNM1B-depleted cells exhibit increased telomere dysfunction-induced foci (TIFs) and telomere fusions, indicative of unprotected chromosome ends [161,179]. Additionally, some telomeres in SNM1B-deficient cells showed two telomeric signals at single-chromatid ends, which suggests abnormal telomere structures [179]. Together, these data reveal an important role for SNM1B in DNA end resection at the telomere to protect it from aberrant DNA repair. Studies have suggested that the generation of 3' overhangs at chromosome ends reflects a role of SNM1B in telomere replication. To separate functions of SNM1B in overhang maintenance and telomere replication, the cellular response to an internal telomeric sequence was examined. SNM1B nuclease activity suppresses the DNA damage response at these internal telomeric sequences and functions in a complementary pathway with TOPIIα to relieve topological stress during telomere replication [158]. These findings provide evidence for a role of SNM1B in protecting telomeres from DSB repair and replicative damage.

SNM1B Protein Interactions

Although TRF2 is the most well studied binding partner of SNM1B, several other proteins have been shown to interact with SNM1B in various contexts (Figure 1.5). Co-immunoprecipitation studies revealed that SNM1B directly interacts with MUS81 and with members of the MRN complex, specifically MRE11 and RAD50 [170]. In the same report, SNM1B was also shown to interact indirectly with the FA protein, FANCD2, and all interactions were mapped to the N-terminal metallo-β-lactamase/βCASP domain of SNM1B [170]. Each of these described binding partners of SNM1B have known roles in

the DNA damage response, but the functional importance of these interactions has yet to be determined.

SNM1B has been previously described to function within the FA pathway, and this is further supported by the finding that SNM1B interacts with FANCP/SLX4 [172]. This interaction was originally mapped to the N-terminal domain of SNM1B, but a recent review suggests that SLX4 instead binds to at least two unreported regions of SNM1B [172,185]. SLX4 and SNM1B function epistatically in the response to MMC-induced ICL damage, and knockdown of SLX4 results in a decrease in SNM1B foci formation [172]. These data provide additional evidence for a functional role of SNM1B in the FA pathway and in the repair of ICLs.

Because SNM1B has known roles in the response to replication stress, it is not surprising that it was found to associate with the replication protein, PSF2 (also known as GINS2) [186]. PSF2 is a member of the GINS complex, which functions in the initiation and elongation steps of DNA replication. The interaction between SNM1B and PSF2 was identified through a yeast two-hybrid screen and validated via co-immunoprecipitation [186]. PSF2 binding was mapped to two regions within SNM1B, one of which encompasses the same site for TRF2 binding. This study concluded that this C-terminal region of SNM1B competes with TRF2 binding and is required for chromatin association through an interaction with PSF2. Alternatively, the more N-terminal binding site within SNM1B promotes the formation of a protein complex involving MUS81 and PSF2, but the functional importance of this complex remains unknown [186]. Interestingly, PSF2 has also been reported to interact with the FA core complex protein, FANCF, and knockdown of PSF2 results in sensitivity to ICLs and a reduction in FA core complex association with chromatin [187]. These data suggest that PSF2 may have a role in loading or stabilizing the FA core complex, and potentially SNM1B, onto chromatin during replication or in response to replication stress.

In another yeast two-hybrid screen, SNM1B was shown to interact with the spindle-associated protein, astrin, through its metallo-β-lactamase domain. It was suggested that this interaction is important for proper activation of the prophase checkpoint during mitosis [174]. Mass spectrometry analyses have revealed additional binding partners of SNM1B, including heat shock proteins HSC70, HSP72, and HSP60,

and the microtubule component, β-tubulin [188]. HSP72 was shown to be required for proper SNM1B foci formation, but additional studies are necessary to elucidate the functional importance of these protein interactions with SNM1B.

SNM1B and Disease

A transcript variant of *hSNM1B* was identified in a patient with Hoyeraal-Hreidarsson (HH) syndrome, a severe form of dyskeratosis congenita [189]. This patient presented with symptoms characteristic of HH syndrome, such as microcephaly, growth retardation, cerebellar hypoplasia, and aplastic anemia [189]. Analyses of primary fibroblasts derived from this patient revealed an intraexonic splice variant of *SNM1B*, which results in a frameshift and premature stop codon in the C-terminal end of the protein. This leads to a loss of the last 116 amino acids, which includes the TRF2 binding domain [189]. The primary fibroblasts displayed a growth defect, increased TIFs, and increased telomere fusions, but no abnormal telomere shortening compared to fibroblasts from healthy controls [189]. However, when cellular senescence is overcome by SV40 large T antigen transformation, expression of the SNM1B variant compromises the completion of lagging-strand replication and results in telomere shortening over time. Ectopic expression of the variant in wildtype cells recapitulates the phenotypes observed in primary patient cells of HH syndrome, suggesting a dominant negative role of the *SNM1B* splice variant [189]. In contrast to defects observed at telomeres, cells expressing the *SNM1B* splice variant did not show sensitivity to MMC or IR [189]. Together, these observations highlight a critical role for SNM1B at telomeres and suggest a separation of function of SNM1B in the DNA damage response and telomere maintenance.

Although only one patient harboring a variant of *SNM1B* has been studied in depth, additional patients with symptoms of HH syndrome have been identified with *SNM1B* variants [190]. Several of these clinical variants have unknown significance, therefore their association with dyskeratosis congenita requires further investigation. Single nucleotide polymorphisms (SNPs) in *SNM1B* have also been evaluated in targeted or genome-wide cancer studies [191–195]. In an examination of DNA repair genes, *SNM1B* variants showed a suggested association with cutaneous malignant

melanoma [191]. Other SNPs in *SNM1B* have been associated with breast cancer, with one specific variant (rs11552449) showing differential splicing of exon 2 and decreased expression levels [193–195]. Cells that were heterozygous for this variant expressed higher levels of *SNM1B* containing exon 2 and were significantly more sensitive to MMC or IR compared to homozygous wildtype controls and showed no alterations in telomere length [196]. Interestingly, when SNM1B was depleted in the breast cancer cell line, SK-BR3, cell proliferation was increased compared to controls, which differs from the phenotype observed in other cancer cells [195]. This suggests that differential expression of *SNM1B* may contribute to the defects associated with cancer and may result in varying phenotypes in different cell lines.

To date, no *SNM1B* null alleles have been identified in humans. However, studies in mice have provided insight into the role of *Snm1B* during development. To study the role of *Snm1B in vivo*, *Snm1B* knockout mice were generated by deletion of exon 4 [157,197]. Deletion of this exon in *Snm1B* eliminates over 66% of the coding region, which includes the TRF2 binding site. *Snm1B* homozygous null mice exhibit perinatal lethality with embryos displaying developmental delays and hypocellularity in multiple organ systems [197]. *Snm1B*$^{-/-}$ primary mouse embryonic fibroblasts (MEFs) generated from these mice showed a proliferation defect and increased apoptosis compared to wildtype controls [197]. This defect was attributed to high levels of telomere fusions, which could be rescued by deletion of the NHEJ factor Ku70 [157,197]. Another mouse model of *Snm1B*, generated by deleting exons 2 and 3, also showed leading-end telomere fusions and a reduction in the telomeric overhang signal [183]. Together, these findings suggest an important role for SNM1B in embryonic development and protection of telomere ends from NHEJ repair. It also indicates that SNM1B might be essential for survival in humans as well as in mice.

Thesis Summary

In this dissertation, I expand on the current knowledge of the functions of SNM1B in the resolution of stalled replication forks and provide insight into the mechanisms of its regulation. In Chapter 2, I discuss our findings on the role of SNM1B in the response to replication stress. We demonstrate that SNM1B is required for preventing the

accumulation of ssDNA intermediates and DSBs at stalled forks, thereby promoting fork stability and restart. We also show that SNM1B facilitates the recombination-mediated repair of replication-associated damage. In Chapter 3, I examine the regulation and post-translational modifications of SNM1B throughout the cell cycle. I characterize a novel SNM1B phosphorylation event that occurs during G2-phase and mitosis to promote protein stability. In Chapter 4, I discuss the implications of my findings and propose additional hypotheses relating to SNM1B and its role in DNA repair processes. Together, these studies define new functions for SNM1B in resolving stalled replication forks and provide a foundation for future explorations on the regulation of pathways that prevent genomic damage.

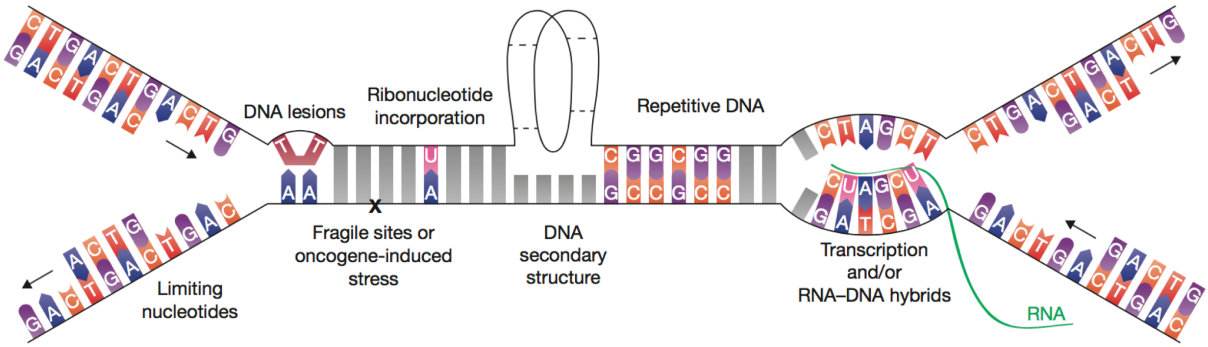

Figure 1.1 Sources of DNA replication stress
Schematic highlighting the various obstacles or barriers that cause replication fork stalling. Adapted from Zeman and Cimprich, 2014 [5].

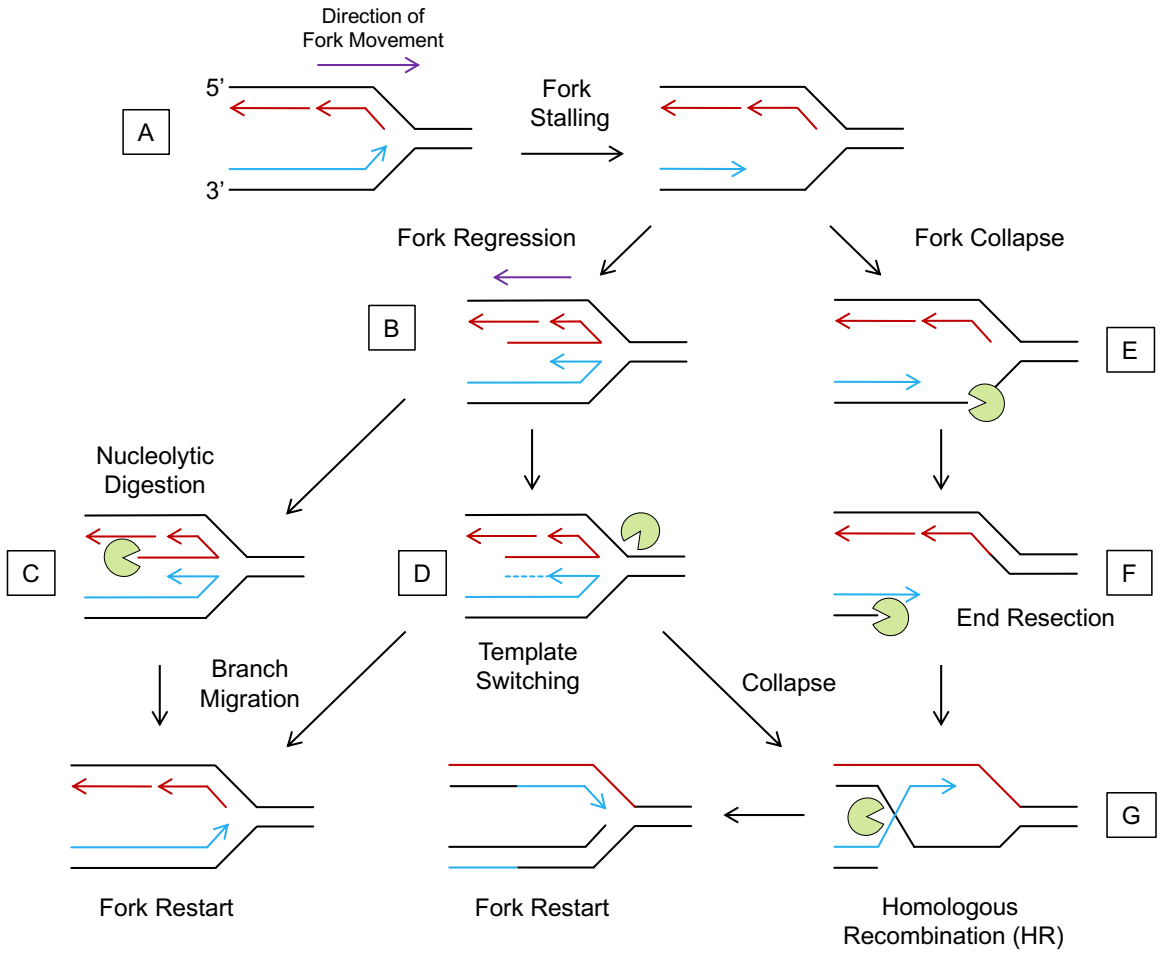

Figure 1.2 Resolution of stalled or collapsed replication forks
Replication fork stalling leads to the accumulation of ssDNA (A). The fork can become stabilized by the formation of a "chicken foot" structure, which entails reannealing of the parental DNA strands through a process called fork regression (B). The nascent arm of the regressed fork can be resected by nucleases (C) or undergo template switching and branch migration (D) to promote fork restart. Prolonged arrest results in fork collapse and the generation of DSBs (E). The DNA ends at DSBs are resected (F) to initiate homologous recombination (G) and fork restart. The purple arrow illustrates the direction of fork movement and the images with green proteins represent DNA structures on which DNA nucleases can act to facilitate repair. Adapted from Petermann and Helleday, 2010 [198].

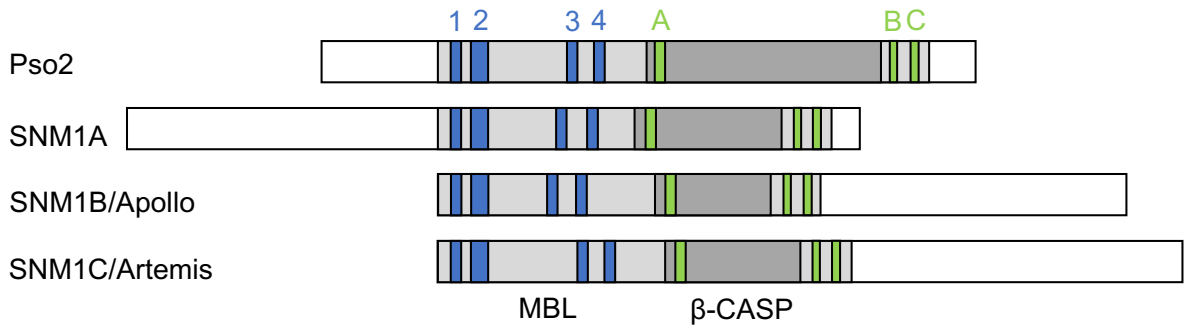

Figure 1.3 Protein domain alignment of the SNM1 family
Alignment of the yeast Pso2 and mammalian SNM1 family of proteins depicting the conserved metallo-β-lactamase (MBL) and βCASP domains in light and dark grey, respectively. The regions that are distinct to each protein are in white. The canonical MBL motifs 1-4 are shown in blue and the βCASP motifs A-C are shaded green. Adapted from Sengerova *et al*., 2012 [159].

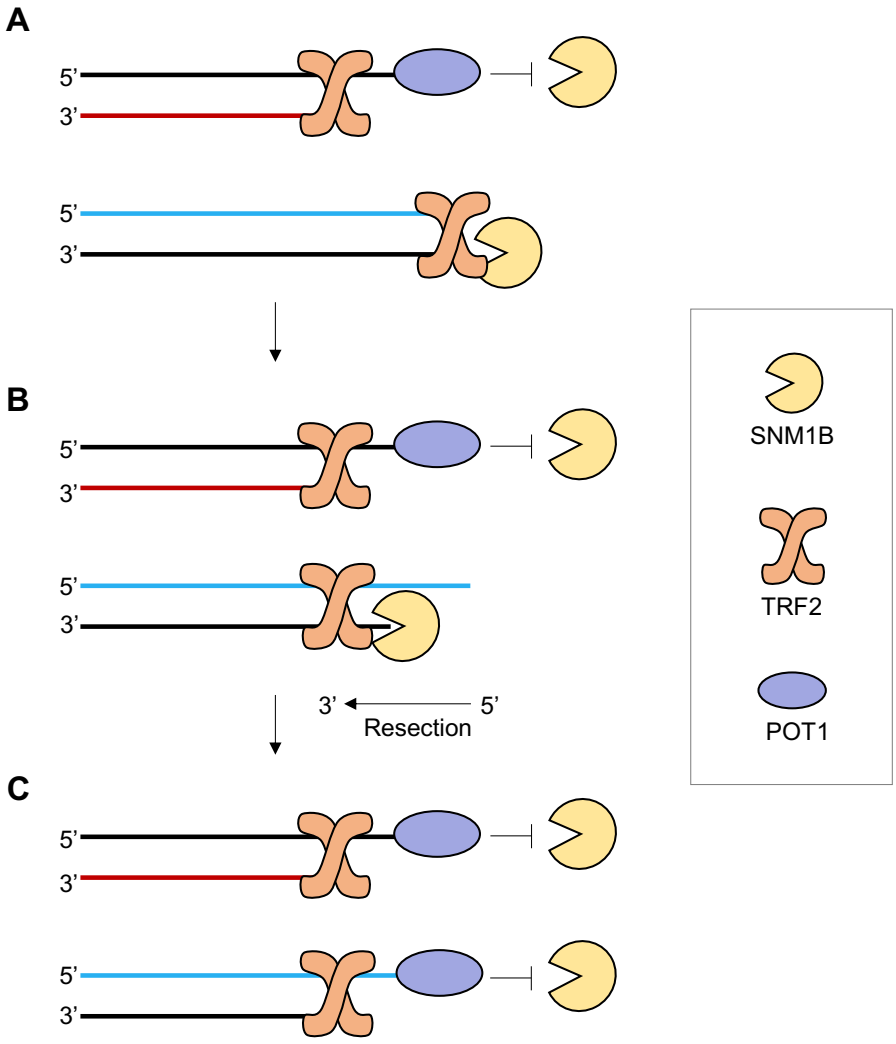

Figure 1.4 SNM1B resects DNA ends at telomeres
(A) Replication results in blunt ends at the leading-strand telomere and a short overhang bound by POT1 at the lagging-strand telomere. **(B)** TRF2 recruits SNM1B to the leading-strand telomere, and SNM1B resects the 5' end to generate an overhang for subsequent processing and T-loop formation. **(C)** POT1 association with the single-strand overhangs inhibits further resection by SNM1B. Adapted from Arnoult and Karlseder, 2016 [199].

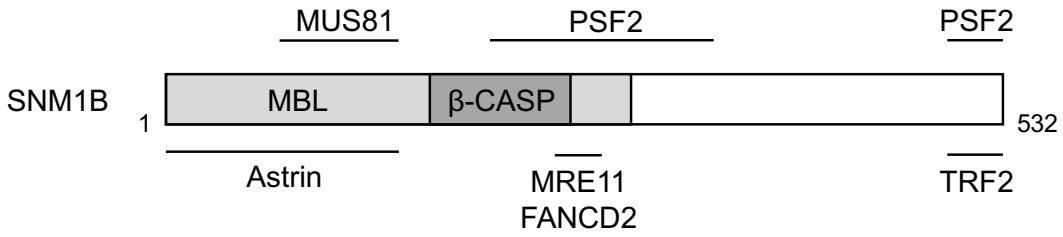

Figure 1.5 Binding partners of SNM1B
Schematic illustrating the functional domains and mapped protein interactions of SNM1B. Unmapped binding partners of SNM1B are not depicted in this figure. MBL, metallo-β-lactamase; βCASP, β-CPSF-Artemis-SNM1/PSO2. Adapted from Schmiester *et al.*, 2017 [185].

References

1. Norbury, C. & Nurse, P. Animal Cell Cycles and Their Control. *Annu. Rev. Biochem.* **61**, 441–468 (1992).
2. Bell, S. P. & Dutta, A. DNA Replication in Eukaryotic Cells. *Annu. Rev. Biochem.* **71**, 333–374 (2002).
3. Masai, H., Matsumoto, S., You, Z., Yoshizawa-Sugata, N. & Oda, M. Eukaryotic Chromosome DNA Replication: Where, When, and How? *Annu. Rev. Biochem.* **79**, 89–130 (2010).
4. Burgers, P. M. J. & Kunkel, T. A. Eukaryotic DNA Replication Fork. *Annu. Rev. Biochem.* **86**, 417–438 (2017).
5. Zeman, M. K. & Cimprich, K. A. Causes and consequences of replication stress. *Nat. Cell Biol.* **16**, 2–9 (2014).
6. Mazouzi, A., Velimezi, G. & Loizou, J. I. DNA replication stress: Causes, resolution and disease. *Exp. Cell Res.* **329**, 85–93 (2014).
7. Hoeijmakers, J. H. J. DNA Damage, Aging, and Cancer. *N. Engl. J. Med.* **361**, 1475–1485 (2009).
8. Ciccia, A. & Elledge, S. J. The DNA Damage Response: Making It Safe to Play with Knives. *Mol. Cell* **40**, 179–204 (2010).
9. Brooks, P. J. & Theruvathu, J. A. DNA adducts from acetaldehyde: implications for alcohol-related carcinogenesis. *Alcohol* **35**, 187–193 (2005).
10. De Bont, R. & van Larebeke, N. Endogenous DNA damage in humans: a review of quantitative data. *Mutagenesis* **19**, 169–185 (2004).
11. Hamperl, S. & Cimprich, K. A. Conflict Resolution in the Genome: How Transcription and Replication Make It Work. *Cell* **167**, 1455–1467 (2016).
12. Bermejo, R., Lai, M. S. & Foiani, M. Preventing Replication Stress to Maintain Genome Stability: Resolving Conflicts between Replication and Transcription. *Mol. Cell* **45**, 710–718 (2012).
13. Helmrich, A., Ballarino, M., Nudler, E. & Tora, L. Transcription-replication encounters, consequences and genomic instability. *Nat. Struct. Mol. Biol.* **20**, 412–418 (2013).
14. Beck, H. *et al.* Cyclin-Dependent Kinase Suppression by WEE1 Kinase Protects the Genome through Control of Replication Initiation and Nucleotide Consumption. *Mol. Cell. Biol.* **32**, 4226–4236 (2012).
15. Debatisse, M., Le Tallec, B., Letessier, A., Dutrillaux, B. & Brison, O. Common fragile sites: mechanisms of instability revisited. *Trends Genet.* **28**, 22–32 (2012).
16. McMurray, C. T. Mechanisms of trinucleotide repeat instability during human development. *Nat. Rev. Genet.* **11**, 786–799 (2010).

17. Bochman, M. L., Paeschke, K. & Zakian, V. A. DNA secondary structures: stability and function of G-quadruplex structures. *Nat. Rev. Genet.* **13**, 770–780 (2012).
18. Glover, T. W., Arlt, M. F., Casper, A. M. & Durkin, S. G. Mechanisms of common fragile site instability. *Hum. Mol. Genet.* **14**, R197–R205 (2005).
19. Glover, T. W. Common fragile sites. *Cancer Lett.* **232**, 4–12 (2006).
20. Durkin, S. G. & Glover, T. W. Chromosome Fragile Sites. *Annu. Rev. Genet.* **41**, 169–192 (2007).
21. Glover, T. W., Wilson, T. E. & Arlt, M. F. Fragile Sites in Cancer: More Than Meets the Eye. *Nat. Rev. Cancer* **17**, 489–501 (2017).
22. Smith, D. I., Zhu, Y., McAvoy, S. & Kuhn, R. Common fragile sites, extremely large genes, neural development and cancer. *Cancer Lett.* **232**, 48–57 (2006).
23. Gao, G. & Smith, D. I. Very large common fragile site genes and their potential role in cancer development. *Cell. Mol. Life Sci.* **71**, 4601–4615 (2014).
24. Wilson, T. E. *et al.* Large transcription units unify copy number variants and common fragile sites arising under replication stress. *Genome Res.* **25**, 189–200 (2015).
25. Le Beau, M. M. *et al.* Replication of a Common Fragile Site, FRA3B, Occurs Late in S Phase and is Delayed Further Upon Induction: Implications for the Mechanism of Fragile Site Induction. *Hum. Mol. Genet.* **7**, 755–761 (1998).
26. Burrow, A. A., Marullo, A., Holder, L. R. & Wang, Y.-H. Secondary structure formation and DNA instability at fragile site FRA16B. *Nucleic Acids Res.* **38**, 2865–2877 (2010).
27. Ozeri-Galai, E. *et al.* Failure of Origin Activation in Response to Fork Stalling Leads to Chromosomal Instability at Fragile Sites. *Mol. Cell* **43**, 122–131 (2011).
28. Sarni, D. & Kerem, B. Oncogene-Induced Replication Stress Drives Genome Instability and Tumorigenesis. *Int. J. Mol. Sci.* **18**, (2017).
29. Vesela, E., Chroma, K., Turi, Z. & Mistrik, M. Common Chemical Inductors of Replication Stress: Focus on Cell-Based Studies. *Biomolecules* **7**, 19 (2017).
30. Lopes, M., Foiani, M. & Sogo, J. M. Multiple Mechanisms Control Chromosome Integrity after Replication Fork Uncoupling and Restart at Irreparable UV Lesions. *Mol. Cell* **21**, 15–27 (2006).
31. Deans, A. J. & West, S. C. DNA interstrand crosslink repair and cancer. *Nat. Rev. Cancer* **11**, 467–480 (2011).
32. Schärer, O. D. DNA Interstrand Crosslinks: Natural and Drug-Induced DNA Adducts that Induce Unique Cellular Responses. *ChemBioChem* **6**, 27–32 (2005).
33. Wang, L. C. & Gautier, J. The Fanconi anemia pathway and ICL repair: implications for cancer therapy. *Crit. Rev. Biochem. Mol. Biol.* **45**, 424–439 (2010).

34. Beranek, D. T. Distribution of methyl and ethyl adducts following alkylation with monofunctional alkylating agents. *Mutat. Res. Mol. Mech. Mutagen.* **231**, 11–30 (1990).

35. Krakoff, I. H., Brown, N. C. & Reichard, P. Inhibition of Ribonucleoside Diphosphate Reductase by Hydroxyurea. *Cancer Res.* **28**, 1559–1565 (1968).

36. Koç, A., Wheeler, L. J., Mathews, C. K. & Merrill, G. F. Hydroxyurea Arrests DNA Replication by a Mechanism That Preserves Basal dNTP Pools. *J. Biol. Chem.* **279**, 223–230 (2004).

37. Hsiang, Y.-H., Lihou, M. G. & Liu, L. F. Arrest of Replication Forks by Drug-stabilized Topoisomerase I-DNA Cleavable Complexes as a Mechanism of Cell Killing by Camptothecin. *Cancer Res.* **49**, 5077–5082 (1989).

38. Deweese, J. E. & Osheroff, N. The DNA cleavage reaction of topoisomerase II: wolf in sheep's clothing. *Nucleic Acids Res.* **37**, 738–748 (2009).

39. Cheng, C. H. & Kuchta, R. D. DNA polymerase .epsilon.: Aphidicolin inhibition and the relationship between polymerase and exonuclease activity. *Biochemistry* **32**, 8568–8574 (1993).

40. Chang, D. J., Lupardus, P. J. & Cimprich, K. A. Monoubiquitination of Proliferating Cell Nuclear Antigen Induced by Stalled Replication Requires Uncoupling of DNA Polymerase and Mini-chromosome Maintenance Helicase Activities. *J. Biol. Chem.* **281**, 32081–32088 (2006).

41. Baranovskiy, A. G. *et al.* Structural basis for inhibition of DNA replication by aphidicolin. *Nucleic Acids Res.* **42**, 14013–14021 (2014).

42. Sirbu, B. M. & Cortez, D. DNA Damage Response: Three Levels of DNA Repair Regulation. *Cold Spring Harb. Perspect. Biol.* **5**, a012724 (2013).

43. Blackford, A. N. & Jackson, S. P. ATM, ATR, and DNA-PK: The Trinity at the Heart of the DNA Damage Response. *Mol. Cell* **66**, 801–817 (2017).

44. Shiloh, Y. & Ziv, Y. The ATM protein kinase: regulating the cellular response to genotoxic stress, and more. *Nat. Rev. Mol. Cell Biol.* **14**, 197–210 (2013).

45. Davis, A. J., Chen, B. P. C. & Chen, D. J. DNA-PK: a dynamic enzyme in a versatile DSB repair pathway. *DNA Repair* **17**, 21–29 (2014).

46. Flynn, R. L. & Zou, L. ATR: a master conductor of cellular responses to DNA replication stress. *Trends Biochem. Sci.* **36**, 133–140 (2011).

47. Zellweger, R. *et al.* Rad51-mediated replication fork reversal is a global response to genotoxic treatments in human cells. *J Cell Biol* **208**, 563–579 (2015).

48. Byun, T. S., Pacek, M., Yee, M., Walter, J. C. & Cimprich, K. A. Functional uncoupling of MCM helicase and DNA polymerase activities activates the ATR-dependent checkpoint. *Genes Dev.* **19**, 1040–1052 (2005).

49. Zou, L. & Elledge, S. J. Sensing DNA Damage Through ATRIP Recognition of RPA-ssDNA Complexes. *Science* **300**, 1542–1548 (2003).

50. Delacroix, S., Wagner, J. M., Kobayashi, M., Yamamoto, K. & Karnitz, L. M. The Rad9–Hus1–Rad1 (9–1–1) clamp activates checkpoint signaling via TopBP1. *Genes Dev.* **21**, 1472–1477 (2007).

51. Lee, J., Kumagai, A. & Dunphy, W. G. The Rad9-Hus1-Rad1 Checkpoint Clamp Regulates Interaction of TopBP1 with ATR. *J. Biol. Chem.* **282**, 28036–28044 (2007).

52. Ceccaldi, R., Sarangi, P. & D'Andrea, A. D. The Fanconi anaemia pathway: new players and new functions. *Nat. Rev. Mol. Cell Biol.* **17**, 337–349 (2016).

53. Thompson, L. H. & Hinz, J. M. Cellular and molecular consequences of defective Fanconi anemia proteins in replication-coupled DNA repair: mechanistic insights. *Mutat. Res.* **668**, 54–72 (2009).

54. Andreassen, P. R., D'Andrea, A. D. & Taniguchi, T. ATR couples FANCD2 monoubiquitination to the DNA-damage response. *Genes Dev.* **18**, 1958–1963 (2004).

55. Collins, N. B. *et al.* ATR-dependent phosphorylation of FANCA on serine 1449 after DNA damage is important for FA pathway function. *Blood* **113**, 2181–2190 (2009).

56. Castella, M. *et al.* FANCI Regulates Recruitment of the FA Core Complex at Sites of DNA Damage Independently of FANCD2. *PLoS Genet.* **11**, (2015).

57. Smogorzewska, A. *et al.* Identification of the Fanconi anemia (FANC) I protein, a monoubiquitinated FANCD2 paralog required for crosslink repair. *Cell* **129**, 289–301 (2007).

58. Hussain, S. *et al.* Direct interaction of FANCD2 with BRCA2 in DNA damage response pathways. *Hum. Mol. Genet.* **13**, 1241–1248 (2004).

59. Taniguchi, T. & D'Andrea, A. D. Molecular pathogenesis of Fanconi anemia: recent progress. *Blood* **107**, 4223–4233 (2006).

60. Wang, X., Andreassen, P. R. & D'Andrea, A. D. Functional Interaction of Monoubiquitinated FANCD2 and BRCA2/FANCD1 in Chromatin. *Mol. Cell. Biol.* **24**, 5850–5862 (2004).

61. Ghosal, G. & Chen, J. DNA damage tolerance: a double-edged sword guarding the genome. *Transl. Cancer Res.* **2**, 107–129 (2013).

62. Atkinson, J. & McGlynn, P. Replication fork reversal and the maintenance of genome stability. *Nucleic Acids Res.* **37**, 3475–3492 (2009).

63. Neelsen, K. J. & Lopes, M. Replication fork reversal in eukaryotes: from dead end to dynamic response. *Nat. Rev. Mol. Cell Biol.* **16**, 207–220 (2015).

64. Meng, X. & Zhao, X. Replication fork regression and its regulation. *FEMS Yeast Res.* **17**, (2017).

65. Gari, K., Décaillet, C., Delannoy, M., Wu, L. & Constantinou, A. Remodeling of DNA replication structures by the branch point translocase FANCM. *Proc. Natl. Acad. Sci.* **105**, 16107–16112 (2008).

66. Bétous, R. *et al.* SMARCAL1 catalyzes fork regression and Holliday junction migration to maintain genome stability during DNA replication. *Genes Dev.* **26**, 151–162 (2012).

67. Blastyák, A., Hajdú, I., Unk, I. & Haracska, L. Role of Double-Stranded DNA Translocase Activity of Human HLTF in Replication of Damaged DNA. *Mol. Cell. Biol.* **30**, 684–693 (2010).

68. Kile, A. C. *et al.* HLTF's Ancient HIRAN Domain Binds 3′ DNA Ends to Drive Replication Fork Reversal. *Mol. Cell* **58**, 1090–1100 (2015).

69. Fugger, K. *et al.* FBH1 Catalyzes Regression of Stalled Replication Forks. *Cell Rep.* **10**, 1749–1757 (2015).

70. Ciccia, A. *et al.* The ZRANB3 translocase associates with poly-ubiquitinated PCNA to promote fork restart and limit recombination after replication stress. *Mol. Cell* **47**, 396–409 (2012).

71. Machwe, A., Xiao, L., Groden, J. & Orren, D. K. The Werner and Bloom Syndrome Proteins Catalyze Regression of a Model Replication Fork. *Biochemistry* **45**, 13939–13946 (2006).

72. Bhat, K. P. & Cortez, D. RPA and RAD51: fork reversal, fork protection, and genome stability. *Nat. Struct. Mol. Biol.* **25**, 446 (2018).

73. Berti, M. *et al.* Human RECQ1 promotes restart of replication forks reversed by DNA topoisomerase I inhibition. *Nat. Struct. Mol. Biol.* **20**, 347–354 (2013).

74. Thangavel, S. *et al.* DNA2 drives processing and restart of reversed replication forks in human cells. *J Cell Biol* **208**, 545–562 (2015).

75. Petermann, E., Orta, M. L., Issaeva, N., Schultz, N. & Helleday, T. Hydroxyurea-Stalled Replication Forks Become Progressively Inactivated and Require Two Different RAD51-Mediated Pathways for Restart and Repair. *Mol. Cell* **37**, 492–502 (2010).

76. Pasero, P. & Vindigni, A. Nucleases Acting at Stalled Forks: How to Reboot the Replication Program with a Few Shortcuts. *Annu. Rev. Genet.* **51**, 477–499 (2017).

77. Chaudhury, I., Stroik, D. R. & Sobeck, A. FANCD2-Controlled Chromatin Access of the Fanconi-Associated Nuclease FAN1 Is Crucial for the Recovery of Stalled Replication Forks. *Mol. Cell. Biol.* **34**, 3939–3954 (2014).

78. Yeo, J. E., Lee, E. H., Hendrickson, E. A. & Sobeck, A. CtIP mediates replication fork recovery in a FANCD2-regulated manner. *Hum. Mol. Genet.* **23**, 3695–3705 (2014).

79. Bryant, H. E. *et al.* PARP is activated at stalled forks to mediate Mre11-dependent replication restart and recombination. *EMBO J.* **28**, 2601–2615 (2009).

80. Hashimoto, Y., Ray Chaudhuri, A., Lopes, M. & Costanzo, V. Rad51 protects nascent DNA from Mre11-dependent degradation and promotes continuous DNA synthesis. *Nat. Struct. Mol. Biol.* **17**, 1305–1311 (2010).

81. Costanzo, V. Brca2, Rad51 and Mre11: Performing balancing acts on replication forks. *DNA Repair* **10**, 1060–1065 (2011).

82. Cotta-Ramusino, C. *et al.* Exo1 Processes Stalled Replication Forks and Counteracts Fork Reversal in Checkpoint-Defective Cells. *Mol. Cell* **17**, 153–159 (2005).

83. Schlacher, K. *et al.* Double-Strand Break Repair-Independent Role for BRCA2 in Blocking Stalled Replication Fork Degradation by MRE11. *Cell* **145**, 529–542 (2011).

84. Schlacher, K., Wu, H. & Jasin, M. A Distinct Replication Fork Protection Pathway Connects Fanconi Anemia Tumor Suppressors to RAD51-BRCA1/2. *Cancer Cell* **22**, 106–116 (2012).

85. Ying, S., Hamdy, F. C. & Helleday, T. Mre11-Dependent Degradation of Stalled DNA Replication Forks Is Prevented by BRCA2 and PARP1. *Cancer Res.* **72**, 2814–2821 (2012).

86. Lemaçon, D. *et al.* MRE11 and EXO1 nucleases degrade reversed forks and elicit MUS81-dependent fork rescue in BRCA2-deficient cells. *Nat. Commun.* **8**, 860 (2017).

87. Hanada, K. *et al.* The structure-specific endonuclease Mus81 contributes to replication restart by generating double-strand DNA breaks. *Nat. Struct. Mol. Biol.* **14**, 1096–1104 (2007).

88. Symington, L. S. & Gautier, J. Double-Strand Break End Resection and Repair Pathway Choice. *Annu. Rev. Genet.* **45**, 247–271 (2011).

89. Mimitou, E. P. & Symington, L. S. Sae2, Exo1 and Sgs1 collaborate in DNA double-strand break processing. *Nature* **455**, (2008).

90. Zhu, Z., Chung, W.-H., Shim, E. Y., Lee, S. E. & Ira, G. Sgs1 helicase and two nucleases Dna2 and Exo1 resect DNA double strand break ends. *Cell* **134**, 981–994 (2008).

91. Gravel, S., Chapman, J. R., Magill, C. & Jackson, S. P. DNA helicases Sgs1 and BLM promote DNA double-strand break resection. *Genes Dev.* **22**, 2767–2772 (2008).

92. Garcia, V., Phelps, S. E. L., Gray, S. & Neale, M. J. Bidirectional resection of DNA double-strand breaks by Mre11 and Exo1. *Nature* **479**, 241–244 (2011).

93. San Filippo, J., Sung, P. & Klein, H. Mechanism of Eukaryotic Homologous Recombination. *Annu. Rev. Biochem.* **77**, 229–257 (2008).

94. Alderton, G. K. *et al.* Seckel syndrome exhibits cellular features demonstrating defects in the ATR-signalling pathway. *Hum. Mol. Genet.* **13**, 3127–3138 (2004).

95. Murga, M. *et al.* A mouse model of the ATR-Seckel Syndrome reveals that replicative stress during embryogenesis limits mammalian lifespan. *Nat. Genet.* **41**, 891–898 (2009).

96. Ogi, T. *et al.* Identification of the First ATRIP–Deficient Patient and Novel Mutations in ATR Define a Clinical Spectrum for ATR–ATRIP Seckel Syndrome. *PLoS Genet.* **8**, (2012).

97. Bachrati, C. Z. & Hickson, I. D. RecQ helicases: guardian angels of the DNA replication fork. *Chromosoma* **117**, 219–233 (2008).

98. Niraj, J., Färkkilä, A. & D'Andrea, A. D. The Fanconi Anemia Pathway in Cancer. *Annu. Rev. Cancer Biol.* **3**, null (2019).

99. Nalepa, G. & Clapp, D. W. Fanconi anaemia and cancer: an intricate relationship. *Nat. Rev. Cancer* **18**, 168–185 (2018).

100. Arlt, M. F., Wilson, T. E. & Glover, T. W. Replication stress and mechanisms of CNV formation. *Curr. Opin. Genet. Dev.* **22**, 204–210 (2012).

101. Zhang, F., Gu, W., Hurles, M. E. & Lupski, J. R. Copy Number Variation in Human Health, Disease, and Evolution. *Annu. Rev. Genomics Hum. Genet.* **10**, 451–481 (2009).

102. Stankiewicz, P. & Lupski, J. R. Structural Variation in the Human Genome and its Role in Disease. *Annu. Rev. Med.* **61**, 437–455 (2010).

103. Lee, J. A., Carvalho, C. M. B. & Lupski, J. R. A DNA Replication Mechanism for Generating Nonrecurrent Rearrangements Associated with Genomic Disorders. *Cell* **131**, 1235–1247 (2007).

104. Hastings, P. J., Ira, G. & Lupski, J. R. A Microhomology-Mediated Break-Induced Replication Model for the Origin of Human Copy Number Variation. *PLOS Genet.* **5**, e1000327 (2009).

105. Huebner, K., Hadaczek, P., Siprashvili, Z., Druck, T. & Croce, C. M. The FHIT gene, a multiple tumor suppressor gene encompassing the carcinogen sensitive chromosome fragile site, FRA3B. *Biochim. Biophys. Acta BBA - Rev. Cancer* **1332**, M65–M70 (1997).

106. Finnis, M. *et al.* Common chromosomal fragile site FRA16D mutation in cancer cells. *Hum. Mol. Genet.* **14**, 1341–1349 (2005).

107. Schrock, M. S. & Huebner, K. WWOX: A fragile tumor suppressor. *Exp. Biol. Med.* **240**, 296–304 (2015).

108. Karras, J. R., Schrock, M. S., Batar, B. & Huebner, K. Fragile Genes That Are Frequently Altered in Cancer: Players Not Passengers. *Cytogenet. Genome Res.* **150**, 208–216 (2016).

109. Wu, X., Wu, G., Yao, X., Hou, G. & Jiang, F. The clinicopathological significance and ethnic difference of FHIT hypermethylation in non-small-cell lung carcinoma: a meta-analysis and literature review. *Drug Des. Devel. Ther.* **10**, 699–709 (2016).

110. Branzei, D. & Foiani, M. Regulation of DNA repair throughout the cell cycle. *Nat. Rev. Mol. Cell Biol.* **9**, 297–308 (2008).

111. Hustedt, N. & Durocher, D. The control of DNA repair by the cell cycle. *Nat. Cell Biol.* **19**, 1–9 (2017).

112. Haber, J. E. Partners and pathways: repairing a double-strand break. *Trends Genet.* **16**, 259–264 (2000).

113. Ferretti, L. P., Lafranchi, L. & Sartori, A. A. Controlling DNA-end resection: a new task for CDKs. *Front. Genet.* **4**, (2013).

114. Huertas, P. & Jackson, S. P. Human CtIP Mediates Cell Cycle Control of DNA End Resection and Double Strand Break Repair. *J. Biol. Chem.* **284**, 9558–9565 (2009).

115. Tomimatsu, N. *et al.* Phosphorylation of EXO1 by CDKs 1 and 2 regulates DNA end resection and repair pathway choice. *Nat. Commun.* **5**, 3561 (2014).

116. Chen, X. *et al.* Cell cycle regulation of DNA double-strand break end resection by Cdk1-dependent Dna2 phosphorylation. *Nat. Struct. Mol. Biol.* **18**, 1015–1019 (2011).

117. Zimmermann, M., Lottersberger, F., Buonomo, S. B., Sfeir, A. & de Lange, T. 53BP1 regulates DSB repair using Rif1 to control 5' end resection. *Science* **339**, 700–704 (2013).

118. Escribano-Díaz, C. *et al.* A Cell Cycle-Dependent Regulatory Circuit Composed of 53BP1-RIF1 and BRCA1-CtIP Controls DNA Repair Pathway Choice. *Mol. Cell* **49**, 872–883 (2013).

119. Callen, E. *et al.* 53BP1 mediates productive and mutagenic DNA repair through distinct phosphoprotein interactions. *Cell* **153**, 1266–1280 (2013).

120. Wyatt, H. D. M., Sarbajna, S., Matos, J. & West, S. C. Coordinated Actions of SLX1-SLX4 and MUS81-EME1 for Holliday Junction Resolution in Human Cells. *Mol. Cell* **52**, 234–247 (2013).

121. Ying, S. *et al.* MUS81 promotes common fragile site expression. *Nat. Cell Biol.* **15**, 1001–1007 (2013).

122. Naim, V., Wilhelm, T., Debatisse, M. & Rosselli, F. ERCC1 and MUS81–EME1 promote sister chromatid separation by processing late replication intermediates at common fragile sites during mitosis. *Nat. Cell Biol.* **15**, 1008–1015 (2013).

123. Minocherhomji, S. *et al.* Replication stress activates DNA repair synthesis in mitosis. *Nature* **528**, 286–290 (2015).

124. Bhowmick, R., Minocherhomji, S. & Hickson, I. D. RAD52 Facilitates Mitotic DNA Synthesis Following Replication Stress. *Mol. Cell* **64**, 1117–1126 (2016).

125. Chan, K. L. & Hickson, I. D. On the origins of ultra-fine anaphase bridges. *Cell Cycle* **8**, 3065–3066 (2009).

126. Chan, K.-L., North, P. S. & Hickson, I. D. BLM is required for faithful chromosome segregation and its localization defines a class of ultrafine anaphase bridges. *EMBO J.* **26**, 3397–3409 (2007).

127. Naim, V. & Rosselli, F. The FANC pathway and BLM collaborate during mitosis to prevent micro-nucleation and chromosome abnormalities. *Nat. Cell Biol.* **11**, 761–768 (2009).

128. Rieder, C. L. & Cole, R. W. Entry into Mitosis in Vertebrate Somatic Cells Is Guarded by a Chromosome Damage Checkpoint That Reverses the Cell Cycle When Triggered during Early but Not Late Prophase. *J. Cell Biol.* **142**, 1013–1022 (1998).

129. Giunta, S., Belotserkovskaya, R. & Jackson, S. P. DNA damage signaling in response to double-strand breaks during mitosis. *J. Cell Biol.* **190**, 197–207 (2010).

130. Orthwein, A. *et al.* Mitosis Inhibits DNA Double-Strand Break Repair to Guard Against Telomere Fusions. *Science* **344**, 189–193 (2014).

131. Lee, D.-H. *et al.* Dephosphorylation enables the recruitment of 53BP1 to double-strand DNA breaks. *Mol. Cell* **54**, 512–525 (2014).

132. Benada, J., Burdová, K., Lidak, T., von Morgen, P. & Macurek, L. Polo-like kinase 1 inhibits DNA damage response during mitosis. *Cell Cycle* **14**, 219–231 (2015).

133. Davies, S. L., North, P. S., Dart, A., Lakin, N. D. & Hickson, I. D. Phosphorylation of the Bloom's Syndrome Helicase and Its Role in Recovery from S-Phase Arrest. *Mol. Cell. Biol.* **24**, 1279–1291 (2004).

134. Leng, M. *et al.* MPS1-dependent mitotic BLM phosphorylation is important for chromosome stability. *Proc. Natl. Acad. Sci.* **103**, 11485–11490 (2006).

135. Hershko, A. & Ciechanover, A. The Ubiquitin System. *Annu. Rev. Biochem.* **67**, 425–479 (1998).

136. Sun, L. & Chen, Z. J. The novel functions of ubiquitination in signaling. *Curr. Opin. Cell Biol.* **16**, 119–126 (2004).

137. Yates, M. & Maréchal, A. Ubiquitylation at the Fork: Making and Breaking Chains to Complete DNA Replication. *Int. J. Mol. Sci.* **19**, 2909 (2018).

138. Wang, J., Chen, J. & Gong, Z. TopBP1 Controls BLM Protein Level to Maintain Genome Stability. *Mol. Cell* **52**, (2013).

139. Kharat, S. S. *et al.* Mitotic phosphorylation of Bloom helicase at Thr182 is required for its proteasomal degradation and maintenance of chromosomal stability. *Oncogene* **35**, 1025–1038 (2016).

140. Kee, Y., Kim, J. M. & D'Andrea, A. Regulated degradation of FANCM in the Fanconi anemia pathway during mitosis. *Genes Dev.* **23**, 555–560 (2009).

141. Gali, H. *et al.* Role of SUMO modification of human PCNA at stalled replication fork. *Nucleic Acids Res.* **40**, 6049–6059 (2012).

142. Ouyang, K. J., Yagle, M. K., Matunis, M. J. & Ellis, N. A. BLM SUMOylation regulates ssDNA accumulation at stalled replication forks. *Front. Genet.* **4**, (2013).

143. Murcia, J. M. de *et al.* Requirement of poly(ADP-ribose) polymerase in recovery from DNA damage in mice and in cells. *Proc. Natl. Acad. Sci.* **94**, 7303–7307 (1997).

144. Haince, J.-F. *et al.* PARP1-dependent Kinetics of Recruitment of MRE11 and NBS1 Proteins to Multiple DNA Damage Sites. *J. Biol. Chem.* **283**, 1197–1208 (2008).

145. Aguilar-Quesada, R. *et al.* Interaction between ATM and PARP-1 in response to DNA damage and sensitization of ATM deficient cells through PARP inhibition. *BMC Mol. Biol.* **8**, 29 (2007).

146. Haince, J.-F. *et al.* Ataxia Telangiectasia Mutated (ATM) Signaling Network Is Modulated by a Novel Poly(ADP-ribose)-dependent Pathway in the Early Response to DNA-damaging Agents. *J. Biol. Chem.* **282**, 16441–16453 (2007).

147. Henriques, J. A. P. & Moustacchi, E. Isolation and Characterization of pso Mutants Sensitive to Photo-Addition of Psoralen Derivatives in SACCHAROMYCES CEREVISIAE. *Genetics* **95**, 273–288 (1980).

148. Ruhland, A., Kircher, M., Wilborn, F. & Brendel, M. A yeast mutant specifically sensitive to bifunctional alkylation. *Mutat. Res. Lett.* **91**, 457–462 (1981).

149. Demuth, I. & Digweed, M. Genomic organization of a potential human DNA-crosslink repair gene, KIAA0086. *Mutat. Res. Repair* **409**, 11–16 (1998).

150. Aravind, L., Walker, D. R. & Koonin, E. V. Conserved domains in DNA repair proteins and evolution of repair systems. *Nucleic Acids Res.* **27**, 1223–1242 (1999).

151. Dronkert, M. L. G. *et al.* Disruption of Mouse SNM1 Causes Increased Sensitivity to the DNA Interstrand Cross-Linking Agent Mitomycin C. *Mol. Cell. Biol.* **20**, 4553–4561 (2000).

152. Jenny, A., Minvielle-Sebastia, L., Preker, P. J. & Keller, W. Sequence Similarity Between the 73-Kilodalton Protein of Mammalian CPSF and a Subunit of Yeast Polyadenylation Factor I. *Science* **274**, 1514–1517 (1996).

153. Takaku, H., Minagawa, A., Takagi, M. & Nashimoto, M. A candidate prostate cancer susceptibility gene encodes tRNA 3′ processing endoribonuclease. *Nucleic Acids Res.* **31**, 2272–2278 (2003).

154. Callebaut, I., Moshous, D., Mornon, J.-P. & de Villartay, J.-P. Metallo-β-lactamase fold within nucleic acids processing enzymes: the β-CASP family. *Nucleic Acids Res.* **30**, 3592–3601 (2002).

155. Cattell, E., Sengerová, B. & McHugh, P. J. The SNM1/Pso2 family of ICL repair nucleases: From yeast to man. *Environ. Mol. Mutagen.* **51**, 635–645 (2010).

156. Pannicke, U. *et al.* Functional and biochemical dissection of the structure-specific nuclease ARTEMIS. *EMBO J.* **23**, 1987–1997 (2004).

157. Lam, Y. C. *et al.* SNMIB/Apollo protects leading-strand telomeres against NHEJ-mediated repair. *EMBO J.* **29**, 2230–2241 (2010).

158. Ye, J. *et al.* TRF2 and Apollo Cooperate with Topoisomerase 2α to Protect Human Telomeres from Replicative Damage. *Cell* **142**, 230–242 (2010).

159. Sengerová, B. *et al.* Characterization of the Human SNM1A and SNM1B/Apollo DNA Repair Exonucleases. *J. Biol. Chem.* **287**, 26254–26267 (2012).

160. Hejna, J., Philip, S., Ott, J., Faulkner, C. & Moses, R. The hSNM1 protein is a DNA 5′-exonuclease. *Nucleic Acids Res.* **35**, 6115–6123 (2007).

161. Lenain, C. *et al.* The Apollo 5′ Exonuclease Functions Together with TRF2 to Protect Telomeres from DNA Repair. *Curr. Biol.* **16**, 1303–1310 (2006).

162. Wang, A. T. *et al.* Human SNM1A and XPF–ERCC1 collaborate to initiate DNA interstrand cross-link repair. *Genes Dev.* **25**, 1859–1870 (2011).

163. Buzon, B., Grainger, R., Huang, S., Rzadki, C. & Junop, M. S. Structure-specific endonuclease activity of SNM1A enables processing of a DNA interstrand crosslink. *Nucleic Acids Res.* **46**, 9057–9066 (2018).

164. Ma, Y., Pannicke, U., Schwarz, K. & Lieber, M. R. Hairpin Opening and Overhang Processing by an Artemis/DNA-Dependent Protein Kinase Complex in Nonhomologous End Joining and V(D)J Recombination. *Cell* **108**, 781–794 (2002).

165. Goodarzi, A. A. *et al.* DNA-PK autophosphorylation facilitates Artemis endonuclease activity. *EMBO J.* **25**, 3880–3889 (2006).

166. Ma, Y. *et al.* The DNA-dependent Protein Kinase Catalytic Subunit Phosphorylation Sites in Human Artemis. *J. Biol. Chem.* **280**, 33839–33846 (2005).

167. Niewolik, D., Peter, I., Butscher, C. & Schwarz, K. Autoinhibition of the Nuclease ARTEMIS Is Mediated by a Physical Interaction between Its Catalytic and C-terminal Domains. *J. Biol. Chem.* **292**, 3351–3365 (2017).

168. Demuth, I., Digweed, M. & Concannon, P. Human SNM1B is required for normal cellular response to both DNA interstrand crosslink-inducing agents and ionizing radiation. *Oncogene* **23**, 8611–8618 (2004).

169. Ishiai, M. *et al.* DNA Cross-Link Repair Protein SNM1A Interacts with PIAS1 in Nuclear Focus Formation. *Mol. Cell. Biol.* **24**, 10733–10741 (2004).

170. Bae, J.-B. *et al.* Snm1B/Apollo mediates replication fork collapse and S Phase checkpoint activation in response to DNA interstrand cross-links. *Oncogene* **27**, 5045–5056 (2008).

171. Mason, J. M. & Sekiguchi, J. M. Snm1B/Apollo functions in the Fanconi anemia pathway in response to DNA interstrand crosslinks. *Hum. Mol. Genet.* **20**, 2549–2559 (2011).

172. Salewsky, B., Schmiester, M., Schindler, D., Digweed, M. & Demuth, I. The nuclease hSNM1B/Apollo is linked to the Fanconi anemia pathway via its interaction with FANCP/SLX4. *Hum. Mol. Genet.* **21**, 4948–4956 (2012).

173. Mason, J. M. *et al.* The SNM1B/APOLLO DNA nuclease functions in resolution of replication stress and maintenance of common fragile site stability. *Hum. Mol. Genet.* **22**, 4901–4913 (2013).

174. Liu, L. *et al.* SNM1B/Apollo interacts with Astrin and is required for the prophase cell cycle checkpoint. *Cell Cycle* **8**, 628–638 (2009).

175. Akhter, S. *et al.* Deficiency in SNM1 Abolishes an Early Mitotic Checkpoint Induced by Spindle Stress. *Mol. Cell. Biol.* **24**, 10448–10455 (2004).

176. de Lange, T. T-loops and the origin of telomeres. *Nat. Rev. Mol. Cell Biol.* **5**, 323–329 (2004).

177. Lange, T. de. Shelterin: the protein complex that shapes and safeguards human telomeres. *Genes Dev.* **19**, 2100–2110 (2005).

178. Palm, W. & de Lange, T. How Shelterin Protects Mammalian Telomeres. *Annu. Rev. Genet.* **42**, 301–334 (2008).

179. van Overbeek, M. & de Lange, T. Apollo, an Artemis-Related Nuclease, Interacts with TRF2 and Protects Human Telomeres in S Phase. *Curr. Biol.* **16**, 1295–1302 (2006).

180. Freibaum, B. D. & Counter, C. M. hSnm1B Is a Novel Telomere-associated Protein. *J. Biol. Chem.* **281**, 15033–15036 (2006).

181. Demuth, I. *et al.* Endogenous hSNM1B/Apollo interacts with TRF2 and stimulates ATM in response to ionizing radiation. *DNA Repair* **7**, 1192–1201 (2008).

182. A Shared Docking Motif in TRF1 and TRF2 Used for Differential Recruitment of Telomeric Proteins | Science. Available at: http://science.sciencemag.org/content/319/5866/1092.long. (Accessed: 22nd November 2018)

183. Wu, P., van Overbeek, M., Rooney, S. & de Lange, T. Apollo Contributes to G Overhang Maintenance and Protects Leading-End Telomeres. *Mol. Cell* **39**, 606–617 (2010).

184. Wu, P., Takai, H. & de Lange, T. Telomeric 3′ Overhangs Derive from Resection by Exo1 and Apollo and Fill-In by POT1b-Associated CST. *Cell* **150**, 39–52 (2012).

185. Schmiester, M., Demuth, I., Schmiester, M. & Demuth, I. SNM1B/Apollo in the DNA damage response and telomere maintenance. *Oncotarget* **8**, 48398–48409 (2017).

186. Stringer, J. R. & Counter, C. M. Snm1B Interacts with PSF2. *PLOS ONE* **7**, e49626 (2012).

187. Tumini, E., Plevani, P., Muzi-Falconi, M. & Marini, F. Physical and functional crosstalk between Fanconi anemia core components and the GINS replication complex. *DNA Repair* **10**, 149–158 (2011).

188. Anders, M., Mattow, J., Digweed, M. & Demuth, I. Evidence for hSNM1B/Apollo functioning in the HSP70 mediated DNA damage response. *Cell Cycle* **8**, 1725–1732 (2009).

189. Touzot, F. *et al.* Function of Apollo (SNM1B) at telomere highlighted by a splice variant identified in a patient with Hoyeraal–Hreidarsson syndrome. *Proc. Natl. Acad. Sci.* **107**, 10097–10102 (2010).

190. Nykamp, K. *et al.* Sherloc: a comprehensive refinement of the ACMG–AMP variant classification criteria. *Genet. Med.* **19**, 1105–1117 (2017).

191. Liang, X. *et al.* Genetic variants in DNA repair genes and the risk of cutaneous malignant melanoma in melanoma-prone families with/without CDKN2A mutations. *Int. J. Cancer J. Int. Cancer* **130**, 2062–2066 (2012).

192. Karami, S. *et al.* Telomere structure and maintenance gene variants and risk of five cancer types. *Int. J. Cancer* **139**, 2655–2670 (2016).

193. Michailidou, K. *et al.* Large-scale genotyping identifies 41 new loci associated with breast cancer risk. *Nat. Genet.* **45**, 353-361e2 (2013).

194. Caswell, J. L. *et al.* Multiple breast cancer risk variants are associated with differential transcript isoform expression in tumors. *Hum. Mol. Genet.* **24**, 7421–7431 (2015).

195. Guo, X. *et al.* A Comprehensive cis-eQTL Analysis Revealed Target Genes in Breast Cancer Susceptibility Loci Identified in Genome-wide Association Studies. *Am. J. Hum. Genet.* **102**, 890–903 (2018).

196. Herwest, S. *et al.* The hSNM1B/Apollo variant rs11552449 is associated with cellular sensitivity towards mitomycin C and ionizing radiation. *DNA Repair* **72**, 93–98 (2018).

197. Akhter, S., Lam, Y. C., Chang, S. & Legerski, R. J. The telomeric protein SNM1B/Apollo is required for normal cell proliferation and embryonic development. *Aging Cell* **9**, 1047–1056 (2010).

198. Petermann, E. & Helleday, T. Pathways of mammalian replication fork restart. *Nat. Rev. Mol. Cell Biol.* **11**, 683–687 (2010).

199. Arnoult, N. & Karlseder, J. Complex interactions between the DNA-damage response and mammalian telomeres. *Nat. Struct. Mol. Biol.* **22**, 859–866 (2015).

Chapter 2

SNM1B is Required for the Repair of Collapsed Replication Forks

Abstract

The efficient resolution of stalled replication forks ensures proper duplication of the genome. Defects in this repair process can result in under-replicated DNA and chromosomal aberrations. The DNA nuclease, SNM1B, has been previously described to function in the repair of stalled and blocked forks to prevent genomic instability. Herein, we expand on the current knowledge of the roles of SNM1B during DNA replication. We demonstrate that SNM1B becomes stabilized in response to agents that induce fork stalling and localizes independently to sites of replication stress after early-response proteins. SNM1B facilitates the stabilization and restart of stalled replication forks by preventing the accumulation of single-stranded DNA intermediates and double-strand breaks (DSBs). Using a chromosomally integrated substrate that models site-specific replication fork arrest by the *E. coli* Tus/*Ter* termination complex, we show that SNM1B is required for the recombination-mediated repair of collapsed forks. Overall, our findings reveal critical functions for SNM1B in accurately processing DNA intermediates during replication stress and in promoting recombinational repair of DSBs that result from prolonged fork arrest.

Jordann Smak designed and performed the experiments shown in Figures 2.1; 2.2C; 2.5; 2.S1; 2.S2; 2.S3
Ishita Das designed and performed the experiments shown in Figures 2.2A,B; 2.3; 2.4

Introduction

The faithful replication of chromosomes is essential for the maintenance of genome stability. However, the progressing DNA replication fork can often encounter impediments, such as unrepaired lesions, secondary DNA structures, or protein-DNA complexes, causing it to stall [1]. If these stalled forks are not properly stabilized or restarted, they can collapse and form DNA double-strand breaks (DSBs), which are then repaired through homologous recombination (HR). Defects in this process can result in detrimental chromosomal breaks, deletions, or aberrant rearrangements associated with human disease and cancer [2–4].

The resolution of stalled replication forks requires the accurate processing of DNA intermediate structures, which is achieved through the coordinated actions of DNA nucleases [5,6]. When a replication fork stalls, it can undergo regression or reversal to generate a "chicken foot" structure. This involves reannealing of the parental DNA strands and annealing of the complementary nascent leading- and lagging-strands [7–9]. One proposed mechanism to resolve this structure and mediate fork restart is through nucleolytic degradation of the annealed nascent DNA. MRE11, a member of the MRE11/RAD50/NBS1 (MRN) complex, is both an endonuclease and 3' to 5' exonuclease that has been implicated in this nucleolytic digestion at regressed forks [10,11]. DNA2, EXO1, and FAN1 are all 5' to 3' exonucleases that have also been described to aid in this process [12–15]. Although nucleolytic resection at regressed forks can mediate fork restart, this process must be tightly regulated to prevent hyper-degradation and deleterious effects [10,11,16,17].

If a stalled replication fork cannot be effectively restarted, it can collapse and generate DSBs. The endonuclease, MUS81, has been implicated in the formation of the DSB intermediate, which is then repaired via HR using the homologous sequence as a template [18,19]. Additional nucleases participate in the HR repair process by resecting the broken DNA ends to allow for strand invasion and subsequent DNA synthesis. The initial limited 5' DNA end resection is catalyzed by the nucleases, MRE11 and CtIP, whereas the processive long-range resection is attributed to the nuclease activities of EXO1 or DNA2, the latter in conjunction with the DNA helicases BLM or WRN [20–25]. Once HR-mediated repair is complete, the replication fork can resume progression. But

if the DSBs persist, the fork remains unrepaired, potentially resulting in detrimental chromosomal aberrations. This highlights the importance of nucleases in processing DNA intermediate structures, but the precise coordination between these enzymes during the resolution of stalled replication forks is not well defined.

The SNM1B DNA nuclease also functions during the resolution of stalled replication forks. SNM1B possesses 5' to 3' exonuclease activity and has known roles in processing DNA intermediates during interstrand crosslink (ICL) repair [26,27]. It is also implicated in DNA end resection at leading-strand telomeres to produce the 3' overhangs for T-loop formation [28–30]. We previously found that SNM1B depletion results in hypersensitivity to the DNA polymerase inhibitor, aphidicolin (Aph). These SNM1B-deficient cells display elevated levels of spontaneous and aphidicolin-induced chromosomal gaps and breaks, including breaks at common fragile sites (CFSs) [31]. CFSs are particularly susceptible to breakage, as they reside in large, actively transcribed genes that are difficult to replicate [32]. Collisions between the replication and transcription machinery can contribute to the instability of these loci during DNA replication. Additionally, we have previously shown that SNM1B localizes to sites of replication stress and is required for efficient recruitment of key DNA repair proteins, including FANCD2 and BRCA1, to stalled forks [27,31]. Studies have revealed that SNM1B physically interacts with FANCD2 and the nuclease, MRE11, which both function in HR [33]. However, the mechanisms underlying the regulation of SNM1B in DNA repair processes and the importance of its nucleolytic functions at stalled forks is not well understood. In this study, we demonstrate that SNM1B is required for the efficient restart of stalled replication forks and that it is involved in the late-stage processing events of HR-mediated repair of DSBs upon fork collapse.

Results

SNM1B accumulates in S-phase cells synchronized by a double thymidine block

DNA repair processes are highly complex and need to be tightly controlled to prevent genome instability. Some DNA repair proteins have multiple roles within different pathways of repair, and therefore need to be precisely regulated to perform the

appropriate functions. One form of regulation is through changes in protein expression or stability. For example, the DNA helicase, BLM, has been shown to be regulated by the cell cycle, with protein levels increasing in S- and G2-phases and decreasing in G1-phase [34]. It is also stabilized in cells after exposure to agents that induce replication stress [34]. The DNA endonuclease, CtIP, is also regulated in a similar cell cycle-specific manner [35]. Therefore, this form of protein regulation could ensure that BLM, CtIP, and potentially other DNA repair proteins are only present and active during the phases in which they are required to function.

Since SNM1B can process DNA intermediates that arise during DNA replication in S-phase, we hypothesized that SNM1B may be cell cycle regulated, similar to BLM and CtIP. Because levels of endogenous SNM1B expression are too low to detect via Western blot, we generated HCT116 cell lines stably expressing an siRNA-resistant, V5-tagged SNM1B cDNA or an empty vector (EV) as a control (Figure 2.S1). Cells expressing wildtype (WT) SNM1B were synchronized in early S-phase by a double thymidine block and released into fresh media for 0, 2, 4, or 6 hours. Cells were harvested at each timepoint and SNM1B protein levels were assessed by immunoblotting. At the time of release, when 45% of cells were in S-phase, SNM1B protein levels were approximately 2-fold higher than in the asynchronous population. After 6 hours, the levels of SNM1B decreased by ~25%, when only 17% of cells remained in S-phase (Figure 2.1A). These results suggest that SNM1B is stabilized in S-phase and that protein levels are reduced as cells progress into G2-phase.

SNM1B protein levels are not altered throughout the cell cycle in unperturbed cells

The double thymidine block is a useful tool for cell synchronization, however, a caveat of this method is that it can induce replication stress through an imbalance of dNTP pools [37–40]. Thus, one potential explanation for the changes in protein levels observed in Figure 2.1A is that SNM1B may be stabilized in response to replication stress induced by the double thymidine block. The levels of SNM1B are then reduced as cells recover from the stress. To address this possibility, we examined SNM1B protein levels in unperturbed cells to see if SNM1B is regulated by the cell cycle. HCT116 cells stably expressing V5-tagged SNM1B were sorted based on their DNA

content using Hoechst staining and flow cytometry. Cyclin A and B1 protein levels were used as controls to assess proper cell sorting. SNM1B protein levels were similar across G1-, S-, and G2/M-phases (Figure 2.1B). These data reveal that the SNM1B protein is not regulated by the cell cycle and that the increase in SNM1B levels after the double thymidine block is most likely due to stabilization in response to replication stress.

SNM1B localizes to stalled forks after the recruitment of DNA repair proteins that function during early repair events

The finding that SNM1B is stabilized in S-phase supports the existing data that SNM1B is involved in the response to stalled replication forks [36]. SNM1B can localize to sites of replication stress and is highly associated with chromatin after treatment with the DNA polymerase inhibitor, aphidicolin (Figure 2.S2) [31]. However, the order of events that occur at these sites or the interplay between the proteins involved is not fully understood.

SNM1B has been previously shown to be dispensable for the early ATR-dependent signaling events in response to aphidicolin-induced stalled forks [31]. It is also not required for the proper localization of RPA and MRE11, which are DNA repair proteins that are involved in the initial response to replication stress. However, there is evidence that SNM1B is necessary for the efficient localization of the downstream factors, FANCD2 and BRCA1, which are both important for recombination events during fork repair [31]. To gain a better understanding of the involvement of SNM1B in early or late repair events, the timing of SNM1B foci formation relative to other DNA repair proteins was analyzed. HCT116 cells stably expressing V5-tagged SNM1B were treated with aphidicolin over a timecourse of 1 to 24 hours, and foci formation of RPA, MRE11, FANCD2, and SNM1B was assessed. Approximately 40% of cells formed RPA and MRE11 foci after 1 hour of aphidicolin treatment, and this level persisted throughout the timecourse. In comparison, only ~15% of cells formed SNM1B foci after 1 hour, and there was a slower accumulation of foci-positive cells over time. Cells did not form FANCD2 foci until approximately 6 hours after aphidicolin treatment, and both SNM1B and FANCD2 foci-positive cells reached a maximum of ~35% after 24 hours (Figure

2.2A,B). These data provide evidence that SNM1B localizes to stalled forks after the early-response proteins, RPA and MRE11, but before FANCD2, which functions downstream within the pathway.

SNM1B recruitment to stalled forks is independent of MRE11 exonuclease activity

Previous studies have reported that the nuclease activity of MRE11 promotes recruitment of BRCA1, FANCD2, and CtIP to aphidicolin-induced stalled forks [41]. SNM1B is also involved in the localization of BRCA1 and FANCD2 and has been shown to physically interact with MRE11 [31,33]. Since we observed that SNM1B forms foci after MRE11, we asked whether MRE11 nuclease activity is also required for recruitment of SNM1B to chromatin after aphidicolin treatment. HCT116 cells stably expressing V5-tagged SNM1B were pre-treated with the MRE11 exonuclease inhibitor, mirin, and then exposed to aphidicolin for 6 or 24 hours. Cellular fractionations were performed to assess the levels of FANCD2, CtIP, and SNM1B in the chromatin fractions. After both 6 and 24 hours of aphidicolin exposure, the levels of CtIP and monoubiquitinated FANCD2 were reduced in the mirin-treated samples compared to the DMSO-treated controls. In contrast, no change in SNM1B chromatin association was observed after mirin treatment (Figures 2.2C; 2.S3). These findings indicate that MRE11 exonuclease activity is dispensable for SNM1B localization to stalled replication forks, but is required for proper recruitment of FANCD2 and CtIP, as previously described [41].

SNM1B suppresses the accumulation of ssDNA at spontaneous and aphidicolin-induced stalled forks

Although RPA localizes to stalled replication forks prior to SNM1B, previous studies revealed that SNM1B depletion leads to an increase in RPA foci formation after aphidicolin treatment [31]. Since RPA binds to ssDNA, these findings suggest that SNM1B knockdown may affect the overall levels of ssDNA in cells exposed to replication stress. To assess the levels of ssDNA, control and SNM1B-depleted cells were labeled with the thymidine analogue, 5-bromo-2'-deoxyuridine (BrdU), for 24 hours to ensure incorporation into both the parental and nascent genomic DNA. Cells were

treated with aphidicolin for 24 hours and fixed using non-denaturing conditions. Staining with an anti-BrdU antibody would therefore detect labeled DNA that becomes single-stranded and exposed. Using immunofluorescence microscopy, BrdU staining was detected and quantitated as the overall fluorescence intensity within each nucleus (Figure 2.3A,B). We observed that a subset of cells had higher levels of detectable ssDNA, therefore the average percentage of cells with high intensity BrdU staining was also calculated (Figure 2.3C). The percentage of cells with high BrdU fluorescence was significantly increased after SNM1B depletion compared to non-silencing (NS) controls. In untreated and aphidicolin-treated cells, this increase was approximately 4-fold and 2-fold, respectively ($p<0.05$; Figure 2.3C). These findings indicate that SNM1B is important for preventing extensive generation of ssDNA at both spontaneous and aphidicolin-induced stalled forks.

SNM1B facilitates the restart of stalled replication forks

If stalled forks are aberrantly processed, then replication cannot restart and proceed in a timely manner. The accumulation of ssDNA in SNM1B-depleted cells suggests that replication intermediates may be unstable and hyper-resected. Several DNA repair factors have been implicated in protecting forks from excessive nucleolytic degradation, thereby promoting efficient recovery and restart [41,42,11]. To determine if SNM1B facilitates replication fork stability and restart, we utilized the established DNA fiber assay. In this assay, progressing replication forks can be sequentially labeled using incorporation of thymidine analogs, specifically iodo-deoxyuridine (IdU) and chloro-deoxyuridine (CldU). The resulting DNA tracts can then be visualized by fluorescent microscopy after immunostaining of each analog. DNA fibers that are able to incorporate both analogs are considered “ongoing” forks (red to green), whereas tracts that only incorporate IdU are described as “stalled or terminated” forks (red only). Alternatively, “new” replication forks are represented by DNA tracts that only incorporate CldU (green only) (Figure 2.3D).

In unperturbed conditions, SNM1B-depleted cells displayed an approximately 4-fold increase in stalled replication forks and a 1.3-fold decrease in ongoing forks compared to the NS controls ($p<0.001$; Figure 2.3E). The percentage of newly initiated

replication forks remained unchanged between the SNM1B-depleted cells and the controls (Figure 2.3E). These findings demonstrate that SNM1B is required for the recovery and restart of spontaneously stalled forks and that it is dispensable for initiating new origin firing.

SNM1B prevents the accumulation of DSBs at stalled forks and promotes RAD51 filament formation

DSBs are often formed as DNA intermediates in the processing of stalled or collapsed replication forks. The histone variant, H2AX, is phosphorylated by both ATM and ATR in response to DSBs and stalled replication forks [43,44]. Although phosphorylated H2AX (γH2AX) is generally considered a maker for DSBs, studies have shown that γH2AX is present at stalled forks well before DSB formation [45]. Previous findings from our lab revealed that aphidicolin induces γH2AX foci formation, but that SNM1B is dispensable for this process [31]. However, since γH2AX is present at early stages of fork stalling, we asked whether these forks are processed into DSBs by examining the colocalization of γH2AX and 53BP1, an important regulator in the response to DSBs. In both untreated and aphidicolin-treated cells, the percentage of γH2AX and 53BP1 colocalization was increased approximately 2-fold upon SNM1B-depletion compared to the controls ($p<0.05$, $p<0.001$; Figure 2.4A). This suggests that SNM1B is important for preventing an accumulation of DSBs at stalled replication forks.

The DSBs that result from replication fork collapse are repaired through HR, which involves the recruitment and coordination of FANCD2, BRCA1/2, and RAD51, among others. In response to both ICLs and aphidicolin-induced stress, SNM1B is required for proper localization of FANCD2 and BRCA1 [27,31]. SNM1B also promotes RAD51 filament formation after ICL damage [30]. Therefore, SNM1B may be involved in the downstream processing of DSBs at replication forks. To examine this further, we assessed the impact of SNM1B depletion on RAD51 foci formation upon exposure to aphidicolin. After 24 hours of aphidicolin treatment, the SNM1B-deficient cells showed a significant 2.5-fold decrease in RAD51 foci formation compared to the controls ($p<0.05$; Figure 2.4B). This finding provides further evidence for a role of SNM1B in DSB repair at stalled forks by promoting RAD51 filament formation at these sites.

HR-mediated repair at Tus/Ter-stalled forks

The precise molecular events that occur during HR at a collapsed replication fork remain to be fully elucidated. The use of DNA damaging agents to induce replication stress have been informative in understanding this process, but they can often cause multiple types of lesions at various sites throughout the genome, making some findings difficult to interpret. For example, ionizing radiation (IR) is mostly used to study the response to DSBs, but it can also induce single-strand breaks and base damage. Additionally, cisplatin can generate a myriad of DNA adducts, such as DNA intra- and interstrand crosslinks, monoadducts, and DNA-protein crosslinks [46]. Therefore, assays have been developed to provide a more detailed and controlled analysis of events that occur at a single perturbed replication fork within a specific location of the genome. One such method utilizes the *Escherichia coli* Tus/*Ter* complex to induce site-specific fork stalling and HR in mammalian cells. In most bacterial species, bidirectional replication of the circular chromosome terminates when the forks converge at a site opposite of the origin. This region contains multiple 23bp terminator sequences (*Ter*), which are bound by the protein Tus to induce polar replication fork trapping. Tus/*Ter* binding forms a barrier to replication fork progression and results in replication termination [47,48]. Tus/*Ter* has been previously used to examine recombination events after fork collapse and provided direct evidence that BRCA1, BRCA2, and RAD51 regulate HR at stalled forks [49]. Since we have shown that SNM1B is involved in the localization of some of these factors to sites of replication stress, we asked whether SNM1B might also be important for regulating recombinational repair.

To examine the specific role of SNM1B in the recombination events that occur as a result of replication fork collapse, we used the previously described Tus/*Ter* reporter system [49] (Figure 2.5D). This reporter was targeted as a single copy to the *ROSA26* locus of the mouse embryonic stem (mES) cell line 11CO/47T (*Brca1*$^{fl/BRCT}$). It contains two tandem enhanced green fluorescent protein (*GFP*) genes, one truncated at its 5' end (5' TR-*GFP*) and the other interrupted by 6x*Ter* sequences adjacent to an I-SceI restriction enzyme cut site (6x*Ter*-I-SceI-*GFP*) [49]. The *E. coli* terminator protein, Tus, can specifically bind to the 6x*Ter* sequences to form a Tus/*Ter* complex that causes bidirectional replication fork stalling. When these stalled forks are processed,

DSBs are generated and repaired through HR. Recombination between the broken *GFP* copy and the 5'-truncated *GFP* of the sister chromatid restores wildtype *GFP* expression. During gene conversion, nascent strand synthesis can extend for short distances (short tract gene conversion – STGC) or for several kilobases (long tract gene conversion – LTGC) prior to termination. LTGC is considered to be error-prone and often results in tandem gene duplication. LTGC is differentiated from STGC in this reporter by the duplication of a red fluorescent protein (*RFP*) gene cassette. Two artificial exons of *RFP* ("A" and "B" in Figure 2.5D) were placed in an inverted orientation between the two copies of *GFP*, and upon duplication, splicing between exon A of the first cassette and exon B of the second generates wildtype *RFP*. Therefore, STGC products are GFP^+RFP^- and LTGC products are GFP^+RFP^+. Additionally, a bias towards error-prone LTCG can be evaluated based on GRP^+RFP^+/Total GFP^+ calculations.

SNM1B was depleted in mES cells containing the Tus/*Ter* reporter, and Tus was expressed to induce site-specific replication fork stalling (Figure 2.5A-C). There was an approximately 2-fold reduction in total HR and Tus-induced STGC in SNM1B-deficient cells compared to NS controls ($p<0.001$; Figure 2.5E,F). Tus-induced LTGC was also reduced in SNM1B-depleted cells compared to the control, however the loss of SNM1B did not significantly bias HR in favor of LTGC (Figure 2.5F). These data indicate that SNM1B is involved in the recombination events at collapsed replication forks, but does not significantly influence the balance between STGC and LTGC.

Discussion

The processing of stalled replication forks must be tightly controlled to allow for the appropriate timing and extent of DNA digestion at intermediate structures. Since SNM1B is a key DNA nuclease involved in the resolution of stalled forks, we first examined whether it was regulated in a way to ensure its activity was limited to S-phase when DNA replication occurs. We used a double thymidine block and Hoechst sorting to determine if SNM1B protein levels were cell cycle regulated. Interestingly, SNM1B was stabilized in S-phase in response to the double thymidine block, but there was no significant change in SNM1B protein levels throughout G1-, S-, or G2/M-phases in

unperturbed cells. This suggests that SNM1B is not regulated by the cell cycle, but is potentially stabilized by agents that induce replication stress. It is necessary to determine whether this form of regulation occurs at the protein level, as opposed to changes in transcription or translation. Since SNM1B in our current study is expressed from a constitutive CMV promoter, we expect transcript levels to be unaltered, however we cannot rule out the possibility that changes in protein levels are due to translational control. Intriguingly, the nuclease CtIP, which also displays elevated levels during S-phase, has been shown to be regulated by the Serpine mRNA binding protein 1 (SERBP1) at the translational level. SERBP1 binds to CtIP mRNA and is required for translational induction of CtIP in S-phase, without affecting the synthesis or stability of CtIP mRNA [50]. Additionally, a number of DNA repair factors, including MRE11, were found to be under translational control throughout the cell cycle in a genome-wide ribosome profiling study [51]. Cyclin A2 has been described to upregulate MRE11 expression by binding to its mRNA and promoting translation [52]. Thus, SNM1B may be regulated in a similar way during S-phase, but this requires further exploration.

In addition to the double thymidine block, SNM1B protein levels are also stabilized in response to aphidicolin treatment and become highly associated with chromatin. It is possible that the increased chromatin association of SNM1B after aphidicolin exposure may aid in its stabilization during S-phase. It would be interesting to examine the effects of other DNA damage-inducing agents on SNM1B protein levels in order to better understand its regulation.

SNM1B has been shown to form subnuclear foci in response to aphidicolin-induced replication stress, but the role of other DNA repair proteins on its recruitment to these sites is unknown [31]. Therefore, we examined the localization of SNM1B to stalled forks relative to both early-response proteins, RPA and MRE11, as well as downstream factors, such as FANCD2. We determined that SNM1B is recruited to aphidicolin-induced stalled forks after RPA and MRE11, but before FANCD2. These findings indicate that SNM1B is not involved in the early response to stalled replication forks, but may function at an intermediate or late stage within the repair process. Interestingly, previous data showed that MRE11 is required for efficient recruitment of monoubiquitinated FANCD2 and CtIP to stalled forks [41]. This prompted us to examine

the role of MRE11 in the localization of SNM1B to chromatin. We found that, unlike FANCD2 and CtIP, the exonuclease activity of MRE11 was not required for recruitment of SNM1B to chromatin after 6 or 24 hours of aphidicolin treatment. This suggests that upon both fork stalling and potentially collapse, SNM1B and MRE11 may localize independently from one another, but are both still required for FANCD2 recruitment [31]. However, since SNM1B and MRE11 have been reported to interact, we cannot eliminate the possibility that the MRE11 protein itself is important for SNM1B localization.

Although the MRE11 nuclease activity is not essential for SNM1B recruitment to stalled forks, it has been reported to be involved in the nucleolytic processing of DNA intermediates after fork regression. If not properly regulated, excessive degradation by MRE11 can result in fork instability. The HR factors, BRCA1 and FANCD2, have been implicated in stabilizing and protecting the fork from excessive degradation by MRE11 [10,11,52]. Since SNM1B is required for the proper recruitment of BRCA1 and FANCD2, we asked whether SNM1B depletion affects the levels of ssDNA at stalled forks [31]. We found that SNM1B-deficient cells displayed a significant increase in the levels of ssDNA compared to controls in both untreated and aphidicolin-treated conditions. This observation indicates that SNM1B may be important for preventing excessive nucleolytic processing by MRE11, potentially through recruitment of members of the FA/BRCA network. Defects in the stabilization of stalled forks can prohibit proper restart and replication progression. Analyses of replication fork dynamics revealed that SNM1B is required for replication restart in unperturbed cells. Therefore, loss of SNM1B can lead to excessive ssDNA formation and instability at stalled forks, resulting in inefficient replication restart.

RAD51 is another HR factor that has been implicated in the stabilization of stalled forks by preventing excessive nascent DNA resection [10,11]. Previous reports have also shown that RAD51 can localize to chromatin in the absence of fork stalling and at early stages of fork repair, before DNA DSBs are generated [53]. To examine whether SNM1B is involved in the localization of RAD51 to stalled forks, we assessed RAD51 foci formation in SNM1B-depleted cells. We found that the percentage of cells with RAD51 foci significantly decreases upon SNM1B knockdown compared to the

controls. RAD51 foci formation requires several kilobases of single-stranded DNA, therefore these results could suggest that RAD51 coats the excessive ssDNA tracts that form upon fork stalling and reversal [54]. However, studies have revealed that the RAD51 accumulation at stalled forks induced by a protein complex barrier was restricted to within a few hundred base pairs of DNA [55]. Therefore, it is more likely that the RAD51 foci formation that we observe is in response to DNA DSBs generated from collapsed replication forks. Consistent with this hypothesis, we also detected an increase in colocalization of γH2AX and 53BP1 foci after SNM1B depletion. Together, these results indicate that SNM1B may be involved in preventing excessive nucleolytic processing at stalled forks that result in instability and DSB accumulation.

Our findings support the notion that SNM1B does not aid in generating the DSBs at collapsed forks, but might be important for the processing events for HR-mediated repair. To examine the role of SNM1B in recombination, we used the Tus/*Ter* reporter system and analyzed gene conversion events after site-specific fork stalling. SNM1B-depleted cells displayed an overall decrease in HR compared to controls, which is similar to previous findings that SNM1B is required for the repair of I-SceI-induced DSBs [30]. Additionally, we found that there was a reduction in both STGC and LTGC products after SNM1B knockdown, with the decrease in STGC being statistically significant. There was also no significant bias of HR towards LTGC in SNM1B-depleted cells compared to the controls. Other members of the FA/BRCA pathway, including BRCA1, BRCA2, RAD51, and FANCP/SLX4, have all been shown to positively regulate STGC after Tus/*Ter*-induced fork stalling [49]. SNM1B has been reported to interact with the nuclease scaffold, FANCP/SLX4, and we have demonstrated that it is necessary for recruitment of BRCA1 and RAD51 to sites of replication stress [31]. Therefore, SNM1B may function with these repair factors to aid in the processing events after replication fork collapse.

Previous studies have demonstrated that Tus/*Ter*-induced HR entails bidirectional fork arrest and that STGC products are the result of canonical synthesis-dependent strand annealing (SDSA) of two DSB ends [49]. The termination mechanism of Tus/*Ter*-induced LTGC products is unknown, but involves extensive nascent strand synthesis that often results in gene duplication. Unlike BRCA1 and RAD51, SNM1B

does not significantly suppress LTGC at stalled forks. These data reveal that SNM1B may be necessary for the initiation of HR-mediated repair after fork collapse, but has a more minor role in the termination mechanism of gene conversion. Since the mES cell line used for this study can express a mutant form of BRCA1, it would be interesting to assess if SNM1B and BRCA1 are epistatic in their functions of HR-mediated repair at collapsed forks.

In conclusion, we demonstrate that SNM1B has critical roles during the resolution of replication stress by promoting replication fork recovery and repair. SNM1B functions at a later stage in the repair process to prevent excessive ssDNA intermediates, facilitate RAD51 recruitment, and repair DSBs after fork collapse. Our findings have provided mechanistic insights into the role of SNM1B in avoiding detrimental replication-associated genome instability.

Materials and Methods

Generation of Cell Lines

A previously described pLL-IRES-GFP lentiviral vector harboring siRNA-resistant SNM1B cDNA was used to generate HCT116 stable cell lines [30]. This SNM1B cDNA contains a C-terminal V5 epitope tag, and an empty vector (EV) was used as a control. Lentiviruses were generated by co-transfecting the lentiviral constructs with packaging plasmids pLP1, pLP2, and pVSVG (Invitrogen) into 293T cells using calcium phosphate. The viral supernatants were collected after 48 hours and filtered through 0.45mm PVDF filters (Millipore). HCT116 cells were transduced with 1 ml viral media containing 4μg/ml polybrene and 1 ml culture media supplemented with 10% FBS for 24 hours. Cells were harvested 24 hours later, and expression of the SNM1B-IRES-GFP cassette was determined by flow cytometry. GFP-positive cells were sorted (UM Flow Cytometry Core) to increase the percentage of cells expressing SNM1B within the population.

Knockdown of SNM1B expression by siRNA

HCT116 cells were plated in 6-well or 12-well plates 24 hours prior to transfection. All siRNAs (50nM) were transfected using Lipofectamine 2000 (Invitrogen)

as per the manufacturer's instructions. Knockdown of mSnm1B for the recombination assay is described below. To verify the extent of knockdown, SNM1B mRNA levels were determined via semi-quantitative RT-PCR. The target sequences for siRNA depletion were as follows: Human siSNM1B: 5′-CCTCTTGCATCGTCACCTACATT-3′; Mouse siSnm1B: 5'-CACTGCTTGCCTCTTGCATCG-3'; NS siRNA (Qiagen AllStars Negative Control) was used as the non-silencing control.

Semi-quantitative RT-PCR

Total RNA (1µg) isolated from cells was reverse transcribed using a poly-dT(20) primer and murine leukemia virus-reverse transcriptase (Invitrogen). Human cDNA was amplified using SNM1B-specific primers located in the 3'UTR and exon 3, and mouse cDNA was amplified using primers located in exons 3 and 4. GAPDH was amplified as a control. Bands were quantitated using ImageJ, and SNM1B cDNA levels were normalized to GAPDH.

Cell Synchronization and Cell Cycle Analyses

For the double thymidine block, HCT116 cells stably expressing WT SNM1B-V5 were treated with 2mM thymidine for 18 hours, released into fresh media for 6 hours, and exposed to 2mM thymidine for an additional 18 hours. After washing with PBS, cells were released from the double thymidine block and harvested at 0, 2, 4, and 6 hours for cell cycle analysis and immunoblotting.

To examine cell cycle profiles after synchronization, cells were fixed with cold 70% ethanol, stored at -20°C, and stained with a solution containing 50µg/ml propidium iodide, 50µg/ml RNase A, and 0.1% Triton X-100 for 30 minutes at room temperature. Cells were analyzed using an Accuri C6 flow cytometer and FlowJo software.

Western Blot Analyses

Cells were harvested and lysed on ice for 1 hour in CSK buffer (10mM PIPES pH 6.8, 100mM NaCl, 300mM sucrose, 1mM $MgCl_2$, 0.1% Triton X-100) containing protease inhibitors (Roche Complete Mini EDTA-free), phosphatase inhibitors (Roche

PhosSTOP), and benzonase (Sigma). Lysates were centrifuged at 14,000 RPM for 20 min and protein concentrations were determined using the Bradford assay (BioRad). Cell extracts were resolved by SDS-PAGE and transferred following standard procedures. Proteins were analyzed using the appropriate primary and secondary antibodies, and bands were visualized and quantitated using Li-Cor Odyssey 2.1 software and ImageJ.

The following primary antibodies were used: V5 (Invitrogen); MRE11 (Cell Signaling); FANCD2 (Novus Biologicals); CtIP (Bethyl); Cyclin B1 (Santa Cruz); Cyclin A (Santa Cruz); H2AX (Millipore); GAPDH (Cell Signaling and Santa Cruz). Secondary antibodies were IRDye conjugated goat anti-rabbit or anti-mouse IgG (Li-Cor Biosciences).

Hoechst Staining and Cell Sorting

HCT116 cells stably expressing WT SNM1B-V5 were suspended at 1.5 x 10^6 cells/ml in McCoy's medium containing 2% FBS. Cells were incubated with Hoechst dye at a final concentration of 5μg/ml for 30 min or 6μg/ml for 90 min at 37°C with intermittent shaking. Fluorescence-activated cell sorting (FACS) was performed to sort the cells into G1-, S-, and G2/M-phase populations based on DNA content. Cells were lysed and immunoblotting was used to assess WT SNM1B-V5 protein levels in each phase of the cell cycle. The average level of SNM1B protein was calculated from three independent experiments.

Immunofluorescence of Subnuclear Foci

HCT116 cells stably expressing WT SNM1B-V5 were grown on glass coverslips in 12-well plates and treated with 0.3μM aphidicolin for 1, 2, 4, 6, or 24 hours. For knockdown experiments, HCT116 cells were grown on glass coverslips in 12-well plates and transfected with NS or siSNM1B siRNAs. At 48 hours post-transfection, cells were treated with 1μM or 2μM aphidicolin for 24 hours. For RPA, MRE11, FANCD2, and γH2AX:53BP1 foci, cells were incubated in cold extraction buffer (20mM HEPES, 50mM NaCl, 300mM sucrose, 3mM $MgCl_2$, 0.5% TX-100) for 5 min followed by fixation in 3% paraformaldehyde/2% sucrose for 20 min. For SNM1B-V5 foci, cells were fixed in ice-

cold 70% methanol/30% acetone for 20 min at -20°C and air-dried at room temperature. For RAD51 foci, cells were fixed in a solution containing 3% paraformaldehyde, 2% sucrose, and 0.5% Triton X-100 for 20 min.

After fixation and permeabilization, cells were stained with the following primary antibodies for 45 min at room temperature or overnight at 4°C (for RAD51): RPA (Calbiochem); MRE11 (Novus Biologicals); FANCD2 (Novus Biologicals); V5 (Invitrogen); γH2AX (Millipore); 53BP1 (Novus Biologicals); RAD51 (GeneTex).

Cells were stained with anti-IgG Alexa Fluor 488 or 594 (Invitrogen Molecular Probes) secondary antibodies for 45 min and coverslips were mounted on slides using ProLong Gold Antifade Reagent with DAPI (Life Technologies). Images were acquired using an Olympus BX61 microscope and FISHview software (Applied Spectral Imaging). Approximately 100 cells per sample were scored from at least three independent experiments.

Cellular Fractionations

HCT116 cells stably expressing WT SNM1B-V5 were treated with 50μM mirin (Cayman Chemical) and 1μM aphidicolin for the indicated times. Cells were harvested and pellets were first resuspended in fractionation buffer I (50mM HEPES pH 7.5, 150mM NaCl, 1mM EDTA, 0.2% NP-40, supplemented with protease and phosphatase inhibitors) for 5 min on ice. After centrifugation at 1000 × g for 5 min, the supernatant was collected (cytoplasmic fraction), and the pellets were washed with fractionation buffer I. The nuclear pellets were then lysed for 40 min on ice with fractionation buffer II (50mM HEPES pH 7.5, 150mM NaCl, 1mM EDTA, 0.5% NP-40, supplemented with protease and phosphatase inhibitors). The supernatants were collected (nuclear faction) after centrifugation at 16,000 × g for 15 min. The final pellets were lysed in RIPA buffer (50mM Tris-HCl pH 8.0, 150mM NaCl, 1% NP-40, 0.5% sodium deoxycholate, 0.1% SDS, supplemented with protease and phosphatase inhibitors), sonicated, and cleared by centrifugation at 16,000 × g for 20 min (chromatin fraction). The whole cell extracts (WCEs) were prepared in a similar manner as the chromatin fractions. Equal concentrations of each fraction were analyzed by immunoblotting, with GAPDH and H2AX serving as controls for cytoplasmic and chromatin fractions, respectively.

ssDNA Immunofluorescence Assay

HCT116 cells were grown on glass coverslips in 12-well plates and transfected with NS or siSNM1B siRNAs for 48 hours. Cells were labeled with 20μM BrdU for 24 hours and treated with 1μM Aphidicolin for an additional 24 hours. Using non-denaturing conditions, cells were incubated in cold extraction buffer (20mM HEPES, 50mM NaCl, 300mM sucrose, 3mM $MgCl_2$, 0.5% Triton X-100) for 5 min and then fixed with 3% paraformaldehyde/2% sucrose for 20 min. Cells were incubated with an anti-BrdU antibody (BD Pharmigen) followed by an anti-IgG Alexa Fluor 488 secondary antibody to visualize BrdU staining. Images were acquired with an Olympus BX61 microscope and FISHview Software. The fluorescence intensity for every nucleus was measured and normalized to background levels for each experiment. At least three independent experiments were performed and approximately 100 cells were analyzed per condition.

DNA Fiber Assay

HCT116 cells were transfected with NS or siSNM1B siRNAs for 48 hours and labeled with 50μM IdU for 20 min followed by 100μM CldU for 20 min. Cells were resuspended at 200 cells/μl in ice-cold PBS and 2μl of the cell suspension was deposited on a silanized slide (Sigma). Approximately 15μl of lysis buffer (200mM Tris pH 7.4, 0.5% SDS, 50mM EDTA) was added to the cells for 10 min, and the slides were tilted to 15° to stretch the DNA fibers. After air-drying for 6-8 hours, slides were fixed in methanol:acetic acid (3:1) for 2 min, dried overnight in the dark, and placed at -20°C for 24 hours. The DNA was denatured with 2.5M HCl for 30 min and stained with mouse anti-IdU (BD Biosciences) and rat anti-CldU (AbD Serotec) primary antibodies. To visualize fibers using immunofluorescence microscopy, cells were stained with anti-IgG Alexa Fluor 594 and 488 secondary antibodies and imaged with an Olympus BX61 microscope and FISHview software. Approximately 200 fibers were scored for each sample from at least three independent experiments. For scoring, red to green tracts were categorized as ongoing forks, red only tracts as stalled forks, and green only tracts as new forks. The average percentage of new forks (or ongoing forks) was calculated

as the number of new forks (or ongoing forks) divided by the total number of ongoing, stalled, and new forks combined.

Recombination Assays

The *Brca1*$^{fl/BRCT}$ mouse embryonic stem (mES) cell line harboring a single copy of a 6x*Ter*/HR reporter at the *ROSA26* locus was generated and cultured as previously described [49]. The mES cells were grown on MEF feeders for approximately one week before they were depleted of MEFs twice over the course of two hours. Cells were then alternately passaged and conditioned on gelatinized plates for use in recombination assays.

Mouse ES cells (1.6×10^5) were transfected in suspension with 20pmol siRNA and 0.35μg pcDNA3β-mycNLS-Tus or control vector using Lipofectamine 2000. Two transfected wells of a 24-well plate were pooled for each condition, and GFP^+RFP^- and GFP^+RFP^+ frequencies were scored 3 days post-transfection by flow cytometry. Approximately 1.5×10^6 total events were scored per sample, and values were corrected for background events and transfection efficiency. Transfection efficiency was measured simultaneously by parallel transfection with 0.035μg of wild-type GFP expression vector, 0.315μg control vector, and 20pmol siRNA. Data represent the mean and SEM of four independent experiments.

Acknowledgements

I would like to thank Ishita Das for her scientific contributions to this chapter. I would also like to thank Nick Willis and Ralph Scully for providing the cell line and reagents for the Tus/*Ter* recombination assay and Hilary Moale for assisting with mES cell culture.

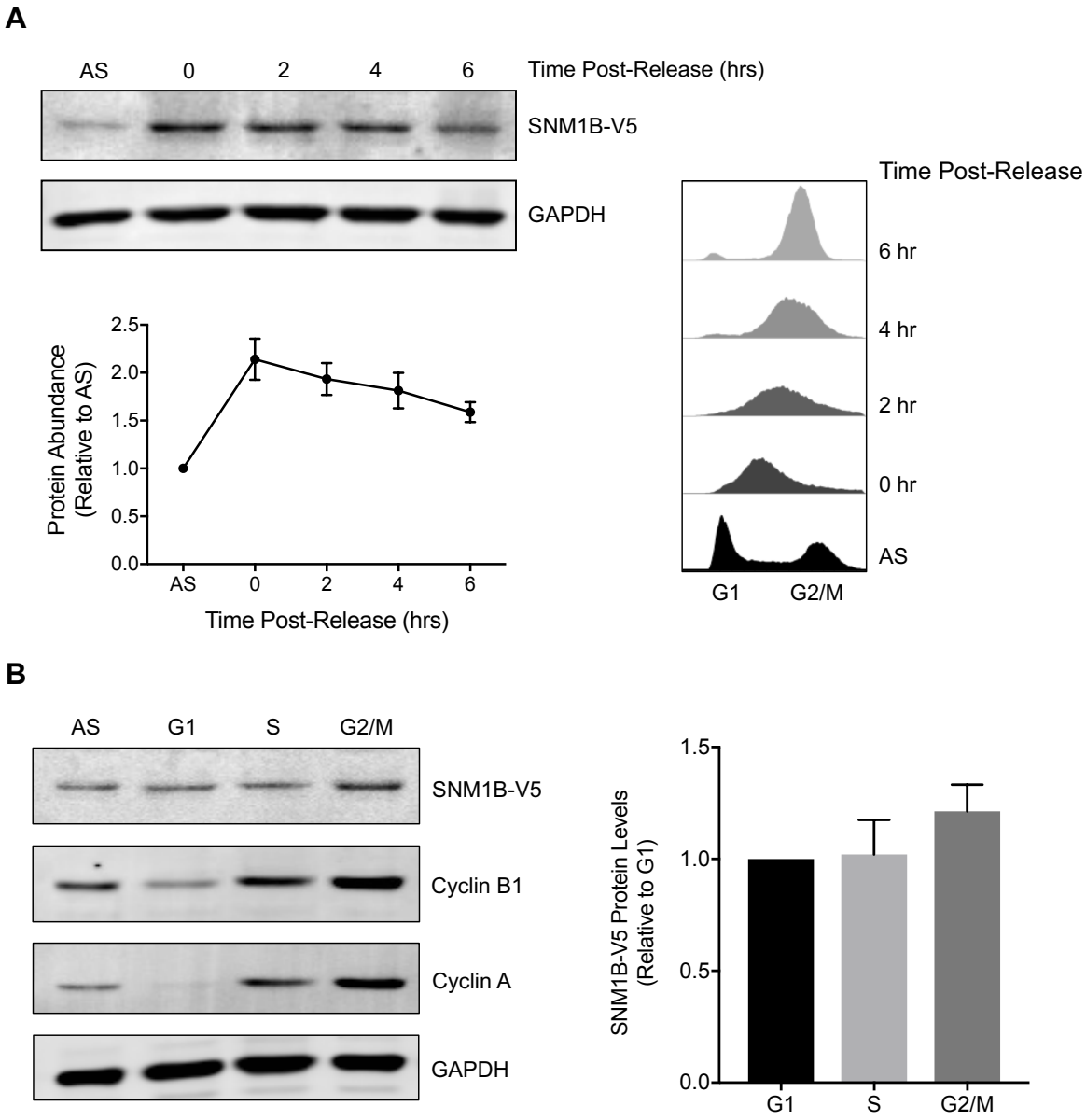
A
AS
0
2
4
6
Time Post-Release (hrs)
SNM1B-V5
GAPDH
Protein Abundance
(Relative to AS)
2.5
2.0
1.5
1.0
0.5
0.0
AS
0
2
4
6
Time Post-Release (hrs)
Time Post-Release
6 hr
4 hr
2 hr
0 hr
AS
G1
G2/M
B
AS
G1
S
G2/M
SNM1B-V5
Cyclin B1
Cyclin A
GAPDH
SNM1B-V5 Protein Levels
(Relative to G1)
1.5
1.0
0.5
0.0
G1
S
G2/M

Figure 2.1 SNM1B protein levels in unperturbed cells and after S-phase synchronization
(A) WT SNM1B HCT116 cells were released from a double thymidine block for the indicated amounts of time and collected for propidium iodide staining and Western blot analysis. Representative cell cycle profiles and Western blot are shown. SNM1B protein levels were quantitated and plotted relative to the asynchronous control. Results are represented as the mean ± SEM from five independent experiments.
(B) WT SNM1B HCT116 cells were incubated with Hoechst dye and sorted using FACS. Sorted cells were lysed for Western blot analysis and protein levels were quantitated relative to the amount in G1-phase. Results are represented as the mean ± SEM from three independent experiments.

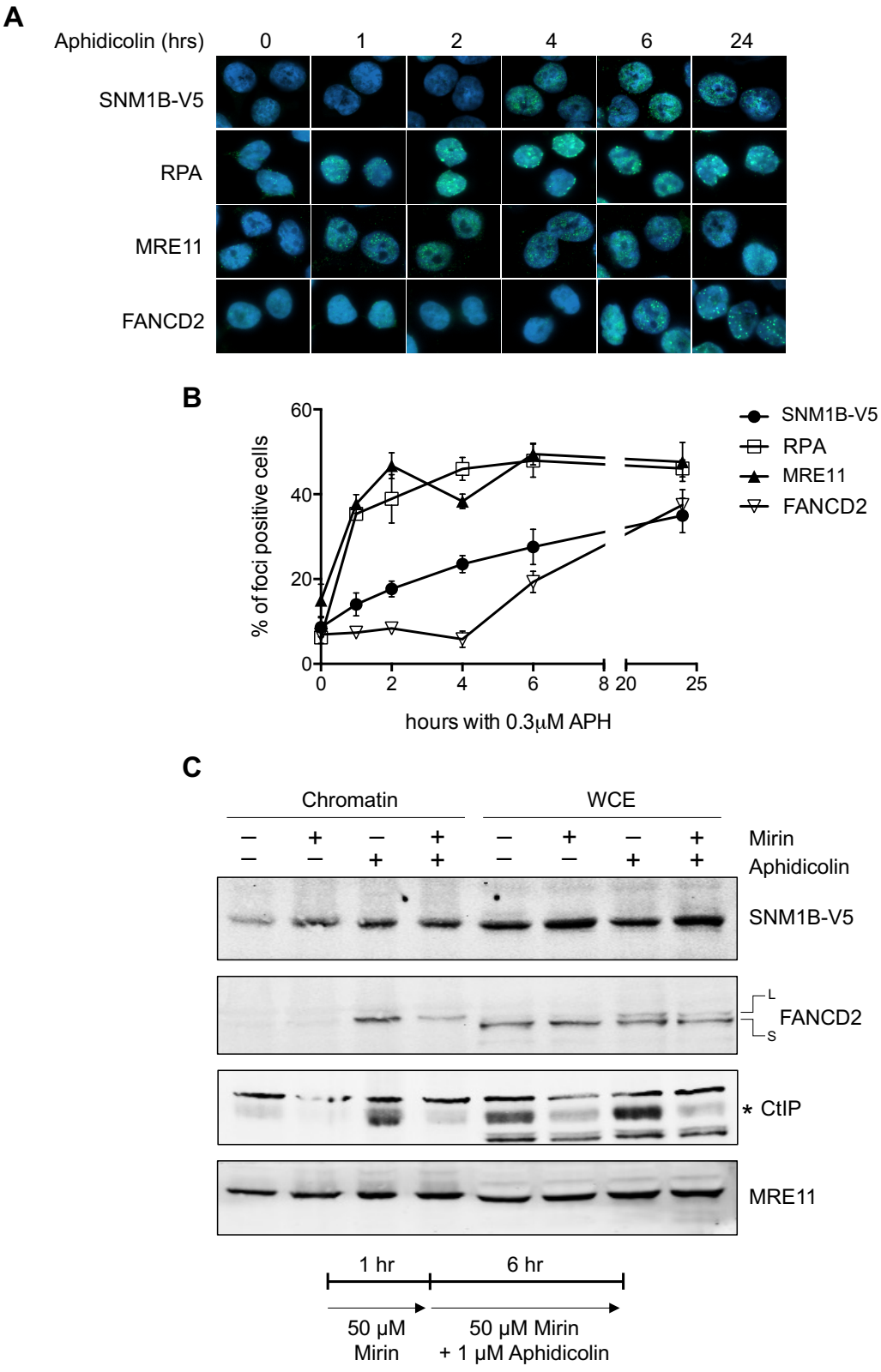
A
Aphidicolin (hrs)
0
1
2
4
6
24
SNM1B-V5
RPA
MRE11
FANCD2
B
% of foci positive cells
60
40
20
0
0
2
4
6
8
20
25
hours with 0.3μM APH
SNM1B-V5
RPA
MRE11
FANCD2
C
Chromatin
WCE
Mirin
Aphidicolin
SNM1B-V5
L
S
FANCD2
* CtIP
MRE11
1 hr
6 hr
50 μM
Mirin
50 μM Mirin
+ 1 μM Aphidicolin

Figure 2.2 SNM1B localization to stalled forks occurs after MRE11 and is independent of MRE11 exonuclease activity
(A) WT SNM1B HCT116 cells were treated with 0.3μM aphidicolin for the indicated times, fixed, and stained for visualization of SNM1B-V5, RPA, MRE11, and FANCD2 subnuclear foci. Representative images are shown for each protein throughout the timecourse. **(B)** The percentage of foci-positive cells was quantitated and plotted as the mean ± SEM. Approximately 100 cells were analyzed from at least three independent experiments. **(C)** WT SNM1B HCT116 cells were pre-treated with 50μM mirin for 1 hr and 1μM aphidicolin was added for an additional 6 hrs. Cells were fractionated and protein levels were assessed via Western blot. The L and S labels represent the monoubiquitinated and unmodified forms of FANCD2, respectively. The asterisk marks the band for CtIP. WCE, whole cell extract; Aph, Aphidicolin

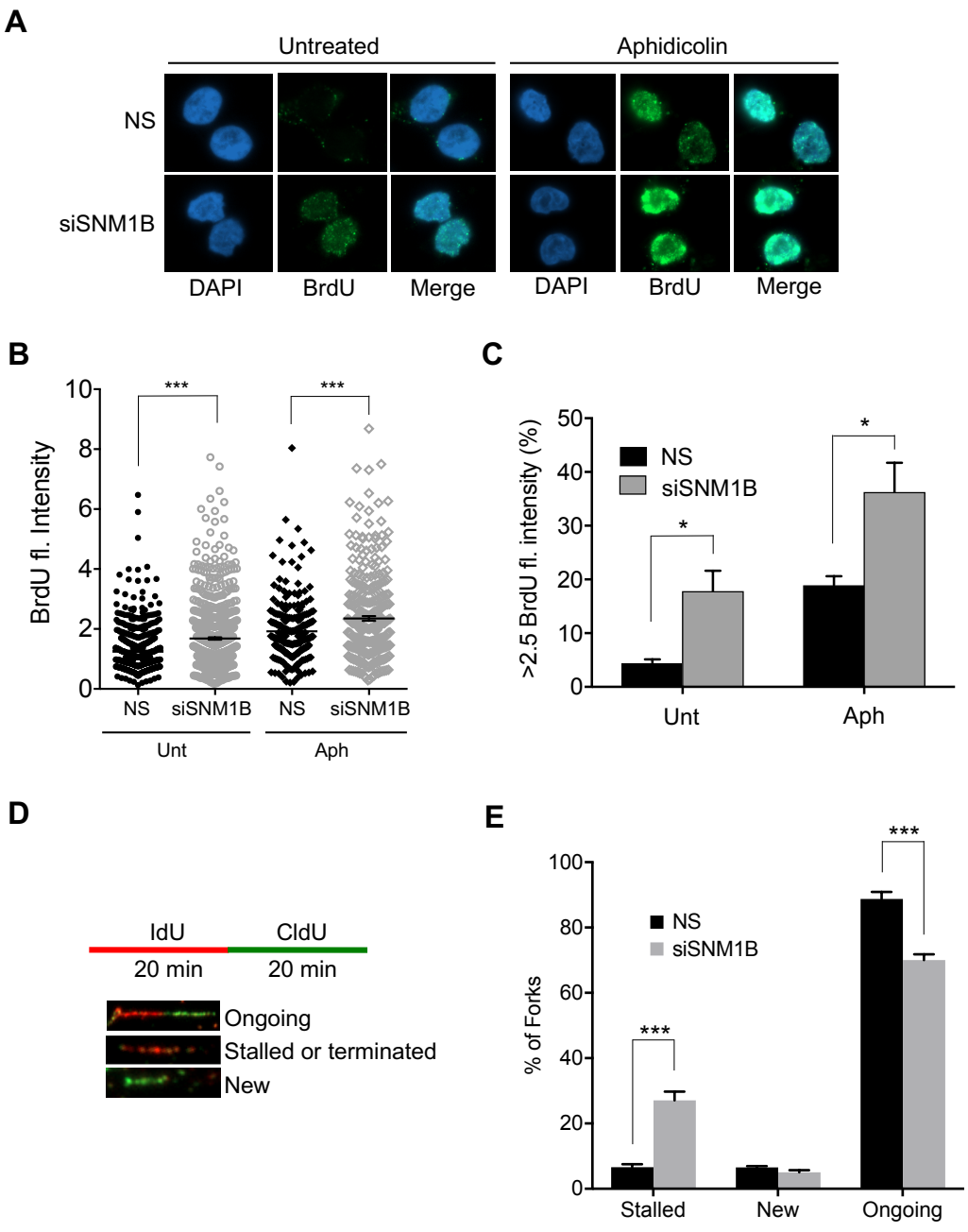
A
Untreated
Aphidicolin
NS
siSNM1B
DAPI
BrdU
Merge
DAPI
BrdU
Merge
B
BrdU fl. Intensity
10
8
6
4
2
0
***
***
NS
siSNM1B
NS
siSNM1B
Unt
Aph
C
>2.5 BrdU fl. intensity (%)
50
40
30
20
10
0
NS
siSNM1B
*
*
Unt
Aph
D
IdU
CldU
20 min
20 min
Ongoing
Stalled or terminated
New
E
% of Forks
100
80
60
40
20
0
NS
siSNM1B
***
***
Stalled
New
Ongoing

Figure 2.3 SNM1B prevents the accumulation of ssDNA at stalled forks and facilitates fork restart

(A) HCT116 cells transfected with NS or siSNM1B siRNAs were allowed to incorporate BrdU for 24 hrs to label parental and nascent DNA. Cells were treated with 1μM aphidicolin for 24 hrs, fixed, and stained with an anti-BrdU antibody in non-denaturing conditions to visualize ssDNA. Representative images are shown. **(B)** The normalized BrdU fluorescence intensity of every nucleus was plotted along with the mean ± SEM. *p<0.001 **(C)** The average percentage of cells with high intensity BrdU staining (>2.5 fluorescence intensity) was plotted ± SEM. Approximately 100 cells were analyzed from at least three independent experiments. *p<0.05 **(D)** HCT116 cells transfected with NS or siSNM1B were incubated with 50μM IdU for 20 min (red), washed, incubated with 100μM CldU for 20 min (green), and then lysed on silanized slides. DNA fibers were spread by gravity, denatured, and visualized by immunofluorescence. Representative DNA fiber images of ongoing, stalled, and new forks are shown. **(E)** The average percentage of each fork type is plotted ± SEM. Approximately 200 fibers were analyzed from at least three independent experiments. ***p<0.001; Unt, Untreated; Aph, Aphidicolin

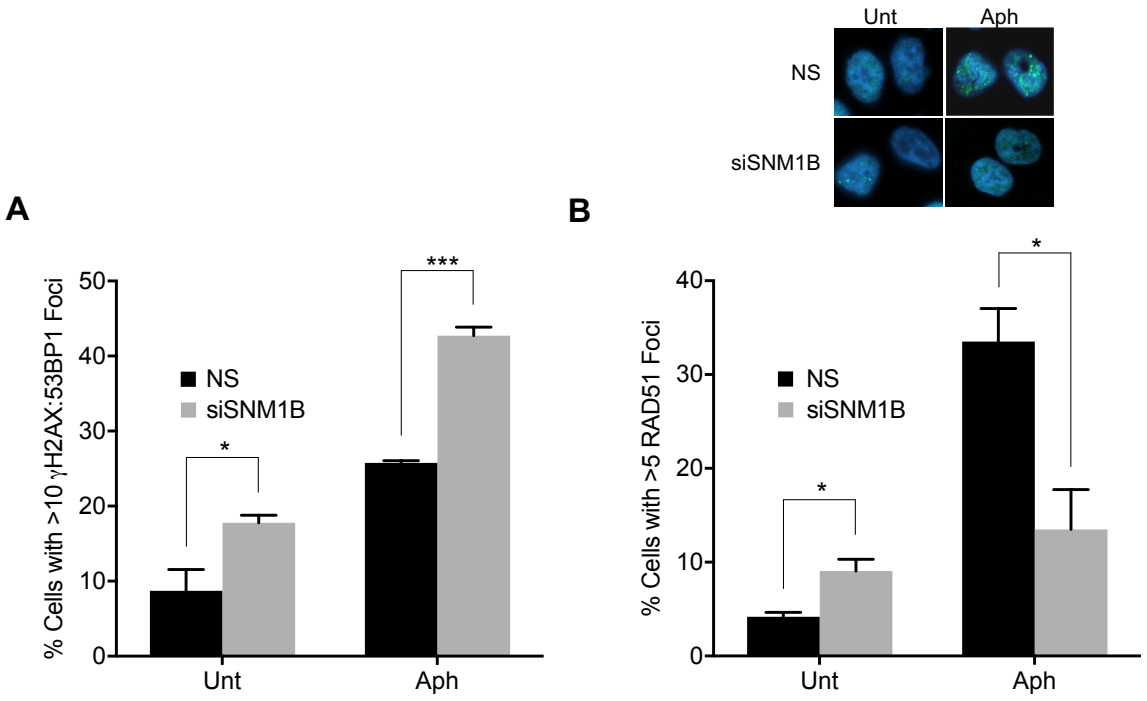

Figure 2.4 SNM1B prevents the accumulation of DNA DSBs and promotes RAD51 filament formation

(A) HCT116 cells transfected with NS or siSNM1B siRNAs were treated with 1μM aphidicolin for 24 hrs, fixed, and stained for γH2AX and 53BP1 foci colocalization. The percentage of cells with >10 foci was quantitated and plotted as the mean ± SEM. *p<0.05, ***p<0.001 **(B)** HCT116 cells transfected with NS or siSNM1B siRNAs were treated with 2μM aphidicolin for 24 hrs, fixed, and stained for RAD51 subnuclear foci. Representative foci images are shown. The percentage of cells with >5 RAD51 foci was quantitated and plotted as the mean ± SEM. Approximately 100 cells were analyzed from at least three independent experiments. *p<0.05; Unt, Untreated; Aph, Aphidicolin

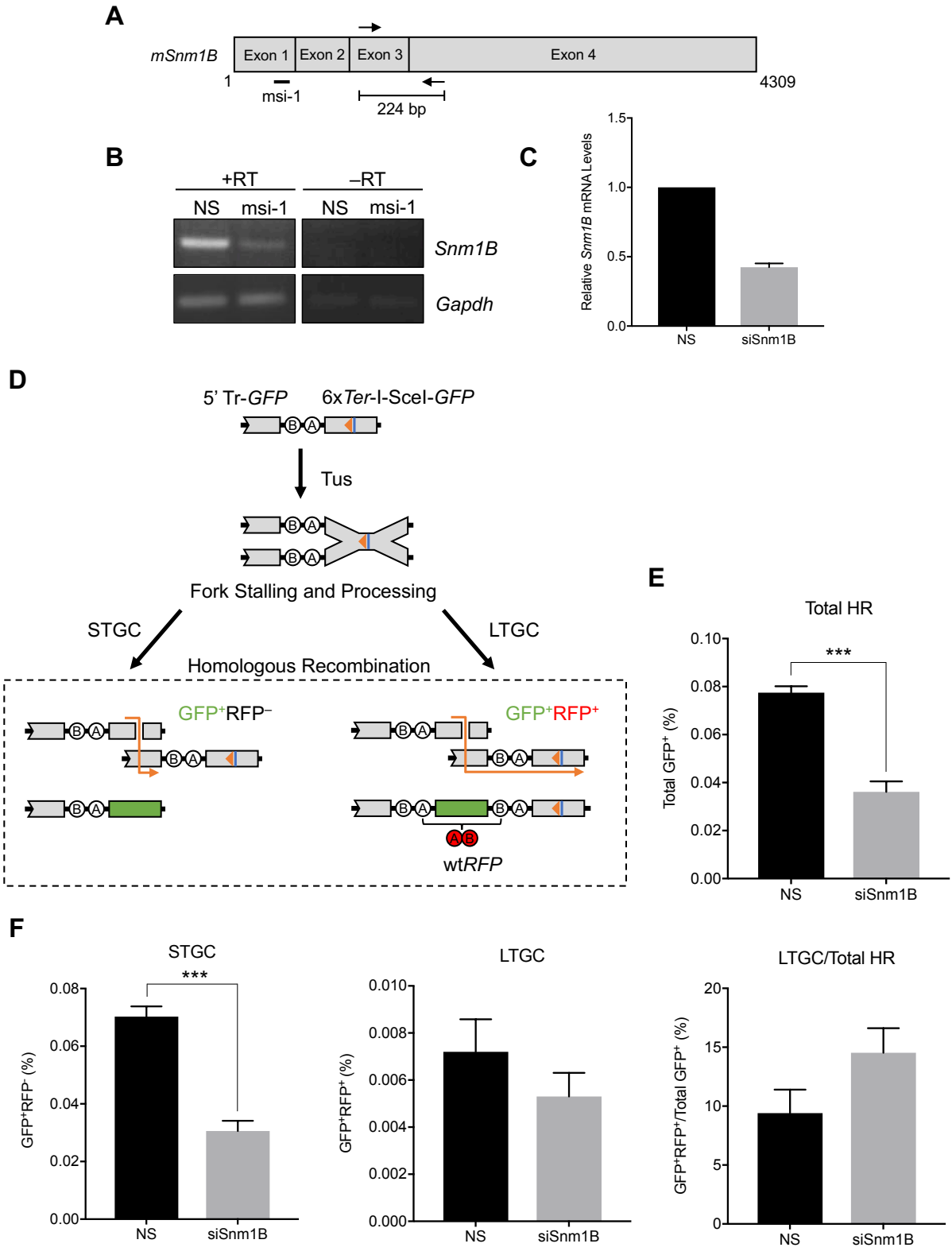
A
mSnm1B
Exon 1
Exon 2
Exon 3
Exon 4
1
4309
msi-1
224 bp
B
+RT
–RT
NS
msi-1
NS
msi-1
Snm1B
Gapdh
C
Relative Snm1B mRNA Levels
1.5
1.0
0.5
0.0
NS
siSnm1B
D
5' Tr-GFP
6xTer-I-SceI-GFP
Tus
Fork Stalling and Processing
STGC
LTGC
Homologous Recombination
GFP+RFP–
GFP+RFP+
wtRFP
E
Total HR
***
Total GFP+ (%)
0.10
0.08
0.06
0.04
0.02
0.00
NS
siSnm1B
F
STGC
***
GFP+RFP– (%)
0.08
0.06
0.04
0.02
0.00
NS
siSnm1B
LTGC
GFP+RFP+ (%)
0.010
0.008
0.006
0.004
0.002
0.000
NS
siSnm1B
LTGC/Total HR
GFP+RFP+/Total GFP+ (%)
20
15
10
5
0
NS
siSnm1B

Figure 2.5 SNM1B is required for the efficient repair of Tus/*Ter*-induced stalled replication forks

(A) Diagram of *mSnm1B* cDNA with locations of the siSnm1B siRNA (msi-1) target site and RT-PCR primers (arrows). **(B)** A representative gel of RT-PCR products from mES cells transfected with NS or msi-1 siRNAs. *Gapdh* was used for normalization of cDNA levels. RT, Reverse Transcriptase **(C)** RT-PCR bands were quantitated using ImageJ and levels were plotted relative to NS controls. Results are represented as the mean ± SEM from four independent experiments. **(D)** Schematic describing the reporter system for Tus/*Ter*-induced fork stalling. The reporter contains a 5' truncated copy of *GFP*, two inverted artificial exons of *RFP*, and *GFP* interrupted by an I-SceI endonuclease site and 6 copies of the bacterial replication terminator sequence (*Ter*). Expression of the Tus protein, which binds to *Ter* sequences, causes replication fork stalling. After collapse, these forks are processed by homologous recombination to produce either short- or long-tract gene conversion products (STGC and LTGC). *wtGFP* expression is restored in both outcomes, whereas *wtRFP* expression is only restored from LTGC products after proper exon splicing. Image adapted from Willis and Scully, 2016. [56] **(E and F)** mES cells harboring a single copy of the 6x*Ter*/HR reporter were transfected with a Tus expression vector and NS or siSnm1B siRNAs. GFP^+ RFP^- and GFP^+RFP^+ frequencies were scored 72 hrs post-transfection by flow cytometry. Data represent the mean ± SEM of four independent experiments. *$p<0.001$

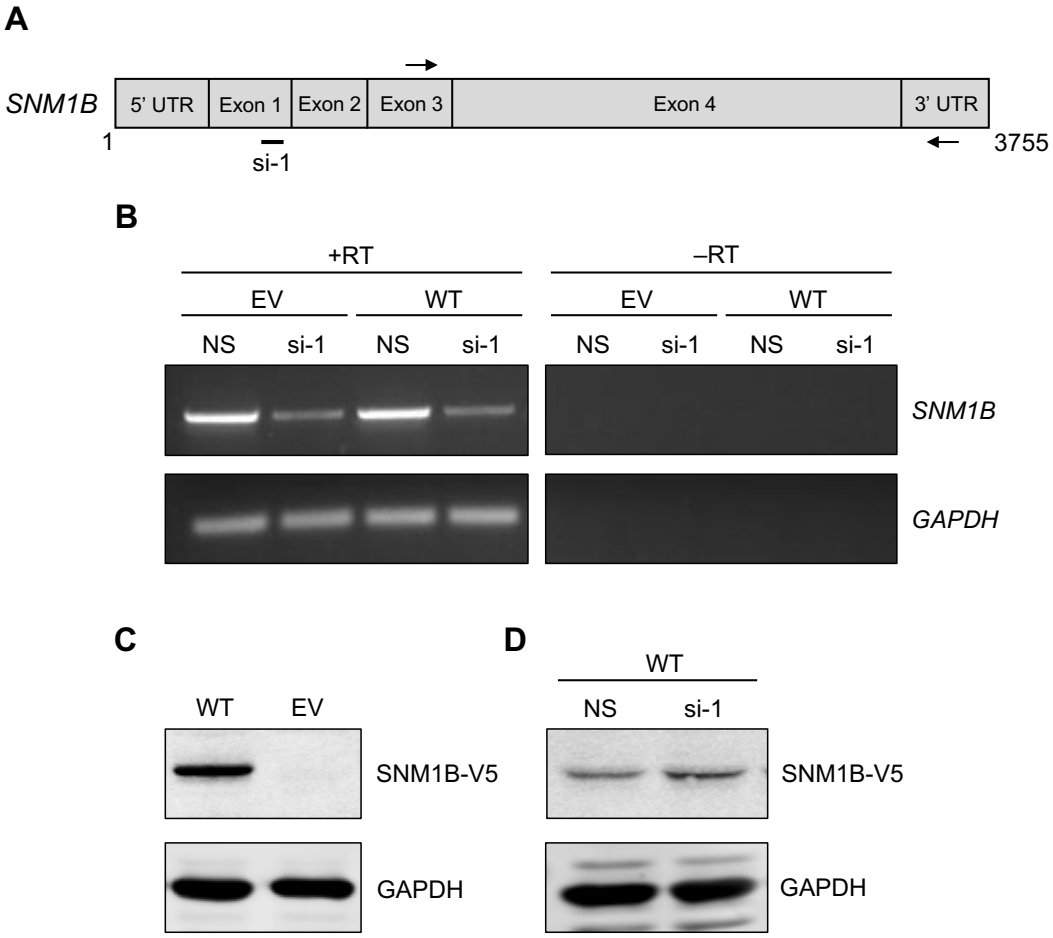

Figure 2.S1 Semi-quantitative RT-PCR and expression of SNM1B
(A) Diagram of *hSNM1B* cDNA with locations of the siSNM1B siRNA (si-1) target site and RT-PCR primers (arrows). **(B)** A representative gel of RT-PCR products from empty vector (EV) or WT SNM1B HCT116 cells transfected with NS or si-1 siRNAs. *GAPDH* was used for normalization of cDNA levels. RT, Reverse Transcriptase
(C) Representative Western blot of WT SNM1B and EV HCT116 protein lysates.
(D) Representative Western blot of lysates from WT SNM1B HCT116 cells transfected with NS or siSNM1B siRNAs.

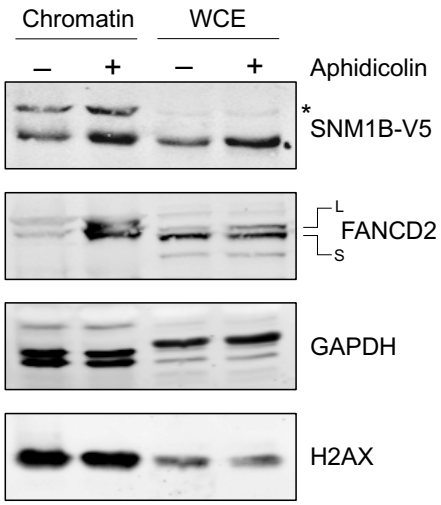

Figure 2.S2 SNM1B is stabilized and enriched on chromatin after aphidicolin treatment

WT SNM1B HCT116 cells were treated with 1μM aphidicolin for 24 hrs, fractionated, and protein levels were assessed via Western blot. The L and S labels represent the monoubiquitinated and unmodified forms of FANCD2, respectively. The asterisk marks a potentially shifted band for SNM1B-V5. WCE, whole cell extract

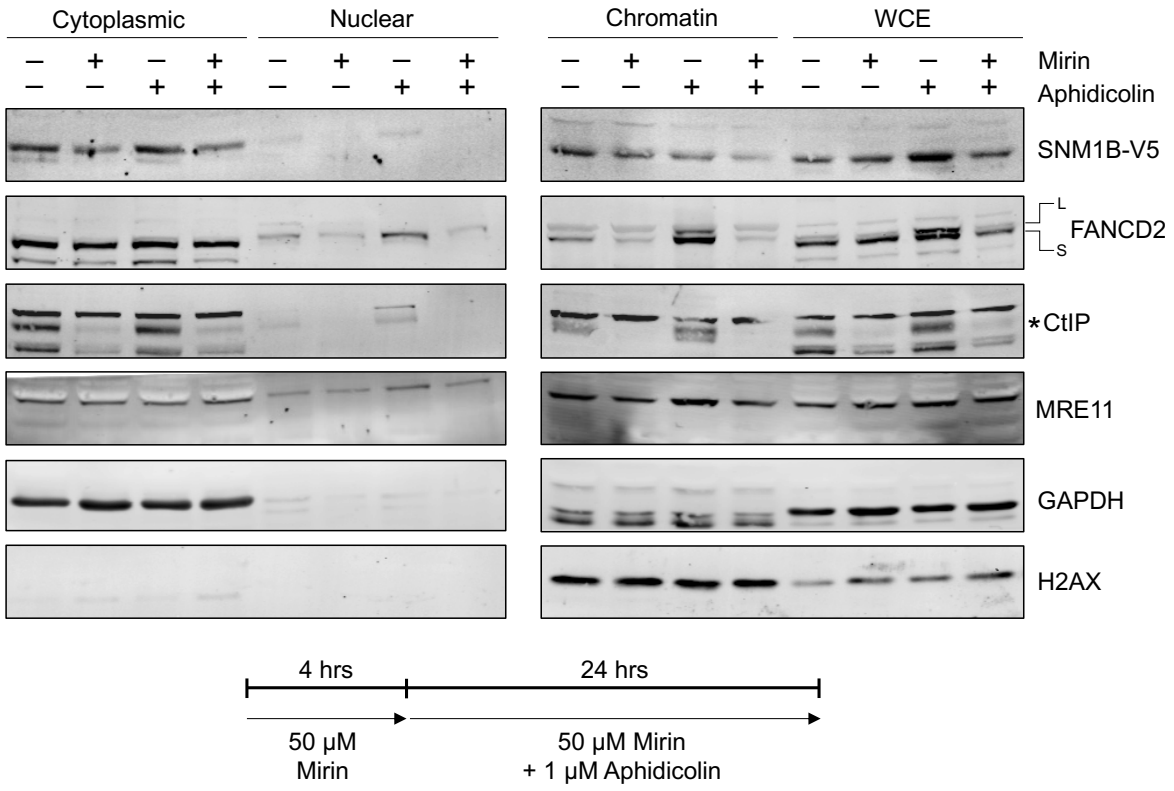

Figure 2.S3 MRE11 exonuclease activity is not required for the chromatin association of SNM1B

WT SNM1B HCT116 cells were pre-treated with 50μM mirin for 4 hrs and 1μM aphidicolin was added for an additional 24 hrs. Cells were fractionated and protein levels were assessed via Western blot. The L and S labels represent the monoubiquitinated and unmodified forms of FANCD2, respectively. The asterisk marks the band for CtIP. WCE, whole cell extract

References

1. Zeman, M. K. & Cimprich, K. A. Causes and consequences of replication stress. *Nat. Cell Biol.* **16**, 2–9 (2014).
2. Jackson, S. P. & Bartek, J. The DNA-damage response in human biology and disease. *Nature* **461**, 1071–1078 (2009).
3. Errico, A. & Costanzo, V. Mechanisms of replication fork protection: a safeguard for genome stability. *Crit. Rev. Biochem. Mol. Biol.* **47**, 222–235 (2012).
4. Yeeles, J. T. P., Poli, J., Marians, K. J. & Pasero, P. Rescuing Stalled or Damaged Replication Forks. *Cold Spring Harb. Perspect. Biol.* **5**, a012815 (2013).
5. Pasero, P. & Vindigni, A. Nucleases Acting at Stalled Forks: How to Reboot the Replication Program with a Few Shortcuts. *Annu. Rev. Genet.* **51**, 477–499 (2017).
6. Bonetti, D., Colombo, C. V., Clerici, M. & Longhese, M. P. Processing of DNA Ends in the Maintenance of Genome Stability. *Front. Genet.* **9**, (2018).
7. Atkinson, J. & McGlynn, P. Replication fork reversal and the maintenance of genome stability. *Nucleic Acids Res.* **37**, 3475–3492 (2009).
8. Neelsen, K. J. & Lopes, M. Replication fork reversal in eukaryotes: from dead end to dynamic response. *Nat. Rev. Mol. Cell Biol.* **16**, 207–220 (2015).
9. Meng, X. & Zhao, X. Replication fork regression and its regulation. *FEMS Yeast Res.* **17**, (2017).
10. Schlacher, K. *et al.* Double-Strand Break Repair-Independent Role for BRCA2 in Blocking Stalled Replication Fork Degradation by MRE11. *Cell* **145**, 529–542 (2011).
11. Schlacher, K., Wu, H. & Jasin, M. A Distinct Replication Fork Protection Pathway Connects Fanconi Anemia Tumor Suppressors to RAD51-BRCA1/2. *Cancer Cell* **22**, 106–116 (2012).
12. Thangavel, S. *et al.* DNA2 drives processing and restart of reversed replication forks in human cells. *J Cell Biol* **208**, 545–562 (2015).
13. Colosio, A., Frattini, C., Pellicanò, G., Villa-Hernández, S. & Bermejo, R. Nucleolytic processing of aberrant replication intermediates by an Exo1-Dna2-Sae2 axis counteracts fork collapse-driven chromosome instability. *Nucleic Acids Res.* **44**, 10676–10690 (2016).
14. Cotta-Ramusino, C. *et al.* Exo1 Processes Stalled Replication Forks and Counteracts Fork Reversal in Checkpoint-Defective Cells. *Mol. Cell* **17**, 153–159 (2005).
15. Chaudhury, I., Stroik, D. R. & Sobeck, A. FANCD2-Controlled Chromatin Access of the Fanconi-Associated Nuclease FAN1 Is Crucial for the Recovery of Stalled Replication Forks. *Mol. Cell. Biol.* **34**, 3939–3954 (2014).

16. Lemaçon, D. *et al.* MRE11 and EXO1 nucleases degrade reversed forks and elicit MUS81-dependent fork rescue in BRCA2-deficient cells. *Nat. Commun.* **8**, 860 (2017).
17. Ait Saada, A. *et al.* Unprotected Replication Forks Are Converted into Mitotic Sister Chromatid Bridges. *Mol. Cell* **66**, 398-410.e4 (2017).
18. Pepe, A. & West, S. C. MUS81-EME2 Promotes Replication Fork Restart. *Cell Rep.* **7**, 1048–1055 (2014).
19. Hanada, K. *et al.* The structure-specific endonuclease Mus81 contributes to replication restart by generating double-strand DNA breaks. *Nat. Struct. Mol. Biol.* **14**, 1096–1104 (2007).
20. Zhu, Z., Chung, W.-H., Shim, E. Y., Lee, S. E. & Ira, G. Sgs1 helicase and two nucleases Dna2 and Exo1 resect DNA double strand break ends. *Cell* **134**, 981–994 (2008).
21. Nicolette, M. L. *et al.* Mre11–Rad50–Xrs2 and Sae2 promote 5′ strand resection of DNA double-strand breaks. *Nat. Struct. Mol. Biol.* **17**, 1478–1485 (2010).
22. Nimonkar, A. V. *et al.* BLM–DNA2–RPA–MRN and EXO1–BLM–RPA–MRN constitute two DNA end resection machineries for human DNA break repair. *Genes Dev.* **25**, 350–362 (2011).
23. Cannavo, E., Cejka, P. & Kowalczykowski, S. C. Relationship of DNA degradation by Saccharomyces cerevisiae Exonuclease 1 and its stimulation by RPA and Mre11-Rad50-Xrs2 to DNA end resection. *Proc. Natl. Acad. Sci.* **110**, E1661–E1668 (2013).
24. Sturzenegger, A. *et al.* DNA2 Cooperates with the WRN and BLM RecQ Helicases to Mediate Long-range DNA End Resection in Human Cells. *J. Biol. Chem.* **289**, 27314–27326 (2014).
25. Anand, R., Ranjha, L., Cannavo, E. & Cejka, P. Phosphorylated CtIP Functions as a Co-factor of the MRE11-RAD50-NBS1 Endonuclease in DNA End Resection. *Mol. Cell* **64**, 940–950 (2016).
26. Demuth, I., Digweed, M. & Concannon, P. Human SNM1B is required for normal cellular response to both DNA interstrand crosslink-inducing agents and ionizing radiation. *Oncogene* **23**, 8611–8618 (2004).
27. Mason, J. M. & Sekiguchi, J. M. Snm1B/Apollo functions in the Fanconi anemia pathway in response to DNA interstrand crosslinks. *Hum. Mol. Genet.* **20**, 2549–2559 (2011).
28. Lam, Y. C. *et al.* SNMIB/Apollo protects leading-strand telomeres against NHEJ-mediated repair. *EMBO J.* **29**, 2230–2241 (2010).
29. Wu, P., van Overbeek, M., Rooney, S. & de Lange, T. Apollo Contributes to G Overhang Maintenance and Protects Leading-End Telomeres. *Mol. Cell* **39**, 606–617 (2010).

30. Wu, P., Takai, H. & de Lange, T. Telomeric 3′ Overhangs Derive from Resection by Exo1 and Apollo and Fill-In by POT1b-Associated CST. *Cell* **150**, 39–52 (2012).
31. Mason, J. M. *et al.* The SNM1B/APOLLO DNA nuclease functions in resolution of replication stress and maintenance of common fragile site stability. *Hum. Mol. Genet.* **22**, 4901–4913 (2013).
32. Wilson, T. E. *et al.* Large transcription units unify copy number variants and common fragile sites arising under replication stress. *Genome Res.* **25**, 189–200 (2015).
33. Bae, J.-B. *et al.* Snm1B/Apollo mediates replication fork collapse and S Phase checkpoint activation in response to DNA interstrand cross-links. *Oncogene* **27**, 5045–5056 (2008).
34. Dutertre, S. *et al.* Cell cycle regulation of the endogenous wild type Bloom's syndrome DNA helicase. *Oncogene* **19**, 2731–2738 (2000).
35. Yu, X. & Baer, R. Nuclear Localization and Cell Cycle-specific Expression of CtIP, a Protein That Associates with the BRCA1 Tumor Suppressor. *J. Biol. Chem.* **275**, 18541–18549 (2000).
36. Bootsma, D., Budke, L. & Vos, O. Studies on synchronous division of tissue culture cells initiated by excess thymidine. *Exp. Cell Res.* **33**, 301–309 (1964).
37. Bostock, C. J., Prescott, D. M. & Kirkpatrick, J. B. An evaluation of the double thymidine block for synchronizing mammalian cells at the G1-S border. *Exp. Cell Res.* **68**, 163–168 (1971).
38. Bolderson, E., Scorah, J., Helleday, T., Smythe, C. & Meuth, M. ATM is required for the cellular response to thymidine induced replication fork stress. *Hum. Mol. Genet.* **13**, 2937–2945 (2004).
39. Darzynkiewicz, Z., Halicka, H. D. & Zhao, H. Cell synchronization by inhibitors of DNA replication induces replication stress and DNA damage response: analysis by flow cytometry. *Methods Mol. Biol. Clifton NJ* **761**, 85–96 (2011).
40. Schmiester, M., Demuth, I., Schmiester, M. & Demuth, I. SNM1B/Apollo in the DNA damage response and telomere maintenance. *Oncotarget* **8**, 48398–48409 (2017).
41. Yeo, J. E., Lee, E. H., Hendrickson, E. A. & Sobeck, A. CtIP mediates replication fork recovery in a FANCD2-regulated manner. *Hum. Mol. Genet.* **23**, 3695–3705 (2014).
42. Chaudhury, I., Sareen, A., Raghunandan, M. & Sobeck, A. FANCD2 regulates BLM complex functions independently of FANCI to promote replication fork recovery. *Nucleic Acids Res.* **41**, 6444–6459 (2013).
43. Burma, S., Chen, B. P., Murphy, M., Kurimasa, A. & Chen, D. J. ATM Phosphorylates Histone H2AX in Response to DNA Double-strand Breaks. *J. Biol. Chem.* **276**, 42462–42467 (2001).

44. Ward, I. M. & Chen, J. Histone H2AX Is Phosphorylated in an ATR-dependent Manner in Response to Replicational Stress. *J. Biol. Chem.* **276**, 47759–47762 (2001).

45. Sirbu, B. M. *et al.* Analysis of protein dynamics at active, stalled, and collapsed replication forks. *Genes Dev.* **25**, 1320–1327 (2011).

46. Vesela, E., Chroma, K., Turi, Z. & Mistrik, M. Common Chemical Inductors of Replication Stress: Focus on Cell-Based Studies. *Biomolecules* **7**, 19 (2017).

47. Hill, T. M. & Marians, K. J. Escherichia coli Tus protein acts to arrest the progression of DNA replication forks in vitro. *Proc. Natl. Acad. Sci.* **87**, 2481–2485 (1990).

48. Mulcair, M. D. *et al.* A Molecular Mousetrap Determines Polarity of Termination of DNA Replication in E. coli. *Cell* **125**, 1309–1319 (2006).

49. Willis, N. A. *et al.* BRCA1 controls homologous recombination at Tus/Ter-stalled mammalian replication forks. *Nature* **510**, 556–559 (2014).

50. Ahn, J.-W. *et al.* SERBP1 affects homologous recombination-mediated DNA repair by regulation of CtIP translation during S phase. *Nucleic Acids Res.* **43**, 6321–6333 (2015).

51. Stumpf, C. R., Moreno, M. V., Olshen, A. B., Taylor, B. S. & Ruggero, D. The translational landscape of the mammalian cell cycle. *Mol. Cell* **52**, 574–582 (2013).

52. Kanakkanthara, A. *et al.* Cyclin A2 is an RNA binding protein that controls Mre11 mRNA translation. *Science* **353**, 1549–1552 (2016).

53. Ying, S., Hamdy, F. C. & Helleday, T. Mre11-Dependent Degradation of Stalled DNA Replication Forks Is Prevented by BRCA2 and PARP1. *Cancer Res.* **72**, 2814–2821 (2012).

54. Petermann, E., Orta, M. L., Issaeva, N., Schultz, N. & Helleday, T. Hydroxyurea-Stalled Replication Forks Become Progressively Inactivated and Require Two Different RAD51-Mediated Pathways for Restart and Repair. *Mol. Cell* **37**, 492–502 (2010).

55. Raderschall, E., Golub, E. I. & Haaf, T. Nuclear foci of mammalian recombination proteins are located at single-stranded DNA regions formed after DNA damage. *Proc. Natl. Acad. Sci.* **96**, 1921–1926 (1999).

56. Willis, N. A., Panday, A., Duffey, E. E. & Scully, R. Rad51 recruitment and exclusion of non-homologous end joining during homologous recombination at a Tus/Ter mammalian replication fork barrier. *PLOS Genet.* **14**, e1007486 (2018).

57. Willis, N. A. & Scully, R. Spatial separation of replisome arrest sites influences homologous recombination quality at a Tus/Ter-mediated replication fork barrier. *Cell Cycle* **15**, 1812–1820 (2016).

Chapter 3

Regulation and Post-Translational Modification of SNM1B

Abstract

Proteins that function in the DNA damage response often have roles in multiple pathways or respond to diverse forms of DNA damage. One such factor is the DNA nuclease, SNM1B, which has known functions in DNA interstrand crosslink repair, double-strand break repair, telomere maintenance, and the resolution of stalled replication forks. However, the precise control of SNM1B within these processes is not well understood. We sought to identify the mechanisms underlying the regulation of SNM1B and its functions within the cell cycle. SNM1B depletion results in decreased cellular survival to spindle stress, suggesting a potential role for SNM1B in mitosis. We determine that SNM1B is phosphorylated during G2/M-phases on its C-terminal residue S481. We also show that SNM1B phosphorylation is dispensable for its localization and binding to the telomere protein, TRF2, but supports protein stability by preventing polyubiquitination during mitosis. Together, these data reveal novel mechanisms for the regulation of SNM1B throughout the cell cycle.

Jordann Smak designed and performed the experiments for all figures.

Introduction

Maintenance of genome stability is critical to ensure normal cell growth and division. It relies on the precise control of DNA replication, DNA repair, and chromosome segregation and their proper integration with cell cycle progression. The cell cycle is intimately linked with genome protection, as the propagation of DNA damage into mitosis can result in chromosomal aberrations and aneuploidy. In addition, the DNA repair pathway choice is partly dictated by the cell cycle phase and type of damage encountered [1,2]. Proteins that function in the DNA damage response (DDR) often have multiple roles within various repair processes, many of which occur at different stages during cell division. Therefore, these factors must be tightly regulated to ensure their timely activation and recruitment for repair.

Most processes of the DDR have been extensively studied in S-phase, since this is the phase in which the bulk of DNA replication occurs. The DNA nuclease, SNM1B, is one DDR protein that has been implicated in facilitating the resolution of stalled replication forks during S-phase. SNM1B is a member of the metallo-β-lactamase/βCASP family of proteins and possesses 5' to 3' exonuclease activity [3]. SNM1B localizes to stalled forks and is required for the efficient recruitment of key DNA repair factors to sites of replication stress [4,5]. Depletion of SNM1B results in hypersensitivity to DNA crosslinking agents and to the DNA polymerase inhibitor, aphidicolin [5–7]. These SNM1B-deficient cells also display elevated levels of genome instability, including chromosomal breaks at difficult to replicate common fragile sites (CFSs) [4–6]. Together, these findings highlight a role for SNM1B during replication fork repair, but the mechanisms regulating its functions remain unknown.

Other DNA nucleases have been described to aid in the resolution of stalled replication forks. The MRE11 nuclease, which has both endo- and exonucleolytic activity, functions by resecting DNA at stalled forks to promote signaling and fork restart. It also partners with CtIP to facilitate end resection of DNA double-strand breaks (DSBs) that can result from fork collapse. During S- and G2-phase, CtIP protein levels increase, and it becomes phosphorylated in order to bind to MRE11 and stimulate DSB repair via homologous recombination (HR) [8–10]. Interestingly, CtIP and MRE11 have also been shown to impact chromosome segregation during mitosis, as depletion or

inhibition of these enzymes leads to defects in spindle assembly and chromosome alignment [11]. CtIP phosphorylation is not required for this mitotic function, thereby emphasizing the importance of post-translational modifications (PTMs) on regulating the various functions of DNA repair proteins in different phases of the cell cycle.

Another repair factor that has multiple roles within the DDR is the BLM DNA helicase. BLM has been shown to function in replication fork stabilization and repair, in the resection and dissolution of HR intermediates, and in chromosome segregation through the resolution of intertwined DNA structures called anaphase bridges [12,13]. Numerous studies have revealed that PTMs play a significant role in fine-tuning its functions in these repair processes [14]. The most striking finding is that BLM becomes hyperphosphorylated during mitosis [15–17]. BLM is phosphorylated on multiple sites to either target it for proteasomal degradation, to maintain checkpoint activation, or to stabilize and localize it to anaphase bridges [16–18]. In addition to its phosphorylation during mitosis, BLM protein levels are also regulated throughout the cell cycle. BLM becomes stabilized during S-phase and its levels are significantly reduced as cells cycle into G1-phase [15]. These changes in protein stability and regulation through PTMs correlate with the distinct roles for BLM in different cell cycle phases.

Similar to BLM, previous data from Chapter 2 demonstrates that the DNA nuclease, SNM1B, also becomes stabilized by agents that induce synchronization in S-phase. Therefore, it is possible that SNM1B may be regulated by similar mechanisms as BLM to dictate its roles throughout the cell cycle. Most of the known functions of SNM1B are specific to S- and G2-phase, but the growing evidence for mitotic functions of other repair proteins, such as CtIP and BLM, prompted us to examine its regulation and role in mitosis.

We found that SNM1B is important for cellular survival in response to spindle stress and that it is phosphorylated during G2-phase and mitosis. SNM1B phosphorylation occurs within its C-terminal domain, specifically on the serine residue 481. Investigations using a non-phosphorylatable mutant revealed that phosphorylation is dispensable for proper localization of SNM1B, but may promote protein stability by preventing polyubiquitination and degradation by the proteasome. Together, these data provide novel insight into the post-translational regulation of SNM1B.

Results

SNM1B-depleted cells are sensitive to microtubule inhibition

Although little is known about SNM1B in mitosis, it has been shown to function in an early mitotic prophase checkpoint, also known as the antephase checkpoint [19]. When cells encounter various stresses, such as chromosomal damage and microtubule stress, the prophase checkpoint delays commitment to mitosis by preventing or reversing chromatin condensation before nuclear envelope breakdown [20]. The metallo-β-lactamase/βCASP family member, SNM1A, and the ubiquitin ligase, checkpoint with FHA and ring finger domains (CHFR), have also been reported to function in the prophase checkpoint [21,22]. Interestingly, knockdown of SNM1A and CHFR sensitizes cells to microtubule inhibitors [21,23]. A similar phenotype was also observed for cells deficient of the Fanconi anemia (FA) protein, FANCA [24]. Since SNM1B functions within the FA pathway and participates in the prophase checkpoint, these findings prompted us to examine whether SNM1B is important in the response to spindle stress.

Endogenous SNM1B is expressed at very low levels and is undetectable using commercially available antibodies [6,3]. Therefore, we generated HCT116 cell lines stably expressing an siRNA-resistant, V5-tagged SNM1B cDNA or an empty vector (EV) as a control. To examine the role of SNM1B in the response to spindle stress, SNM1B was knocked down in the HCT116 EV cell line using a previously characterized siRNA and treated with nocodazole, a reversible inhibitor of microtubule polymerization that stalls cells in prometaphase [4]. After 24 hours, the mitotic shake-off cells were replated at low density, and sensitivity to nocodazole was assessed using crystal violet staining of surviving colonies. SNM1B-depleted cells were significantly more sensitive to nocodazole treatment compared to the non-silencing (NS) controls, with cellular survival reduced to approximately 15% compared to 80% ($p<0.01$; Figure 3.1A). This suggests that SNM1B may have a functional role during mitosis, specifically in response to spindle stress.

SNM1B is phosphorylated in G2-phase and mitosis

The finding that SNM1B is important for survival after nocodazole release prompted us to examine the protein dynamics of SNM1B as cells enter G2/M-phases. Considering that several DNA repair proteins are phosphorylated in mitosis, we were particularly interested in PTMs. HCT116 cells expressing V5-tagged SNM1B were treated with nocodazole to synchronize cells in mitosis, and a prominent, slow-migrating band was observed for SNM1B in the Western blot (Figure 3.1B; 3.S1A). Similar results were seen in the osteosarcoma U2OS cell line and in the transformed embryonic kidney 293T cell line, suggesting that the shift is not cell type-specific or characteristic to cancer cells (Figure 3.S1B). Together, these data provide evidence that SNM1B is post-translationally modified during mitosis.

Protein phosphorylation is a common PTM that serves as a key regulatory mechanism during the progression of mitosis. To determine whether the observed modification of SNM1B is phosphorylation, cell lysates were treated with lambda protein phosphatase (λPPase), which releases phosphate groups from serine, threonine, and tyrosine residues. The shifted band was eliminated by lambda phosphatase treatment and retained with addition of phosphatase inhibitors (Figure 3.1C). This finding indicates that the shifted form of SNM1B during mitosis is due to phosphorylation. The shifted band is also observed in a Phos-tag SDS-PAGE gel, which specifically retards the migration of phosphorylated proteins (Figure 3.S1C). This provides further evidence that the modification of SNM1B is phosphorylation.

To verify that phosphorylation of SNM1B is not solely in response to microtubule inhibition, the appearance of the shifted band was examined in unperturbed conditions. Cells were sorted into G1-, S-, and G2/M-phases of the cell cycle using Hoechst staining and flow cytometry. SNM1B phosphorylation was more prominent in G2/M- compared to G1- or S-phase cells (Figure 3.1D). We also examined the dynamics of phosphorylated SNM1B by synchronizing and releasing cells from a double thymidine block, which reversibly stalls cells in early S-phase. The level of phosphorylated SNM1B was lower in thymidine-blocked cells compared to nocodazole-synced cells (Figure 3.S1C), and the modified form accumulated as cells were released from the

thymidine block into G2/M (Figure 3.1E). The ratio of modified SNM1B/unmodified SNM1B protein was approximately 0.5 when 65% of the cells were in G2/M compared to 0.2 when only 10% of the cells were in G2/M (Figure 3.1F). This supports the finding that SNM1B is preferentially phosphorylated in G2/M-phases compared to other stages of the cell cycle.

To verify that SNM1B is phosphorylated in G2-phase in addition to mitosis, cells were synchronized using the cyclin-dependent kinase 1 (CDK1) inhibitor, RO3306 (CDK1i). This inhibitor is effective against both CDK1/cyclin B and CDK1/cyclin A complexes, and it reversibly stalls cells in late G2-phase (Figure 3.S1A) [25]. SNM1B was phosphorylated in cells treated with the CDK1 inhibitor for 20 hours, revealing that this modification arises as early as late G2-phase (Figure 3.1G).

Dependence of SNM1B phosphorylation on the ATM, ATR, or DNA-PKcs kinases

ATM, DNA-PKcs, and ATR are members of the phosphatidylinositol 3-kinase-related kinase (PIKK) family of serine/threonine kinases which function in DNA repair pathways. ATM acts as an apical activator of the DNA DSB response by controlling an extensive signaling network, whereas DNA-PKcs is involved in DSB repair though it roles in non-homologous end-joining [26,27]. ATR is also activated by DSBs, but it responds to a broader spectrum of DNA damage and plays a central role in the response to replication stress [28]. Since SNM1B is a nuclease that functions in the response to DNA damage and replication stress, I first examined whether ATM, DNA-PKcs, or ATR were involved in SNM1B phosphorylation. Treatment with inhibitors of these kinases resulted in no change in the phosphorylation status of SNM1B during mitosis (Figure 3.2A,B). Cells treated with bleomycin or UV were used as controls to evaluate successful kinase inhibition (Figure 3.S2A,B).

ATM, ATR, and DNA-PKcs recognize and phosphorylate a consensus sequence of S/TQ, which usually reside in clusters within the protein substrate [29]. SNM1B has three S/TQ sites, one of which (S444) was previously reported in a mass spectrometry study for identification of ATM/ATR targets [30]. We mutated this serine, along with another SQ site (S418), and examined the phosphorylation of SNM1B during mitosis. After nocodazole treatment, both serine to alanine mutants displayed a discernable shift

in the Western blot, suggesting that these sites are not the major sites for phosphorylation (Figure 3.2C). In concert with the inhibitor data, these findings suggest that the DNA repair kinases, ATM, ATR, and DNA-PKcs, are not responsible for the observed phosphorylation of SNM1B.

Dependence of SNM1B phosphorylation on mitotic kinases

Because the phosphorylation of SNM1B is prominent during late G2-phase and mitosis, we investigated the potential role of mitotic kinases in this phosphorylation event. These kinases included CDK1, Aurora A, Aurora B, NEK2, and PLK1. CDK1 is considered the master regulator of mitosis. Entry into mitosis depends on CDK1 dephosphorylation and activation, whereas exit from mitosis depends on its deactivation as a consequence of cyclin destruction. CDK1 has been shown to phosphorylate several DNA nucleases, including MRE11, CtIP, and EXO1, to regulate DNA end resection throughout the cell cycle [31–34]. The Aurora kinase family, polo-like kinase 1 (PLK1), and NIMA related kinase 2 (NEK2) all play important roles in the progression of mitosis. Aurora A promotes mitotic spindle assembly and centrosome maturation, whereas Aurora B functions primarily in chromosome segregation and kinetochore attachment [35]. PLK1 is involved in centrosome maintenance, chromosome dynamics, and mitotic exit, and NEK2 functions in regulating centrosome architecture [36,37]. PLK1 and NEK2 have also been shown to phosphorylate DNA repair proteins in various cellular processes [24,38,39].

SNM1B was identified as a potential substrate of Aurora kinases in a phosphoproteomic study [40]. Therefore, I first examined the potential role of Aurora B in SNM1B phosphorylation. Cells expressing V5-tagged SNM1B were synchronized with nocodazole for 18 hours and treated with the Aurora B inhibitor, ZM447439 (AurBi), for an additional 1 hour. Phosphorylated SNM1B was dramatically decreased upon treatment with the Aurora B inhibitor compared to the DMSO-treated control (Figure 3.2D). Histone H3 S10 is a known substrate for Aurora B, and its phosphorylation was used as a control to ensure successful kinase inhibition.

I next examined the full panel of mitotic kinase inhibitors to assess their effect on SNM1B phosphorylation. There was no change in phosphorylated SNM1B after

treatment with inhibitors against PLK1 or NEK2. However, similar to Aurora B inhibition, phosphorylation of SNM1B was decreased after treatment with Aurora A or CDK1 inhibitors (Figure 3.2E). The concentration of inhibitor used to target Aurora A in this assay could also potentially inhibit Aurora B [41]. Therefore, lower doses were tested and found to cause no change in phosphorylated SNM1B (Figure 3.S2C). These data provide evidence that Aurora A, PLK1, and NEK2 are likely not involved in SNM1B phosphorylation during mitosis.

To further investigate the potential role of Aurora B in SNM1B phosphorylation, alanine point mutations were generated for several serine or threonine residues that reside in Aurora kinase consensus sites within SNM1B (Figure 3.3A). Some of these residues are more evolutionarily conserved than others, and one site does not conform to the general consensus sequence for Aurora targets (S311). This site was chosen because it was previously identified as a potential Aurora kinase substrate in a mass spectrometry study [40]. HCT116 cells were transiently transfected with plasmids expressing the V5-tagged SNM1B point mutants and treated with nocodazole for 18 hours. The phosphorylation status of each point mutant was assessed using the Phos-tag SDS-PAGE system (Figure 3.3B) or traditional SDS-PAGE (Figure 3.3C) followed by Western blotting. None of the examined point mutants altered SNM1B phosphorylation during mitosis. This suggests that SNM1B may not be a direct target of Aurora B kinase activity or that SNM1B is phosphorylated at alternative sites by Aurora B or other kinases.

Phosphorylated SNM1B is reduced as cells exit mitosis

The decrease in SNM1B phosphorylation after Aurora B or CDK1 inhibition could suggest a role for these kinases in the indirect phosphorylation of SNM1B. However, there is evidence that demonstrates that Aurora B or CDK1 inhibition can lead to spindle assembly checkpoint (SAC) bypass [25,42–44]. The SAC ensures that all chromosomes are correctly attached to spindle microtubules before division, and its activation halts the metaphase-anaphase transition. SAC bypass would allow the cells to continue through mitosis despite perturbed mitotic spindle formation induced by nocodazole. As shown in cell cycle profiles, prolonged inhibition of Aurora B after SAC activation induces a

broadening and decrease in G2/M peak height, indicative of possible SAC bypass (Figure 3.S3A). Therefore, SNM1B phosphorylation could be decreased after Aurora B inhibition due to progression through mitosis and the events that take place during this process. One major event that is essential for mitotic exit is the degradation of cyclin B by the proteasome [45]. To prevent this degradation process and the resulting mitotic progression, cells were treated with the proteasome inhibitor, MG132, in the presence or absence of the Aurora B inhibitor after SAC activation. Cell cycle profiles reveal that Aurora B inhibition reduced G2/M peak height, whereas the profiles remain unaltered in samples treated with MG132 (Figure 3.S3B). In the Western blot analysis, SNM1B was still phosphorylated when mitotic cells were treated with MG132 alone or in combination with AurBi (Figure 3.4A). The same was observed for co-treatment of mitotic cells with MG132 and CDK1i (Figure 3.S3C). This suggests that proteasome inhibition prevents the loss of phosphorylated SNM1B. In addition, treatment with the CDK1i or AurBi without prior SAC activation still induces SNM1B phosphorylation (Figure 3.1G; 3.S3D). Together, these data support the hypothesis that Aurora B or CDK1 inhibition may promote the loss of SNM1B phosphorylation via SAC bypass.

To further examine SNM1B phosphorylation after mitotic exit, cells were blocked with nocodazole for 18 hours and released into drug-free media for 4 or 8 hours to allow for cell cycle progression. Progression was monitored by cyclin A and B1 levels, which increased and decreased after release, respectively. Phosphorylated SNM1B was no longer detected after mitotic release at either the 4 or 8 hour timepoint (Figure 3.4B). These results indicate that SNM1B is no longer phosphorylated as cells exit mitosis.

Identification of a major phosphorylation site on SNM1B

To identify the phosphorylation site(s) on SNM1B, deletion mutants were generated (Figure 3.5A). All mutants harbored a V5 tag at the C-terminus and retained the TRF2 binding domain within residues 496-532. Upon treatment with nocodazole, the SNM1B mutant consisting of only the catalytic N-terminal domain (N-term SNM1B-V5) did not show a mobility shift similar to the WT protein (Figure 3.5B). This indicates that SNM1B is phosphorylated on its C-terminus. Upon examination of SNM1B mutants lacking various regions of the C-terminal domain, only the Δ399-465 and the Δ466-495

mutants lacked a discernable shift in the Western blot after treatment with nocodazole (Figure 3.5C). Upon further investigation using the Phos-tag SDS-PAGE system, the Δ399-465 mutant revealed a more drastically shifted band compared to the Δ466-495 mutant after exposure to nocodazole (Figure 3.5D). This suggests that a major phosphorylation site resides within residues 466-495 of SNM1B. There are only three highly conserved serine or threonine residues within this region of SNM1B – S474, S481, and S487 (Figure 3.5E). These residues were mutated to alanines by site-directed mutagenesis to create a triple point mutant (3SA SNM1B). When cells expressing this mutant form of SNM1B were treated with nocodazole, there was no distinct shift observed in the Western blot, suggesting that SNM1B is phosphorylated at one or several of these sites during mitosis (Figure 3.5F). The S474A and S481A individual point mutants were generated, and only the S481A mutant showed decreased phosphorylation after nocodazole treatment (Figure 3.5G). These findings reveal that S481 is a major phosphorylation site on SNM1B.

SNM1B phosphorylation is dispensable for its localization to stalled forks and for its interaction with TRF2

To ensure that the point mutations do not potentially disrupt known functions of SNM1B in response to replication stress, cellular localization was examined by fractionations and foci formation. Previous studies demonstrate that SNM1B forms subnuclear foci in response to the polymerase inhibitor, aphidicolin, and data from Chapter 2 shows that SNM1B becomes highly associated with chromatin after aphidicolin treatment [5]. Both WT and 3SA SNM1B displayed an increase in chromatin association after exposure to aphidicolin, revealing that the mutations in SNM1B do not alter the localization of the protein in response to replication stress (Figure 3.6A). This is supported by the finding that, similar to WT SNM1B, the 3SA mutant exhibits increased foci formation after aphidicolin-induced fork stalling compared to the untreated controls (Figure 3.6B) [5]. This increase was approximately 4-fold and 2.3-fold for the WT and 3SA mutant, respectively. The percentage of cells with foci formation was slightly higher in all conditions for 3SA SNM1B compared to WT, but this finding needs to be further investigated.

Phosphorylation can often serve as a key regulator of protein interactions during cellular processes. Phosphorylation can both initiate new protein complex formation and cause dissociation of existing binding partners. One major binding partner of SNM1B is the telomere protein, TRF2. SNM1B has been shown to interact with TRF2 for the protection of telomere ends during DNA replication in S-phase [46]. It is unknown whether or not SNM1B and TRF2 maintain their association during mitosis, or if their interaction is affected by protein modifications. To examine this, SNM1B was immunoprecipitated from nocodazole-treated cells expressing Myc-TRF2. Myc-TRF2 co-immunoprecipitated with N-term SNM1B in both asynchronous and nocodazole-treated cells (Figure 3.6C). The same result was observed when the 3SA SNM1B mutant was immunoprecipitated (Figure 3.6D). These data suggest that the phosphorylation of SNM1B does not affect the interaction between TRF2 and SNM1B during mitosis.

S481A SNM1B mutant is polyubiquitinated during mitosis

Several DNA repair proteins have been previously shown to undergo proteasomal degradation after phosphorylation in mitosis. FANCM, a member of the FA pathway, becomes hyperphosphorylated and subsequently degraded during mitosis to allow for the release of the FA core complex from chromatin [47]. Additionally, the BLM helicase contains a phospho-degron recognized by the E3 ubiquitin ligase, Fbw7α, that polyubiquitinates and targets BLM for degradation [17]. Based on the findings that phosphorylated SNM1B is reduced as cells exit mitosis, I hypothesized that phosphorylated SNM1B may be similarly targeted for degradation by the proteasome. To examine this, HCT116 cells were transiently transfected with plasmids expressing WT or S481A SNM1B-V5, treated with nocodazole and MG132, and harvested for immunoprecipitation of K48-linked ubiquitin. After MG132 treatment, a distinct smearing pattern representing polyubiquitination was observed for the S481A mutant that was not observed for the WT control (Figure 3.7). This demonstrates that phosphorylation on S481 may be important for preventing polyubiquitination and subsequent degradation of SNM1B in mitosis.

Discussion

This study has revealed a novel modification of SNM1B during mitosis, a phase of the cell cycle in which little is known about the functions of SNM1B. I have shown that SNM1B is predominantly phosphorylated in G2/M-phases and that phosphorylated SNM1B is drastically reduced as cells exit mitosis. The PIKK members, ATM, ATR, and DNA-PKcs, which function in DNA repair pathways, are not involved in the phosphorylation of SNM1B. Additionally, inhibition of mitotic kinases during SAC activation revealed that PLK1 and NEK2 do not alter the phosphorylation status of SNM1B. However, inhibition of Aurora A, Aurora B, and CDK1 resulted in a reduction of phosphorylation, which is most likely due to SAC bypass. This finding is supported by evidence that SNM1B phosphorylation is reduced as cells are released from mitotic arrest in the absence of mitotic kinase inhibitors. I have also identified that S481 is a major site of phosphorylation on SNM1B, and that mutation of this serine to an alanine does not disrupt SNM1B localization during replication stress or its interaction with the telomere protein, TRF2. However, the S481A mutation does promote polyubiquitination of SNM1B, suggesting that phosphorylation may play a role in regulating SNM1B stability.

SNM1B has been previously shown to function in the prophase checkpoint during mitosis. Upon exposure to microtubule inhibitors, SNM1B-deficient cells exhibit increased levels of phospho-histone H3 and a failure to arrest in prophase with uncondensed chromatin [19]. Similar phenotypes were observed for the metallo-β-lactamase/βCASP family member, SNM1A, and for the ubiquitin ligase, CHFR, both of which have been implicated in the early mitotic checkpoint [21,22]. Knockdown of SNM1A and CHFR also sensitizes cells to microtubule inhibitors, such as nocodazole [21,23]. This observation prompted us to examine the potential role of SNM1B in cellular survival after spindle stress.

Cells that experience prolonged mitotic arrest upon microtubule inhibition (MTI) can succumb to one of several fates. They can resume normal cell division, undergo apoptosis soon after mitosis, or fail cytokinesis and enter the tetraploid state. These tetraploid cells can continue dividing, become senescent, or execute cell death at a later point in time [48–50]. These fates differ depending on the cell type and the MTI used to

induce arrest. In response to nocodazole-induced arrest, most HCT116 cells are able to eventually exit mitosis, with a small proportion of cells undergoing apoptosis in the following interphase [51]. Since SNM1B-depleted HCT116 cells exhibit increased sensitivity to nocodazole treatment in a long-term colony formation assay, it is possible that knockdown cells apoptose in the following interphase or in a tetraploid state after release from microtubule inhibition. This is supported by findings that SNM1B-deficient cells display binucleation and proliferation defects through apoptosis, even in the absence of spindle stress [52–55].

Interestingly, prolonged mitotic arrest induces telomere uncapping, increased telomere dysfunction-induced foci (TIF), and loss of telomeric 3' overhangs [56]. Telomeres are normally protected by the shelterin complex and the formation of a T-loop structure, which involves insertion of the 3' overhang back into the double-stranded portion of the DNA [57,58]. Knockdown of the shelterin protein, TRF2, has been shown to exacerbate telomere deprotection and increase mitotic cell death [59]. Since SNM1B physically interacts with TRF2 and has been implicated in the generation of 3' overhangs at leading-strand telomeres, SNM1B depletion could also promote telomere deprotection. If so, this may provide an explanation as to why knockdown of SNM1B sensitizes cells to nocodazole. To determine if this phenotype is associated with telomere uncapping, TIF formation could be analyzed after SNM1B knockdown and mitotic arrest. It would also be interesting to examine the sensitivity of other cell lines to nocodazole and to additional types of microtubule inhibitors.

The phosphorylation of SNM1B that we observed in this study was most prominent during G2-phase and mitosis, suggesting that mitotic kinases may contribute to this modification. Interestingly, inhibition of Aurora B and CDK1 both reduced SNM1B phosphorylation, but only after prior SAC activation induced by nocodazole. Therefore, we hypothesize that this loss of SNM1B phosphorylation could be due to SAC bypass, as studies have shown that Aurora B and CDK1 inhibition during MTI-induced mitotic arrest leads to bypass of this checkpoint [25,42,44]. After nocodazole treatment, CDK1-inhibited cells can rapidly exit mitosis, whereas cells exposed to Aurora B inhibitors stay arrested for a longer period of time [25,42–44,60]. This supports the finding that SNM1B phosphorylation is completely lost in nocodazole and CDK1i-treated

cells, compared to AurBi-treated cells where some SNM1B phosphorylation is retained. Although Aurora B and CDK1 inhibition can lead to SAC bypass, these effects can be suppressed by co-treatment with the proteasome inhibitor, MG132 [43,44]. It is well established that APC-mediated degradation of cyclin B serves as a key regulator of mitotic exit, and by preventing this degradation process with the addition of MG132, cells will remain stalled in metaphase [45,61]. Based on the findings in this current study, co-treatment of AurBi or CDK1i with MG132 results in retention of phosphorylated SNM1B. This suggests that MG132 may be suppressing SAC bypass, therefore preventing the loss of SNM1B phosphorylation that is normally observed in AurBi- or CDK1i-treated cells. This concurs with data showing that SNM1B phosphorylation is reduced as cells are released from nocodazole arrest in the absence of kinase inhibitors. The loss of SNM1B phosphorylation coincides with increased levels of phosphatase activity upon mitotic exit, therefore the role of protein phosphatases in the potential dephosphorylation of SNM1B should be examined as well.

SAC bypass has also been observed in response to Aurora A inhibition in MTI-arrested cells [62,63]. Treatment with lower concentrations of the Aurora A inhibitor, MLN8237, produced no change in SNM1B phosphorylation. However, at a higher concentration of 1μM, SNM1B phosphorylation was reduced to similar levels as observed for Aurora B inhibition. It has been previously reported that MLN8237 concentrations higher than 50nM could also potentially inhibit Aurora B [41]. This suggests that treatment with MLN8237 at higher doses could promote SAC bypass, either through inhibition of Aurora A and/or Aurora B. Nonetheless, my findings indicate that mitotic kinases regulate the phosphorylated state of SNM1B, either directly or indirectly.

It would be interesting to determine whether other kinases contribute to SNM1B phosphorylation. The identification of S481 as a major SNM1B phosphorylation site could guide future studies to determine the kinase involved in this PTM. The S481 residue resides in a common pSP or pSP-like motif that is recognized by several families of kinases, including ERK/MAPK and other CDKs [64]. Using kinase prediction software, JNK, p38 MAPK, and CDK5 have been identified as the top potential kinases acting on S481 in SNM1B [65]. Studies have shown that p38 MAPK and JNK, kinases generally involved in stress response pathways, are activated in mitosis in response to

microtubule inhibition [66–68]. CDK5 is a member of the CDK family and has been mainly associated with regulating the cytoarchitecture of the central nervous system [69]. However, it has also been implicated in the regulation of actin dynamics and microtubule stability [69]. Since the MAPK and CDK5 kinases have been reported to be active in mitosis or function in processes that are required for spindle formation, they may have a yet unknown role in SNM1B phosphorylation. These kinases, and potentially others, should be tested for their effect on the modification of SNM1B.

Although SNM1B phosphorylation is dispensable for its known interaction with TRF2, it is possible that this PTM can alter other protein interactions involving SNM1B. For example, SNM1B has been reported to interact with PSF2, a member of the GINS complex that is important for initiation of DNA replication [70]. SNM1B may interact with PSF2 during replication in S-phase, and phosphorylation could allow it to disassociate from PSF2 as cells enter mitosis. However, the role of phosphorylation and the dynamics of this interaction is still unknown and requires further investigation. SNM1B has also been reported to interact with proteins that function in spindle assembly during mitosis, specifically β-tubulin and astrin [19,71]. Mass spectrometry experiments revealed an association between SNM1B and β-tubulin, which is a major component of cytoskeletal microtubules and mitotic spindles [71]. However, the functional importance of this interaction has yet to be elucidated. Astrin is a mitotic spindle-associated protein that is essential for progression through mitosis, and knockdown of astrin results in multipolar or disordered spindles and cell death [72]. The interaction between SNM1B and astrin is enhanced after mitotic arrest by nocodazole, and both proteins have been shown to localize to the centrosome [19]. Therefore, we cannot rule out the possibility that SNM1B phosphorylation affects this interaction with astrin or alters its localization to centrosomes during mitosis.

Several DNA repair proteins undergo proteasomal degradation after phosphorylation in mitosis. For example, FANCM and BLM are both phosphorylated to target them for subsequent polyubiquitination, which in turn regulates various repair processes within the cell [41,77]. Based on the findings that phosphorylated SNM1B is reduced as cells exit mitosis, I hypothesized that phosphorylated SNM1B may be degraded by the proteasome. Unexpectedly, the S481A SNM1B mutant, which disrupts

phosphorylation of SNM1B during mitosis, exhibited increased polyubiquitination compared to the WT control. This suggests that the loss of phosphorylation promotes polyubiquitination and subsequent degradation of SNM1B rather than preventing it. SNM1B has previously been shown to be polyubiquitinated, and this polyubiquitination can be prevented by binding to TRF2 [73]. I have shown that non-phosphorylatable SNM1B mutants can still interact with TRF2, indicating that polyubiquitination of the S481A mutant is not induced by disruption of TRF2 binding. However, it is possible that phosphorylation facilitates an unknown interaction with another protein that regulates the stability of SNM1B. Loss of this phosphorylation, and therefore loss of the stabilizing interaction, could then lead to proteasomal degradation.

Overall, results from this study reveal an important role for SNM1B in mitosis and provide insight into the regulation of SNM1B by post-translational modifications. Because SNM1B functions during various processes within the DDR, elucidating the mechanisms that control its functions will help us understand how it prevents genomic instability.

Materials and Methods

Generation of Cell Lines and SNM1B Mutants

SNM1B deletion constructs and point mutants were generated using Q5 site-directed mutagenesis (NEB) according to the manufacturer's instructions. A previously described pLL-IRES-GFP lentiviral vector harboring siRNA-resistant SNM1B cDNA was used as the template for mutagenesis [4]. This SNM1B cDNA contains a C-terminal V5 epitope tag, and an empty vector (EV) was used as a control. Lentiviruses were generated by co-transfecting the lentiviral constructs with packaging plasmids pLP1, pLP2, and pVSVG (Invitrogen) into 293T cells using calcium phosphate. The viral supernatants were collected after 48 hours and filtered through 0.45mm PVDF filters (Millipore). HCT116 and U2OS cells were transduced with 1 ml viral media containing 4μg/ml polybrene and 1 ml culture media supplemented with 10% FBS for 24 hours. Cells were harvested 24 hours later, and expression of the SNM1B-IRES-GFP cassette was determined by flow cytometry. GFP-positive HCT116 cells were sorted (UM Flow

Cytometry Core) to increase the percentage of cells expressing SNM1B within the population.

Nocodazole Sensitivity Assay

HCT116 EV cells were transfected with 50nM NS or siSNM1B siRNAs using Lipofectamine 2000 (Invitrogen) and treated with 60ng/ml nocodazole at 48 hours post-transfection. After 24 hours in nocodazole, cells were harvested by mitotic shake-off, thoroughly washed in PBS, and plated at low density in 12-well plates in triplicate. Cells were grown for 6-9 days and fixed with 10% methanol/10% acetic acid for 10 min at room temperature. Cells were stained with 1% crystal violet in methanol for 10 min, washed thoroughly, and air-dried overnight. Crystal violet was resolubilized using 0.1% SDS in methanol and absorbance was measured at 595nm. Percent survival was calculated relative to DMSO-treated controls and plotted as the mean and SEM from three independent experiments.

Cell Synchronization and Cell Cycle Analyses

For the double thymidine block, HCT116 cells stably expressing WT SNM1B-V5 were treated with 2mM thymidine for 18 hours, released into fresh media for 6 hours, and exposed to 2mM thymidine for another 18 hours. After washing with PBS, cells were released from the block and harvested at 0, 2, 4, 6, and 8 hours for cell cycle analysis and immunoblotting. For synchronization in G2-phase or mitosis, cells were treated with 9μM RO3306 (CDK1i; Cayman Chemical) for 20 hours or 400ng/ml nocodazole for 18 hours, respectively. For nocodazole release experiments, a final concentration of 100ng/ml was used. All mitotic cells were harvested by mitotic shake-off.

To examine cell cycle profiles after synchronization, cells were fixed with cold 70% ethanol, stored at -20°C, and stained with a solution containing 50μg/ml propidium iodide, 50μg/ml RNase A, and 0.1% Triton X-100 for 30 minutes at room temperature. Cells were analyzed using an Accuri C6 or Novocyte flow cytometer and FlowJo software.

Protein Kinase Inhibition

Protein kinase inhibitors were used as follows: ATM, KU-55933 (10μM, Cayman Chemical); ATR, VE-822 (1μM, Cayman Chemical); DNA-PKcs, NU7026 (20μM, Tocris Biosciences); Aurora A, MLN8237 (20nM, 100nM, 1μM, Cayman Chemical); Aurora B, ZM447439 (5μM, Tocris Biosciences); PLK1, BI-6727 (25nM, 1μM, Cayman Chemical); NEK2, INH6 (50μM, Cayman Chemical); CDK1, RO3306 (9μM, Cayman Chemical).

Transient Transfections

HCT116 or 293T cells were plated in 6-well plates and transfected with 2.5μg WT or mutant SNM1B-V5 lentiviral vector using Lipofectamine 2000 as instructed by the manufacturer. At 24 hours post-transfection, cells were treated with 400ng/ml nocodazole and harvested 18 hours later by mitotic shake-off. For ubiquitin co-immunoprecipitation experiments, HCT116 cells were plated in 10cm dishes and transfected with 10μg WT or mutant SNM1B-V5 pEF6 vector using Lipofectamine 2000. At 24 hours post-transfection, cells were treated with 400ng/ml nocodazole for 18 hours, treated with or without 40μM MG132 (Sigma) for 1 hr, and harvested by mitotic shake-off. For TRF2 co-immunoprecipitations, HCT116 cells were co-transfected with 5μg WT or mutant SNM1B-V5 lentiviral vector and 5μg of a construct expressing Myc-TRF2 using Lipofectamine 2000. At 24 hours post-transfection, cells were treated with 400ng/ml nocodazole for 18 hours and harvested by mitotic shake-off.

Western Blot Analyses

Cells were harvested and lysed on ice for 1 hour in CSK buffer (10mM PIPES pH 6.8, 100mM NaCl, 300mM sucrose, 1mM $MgCl_2$, 0.1% Triton X-100) containing protease inhibitors (Roche Complete Mini EDTA-free), phosphatase inhibitors (Roche PhosSTOP), and benzonase (Sigma). Lysates were centrifuged at 14,000 RPM for 20 min and protein concentrations were determined using the Bradford assay (BioRad). Cell extracts were resolved by SDS-PAGE and transferred following standard procedures. For Phos-tag SDS-PAGE, 25-50μM phos-binding reagent acrylamide (APExBIO) and 10mM $ZnCl_2$ were added to bis-tris-HCl resolving gels before

polymerization. Separation and transfer were performed as previously described [74]. Proteins were analyzed using the appropriate primary and secondary antibodies, and bands were visualized using Li-Cor Odyssey 2.1 software or the SuperSignal West Pico system (Pierce). ImageJ was used for Western blot protein quantifications.

The following primary antibodies were used: V5 (Invitrogen); BLM (Novus Biologicals); Cyclin B1 (Santa Cruz); Cyclin A (Santa Cruz); phospho-histone H3 S10 (Cell Signaling); phospho-KAP1 S824 (Bethyl); phospho-CHK1 S345 (Cell Signaling); H2AX (Millipore); Myc-tag (Cell Signaling); Vinculin (Cell Signaling); GAPDH (Cell Signaling and Santa Cruz). Secondary antibodies were: IRDye conjugated goat anti-rabbit or anti-mouse IgG (Li-Cor Biosciences) and HRP-conjugated anti-mouse IgG (Jackson ImmunoResearch).

Lambda Phosphatase Treatment

HCT116 cells stably expressing WT SNM1B-V5 were treated with DMSO or 400ng/ml nocodazole for 18 hours. Cells were lysed as described above without the addition of phosphatase inhibitors. Extracts were treated with lambda protein phosphatase (NEB) according to the manufacturer's instructions and incubated at 30°C for 20 min. Controls were incubated on ice with an equivalent amount of buffer without lambda phosphatase and phosphatase inhibitors were added to one sample to inhibit enzymatic activity. BLM phosphorylation was analyzed as a control.

Hoechst Staining and Cell Sorting

HCT116 cells stably expressing WT SNM1B-V5 were suspended at 1.5 x 10^6 cells/ml in McCoy's medium containing 2% FBS. Cells were incubated with Hoechst dye at a final concentration of 5μg/ml for 30 min at 37°C with intermittent shaking. Fluorescence-activated cell sorting (FACS) was performed to sort the cells into G1-, S-, and G2/M-phase populations based on DNA content. Cells were lysed, and immunoblotting was used to assess WT SNM1B-V5 protein levels in each phase of the cell cycle.

Cellular Fractionations

HCT116 cells stably expressing WT or 3SA SNM1B-V5 were treated with DMSO or 1μM aphidicolin for 24 hours. Cells were harvested and pellets were first resuspended in fractionation buffer I (50mM HEPES pH 7.5, 150mM NaCl, 1mM EDTA, 0.2% NP-40, supplemented with protease and phosphatase inhibitors) for 5 min on ice. After centrifugation at 1000 × g for 5 min, the supernatant was collected (cytoplasmic fraction), and the pellets were washed with fractionation buffer I. The nuclear pellets were then lysed for 40 min on ice with fractionation buffer II (50mM HEPES pH 7.5, 150mM NaCl, 1mM EDTA, 0.5% NP-40, supplemented with protease and phosphatase inhibitors). The supernatants were collected (nuclear faction) after centrifugation at 16,000 × g for 15 min. The final pellets were lysed in RIPA buffer (50mM Tris-HCl pH 8.0, 150mM NaCl, 1% NP-40, 0.5% sodium deoxycholate, 0.1% SDS, supplemented with protease and phosphatase inhibitors), sonicated, and cleared by centrifugation at 16,000 × g for 20 min (chromatin fraction). The whole cell extracts (WCEs) were prepared in a similar manner as the chromatin fractions. Equal concentrations of each fraction were analyzed by immunoblotting, with GAPDH and H2AX serving as controls for cytoplasmic and chromatin fractions, respectively.

Immunofluorescence of Subnuclear Foci

HCT116 cells stably expressing WT or 3SA SNM1B-V5 were grown on glass coverslips in 12-well plates and treated with DMSO or 1μM aphidicolin for 24 hours. Cells were fixed in ice-cold 70% methanol/30% acetone for 20 min at -20°C and air-dried at room temperature. Cells were stained with primary anti-V5 antibody (Invitrogen) for 45 min followed by anti-mouse Alexa Fluor 488 secondary antibody (Invitrogen Molecular Probes) for 45 min. Coverslips were mounted on slides using ProLong Gold Antifade Reagent with DAPI (Life Technologies) and images were acquired using an Olympus BX61 microscope and FISHview software (Applied Spectral Imaging).

Co-Immunoprecipitations

Cells were lysed for 1 hour at 4°C with rotation in CSK buffer (10mM PIPES pH 6.8, 100mM NaCl, 300mM sucrose, 1mM $MgCl_2$, 0.1% Triton X-100) containing protease inhibitors (Roche Complete Mini EDTA-free), phosphatase inhibitors (Roche PhosSTOP), and benzonase (Sigma). Lysates were centrifuged at 14,000 RPM for 20 min and protein concentrations were determined using the Bradford assay (BioRad). Lysates (1-2mg) were pre-cleared for 30 min with washed Protein G Sepharose (GE Healthcare) or Protein A Agarose (Roche) beads and incubated with anti-V5 antibody (Invitrogen) or anti-Ubiquitin K48-specific antibody (Millipore) for 15 min at 4°C with rotation. Beads were added to the samples and rotated for an additional 2 hours. Samples were washed 3 times with CSK buffer and proteins were eluted from the beads with Laemmli buffer (BioRad) by heating at 95°C for 5 min.

Acknowledgements

I would like to thank Mariela Hurtado Garcia for assistance in generating and testing the SQ point mutants.

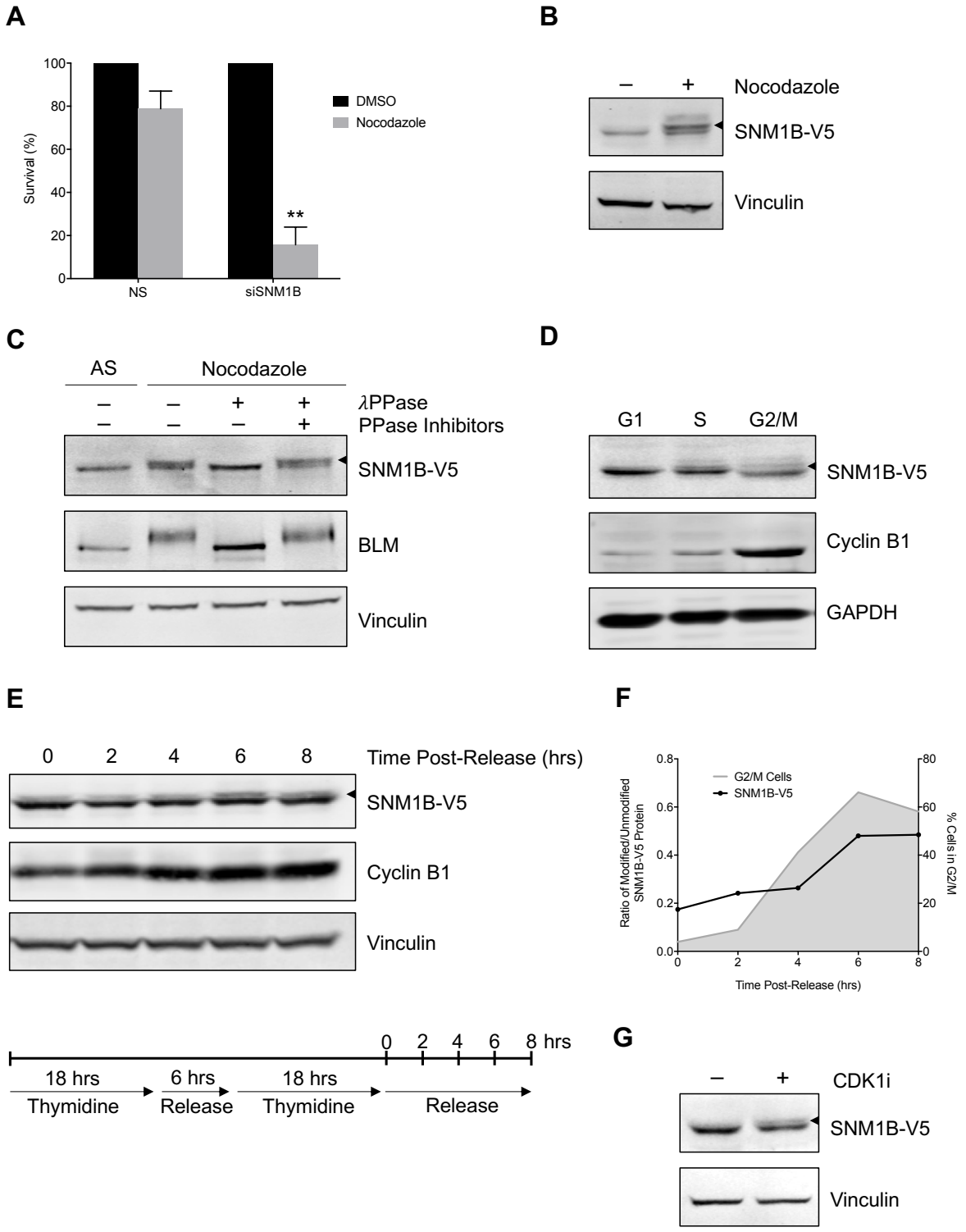
A
100
80
60
40
20
0
Survival (%)
DMSO
Nocodazole
**
NS
siSNM1B
B
–
+
Nocodazole
SNM1B-V5
Vinculin
C
AS
Nocodazole
–
–
+
+
λPPase
–
–
–
+
PPase Inhibitors
SNM1B-V5
BLM
Vinculin
D
G1
S
G2/M
SNM1B-V5
Cyclin B1
GAPDH
E
0
2
4
6
8
Time Post-Release (hrs)
SNM1B-V5
Cyclin B1
Vinculin
0
2
4
6
8 hrs
18 hrs
Thymidine
6 hrs
Release
18 hrs
Thymidine
Release
F
0.8
0.6
0.4
0.2
0.0
Ratio of Modified/Unmodified SNM1B-V5 Protein
G2/M Cells
SNM1B-V5
80
60
40
20
0
% Cells in G2/M
0
2
4
6
8
Time Post-Release (hrs)
G
–
+
CDK1i
SNM1B-V5
Vinculin

Figure 3.1 SNM1B is phosphorylated during G2-phase and mitosis
(A) EV HCT116 cells transfected with NS or siSNM1B siRNAs were treated with 60ng/ml nocodazole for 24 hrs. Mitotic shake-off cells were plated at low density and allowed to proliferate for 6-9 days. Percent survival was determined relative to a DMSO-treated control. Data represent the mean ± SEM of three independent experiments. **p<0.01 **(B)** WT SNM1B HCT116 cells were treated with 400ng/ml nocodazole for 18 hrs and harvested by mitotic shake-off. Cells were lysed and proteins were analyzed by Western blot. **(C)** WT SNM1B HCT116 cells were synchronized as in (B) and lysates were treated with or without lambda phosphatase (λPPase). Phosphorylation status of SNM1B-V5 was examined via Western blot. **(D)** WT SNM1B HCT116 cells were incubated with 5μg/ml Hoechst dye for 30 min and sorted using FACS. Sorted cells were lysed for Western blot analysis. **(E and F)** WT SNM1B HCT116 cells were released from a double thymidine block for the indicated amounts of time and collected for propidium iodide staining and Western blot analysis. The ratio of modified/unmodified SNM1B-V5 protein was calculated and plotted along with the percentage of cells in G2/M-phase. **(G)** WT SNM1B HCT116 cells were treated with 9μM RO3306 (CDK1i) for 20 hrs and harvested for Western blot analysis. The arrowhead labels the shifted, phosphorylated form of SNM1B. AS, Asynchronous

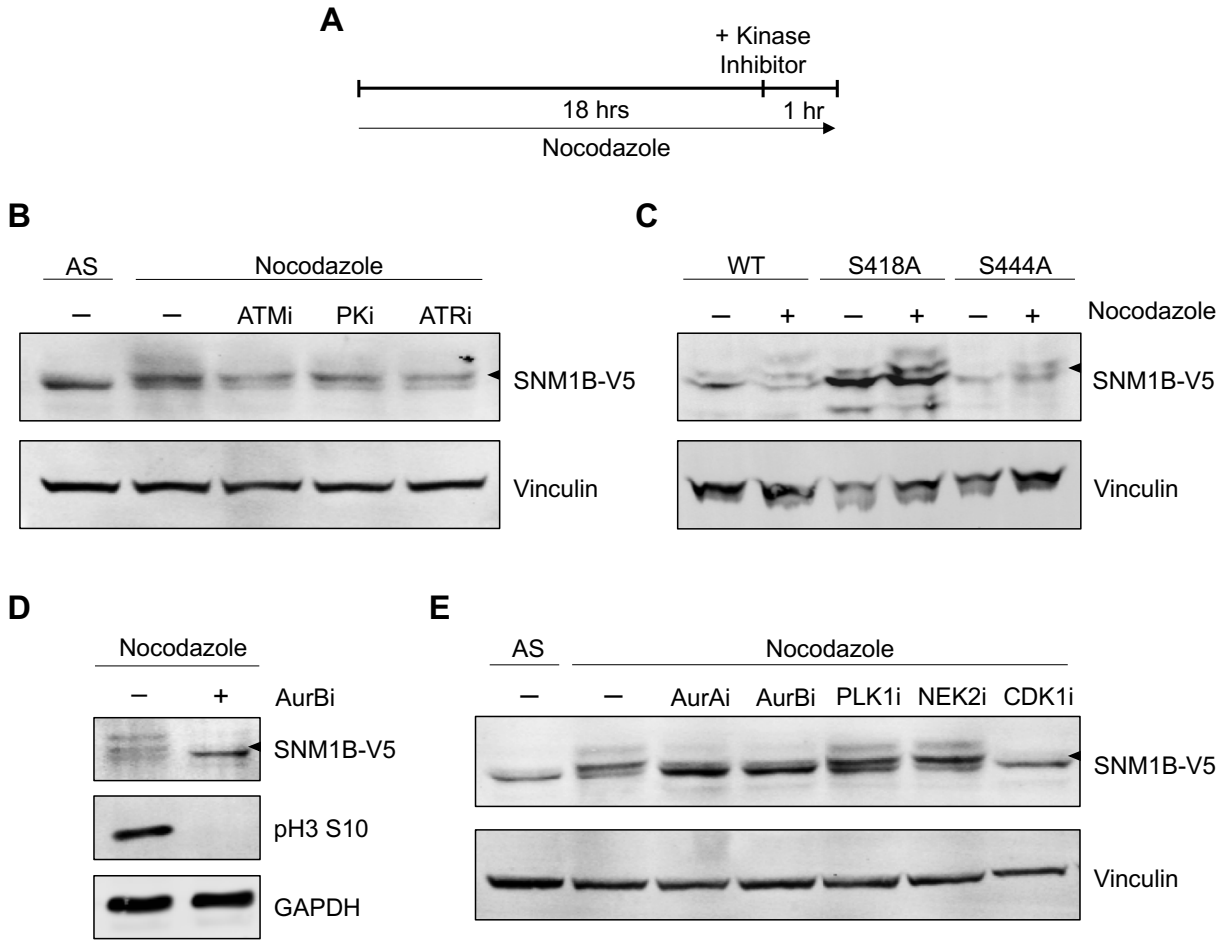

Figure 3.2 Dependence of SNM1B phosphorylation on PIKK and mitotic kinases
(A) Experimental timeline for kinase inhibitor experiments in panels B, D, and E. WT SNM1B HCT116 cells were treated with 400ng/ml nocodazole for 18 hrs followed by the addition of each kinase inhibitor for 1 hr. **(B)** Western blot analysis of cells treated with PIKK inhibitors. ATMi, ATM (10μM); PKi, DNA-PKcs (20μM); ATRi, ATR (1μM) **(C)** HCT116 cells were transfected with plasmids expressing WT and mutant SNM1B-V5 and treated with 400ng/ml nocodazole for 18 hrs. Phosphorylation status was examined via immunoblotting. **(D)** Western blot analysis of cells treated with the Aurora B inhibitor, AurBi. pH3 S10 was used as a control to validate kinase inhibition. **(E)** Western blot analysis of cells treated with mitotic inhibitors. AurAi, Aurora A (1μM); AurBi, Aurora B (5μM); PLK1i, PLK1 (1μM); NEK2i, NEK2 (50μM); CDK1i, CDK1(9μM). The arrowhead labels the shifted, phosphorylated form of SNM1B. AS, Asynchronous

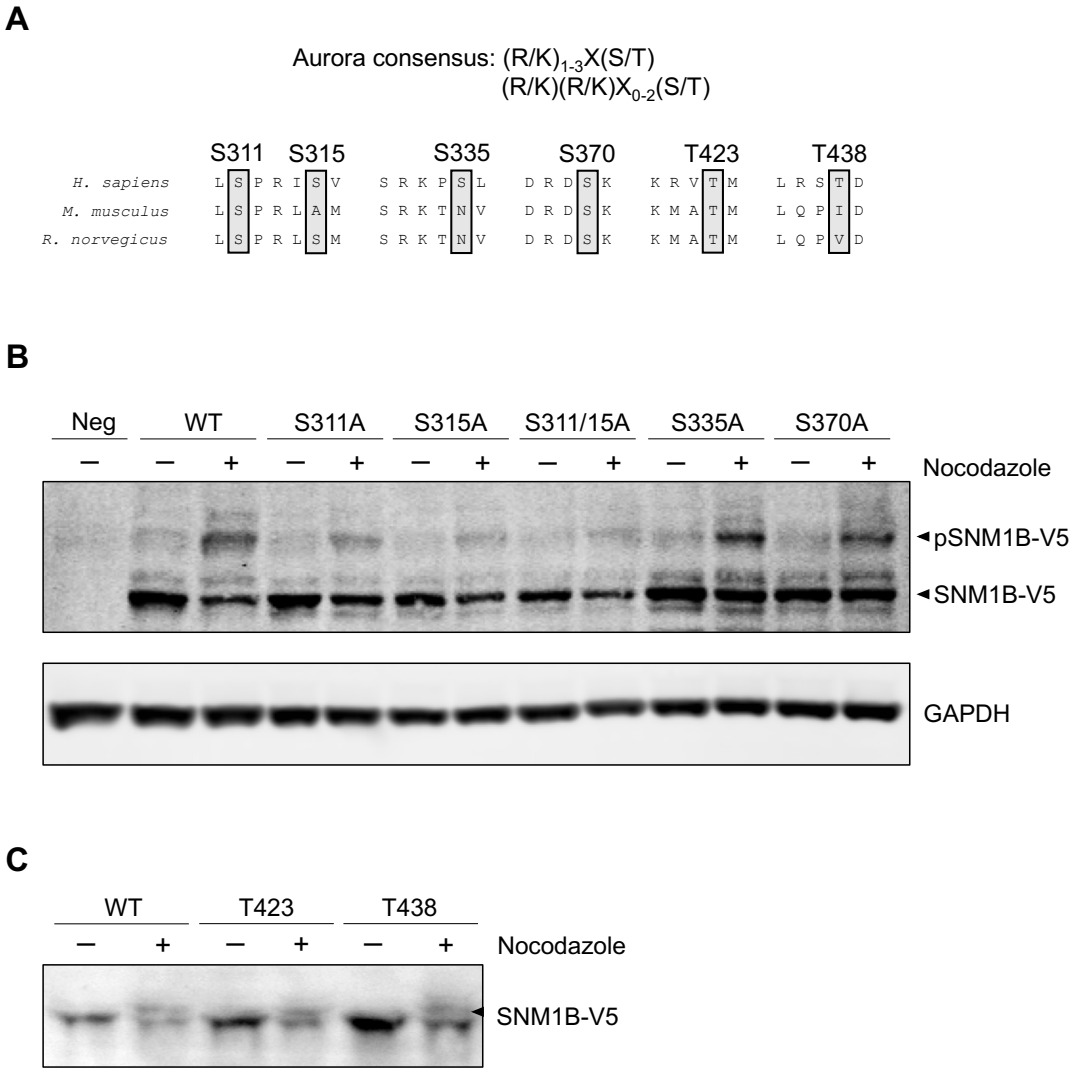

Figure 3.3 Evaluation of SNM1B phosphorylation on Aurora consensus sites
(A) Protein sequence alignments for Aurora consensus sites within SNM1B. The predicted serine or threonine for phosphorylation is boxed. **(B)** HCT116 cells were transfected with vectors expressing WT or mutant SNM1B-V5 and treated with 400ng/ml nocodazole for 18 hrs. Cells were lysed and protein extracts were resolved using Phos-tag SDS-PAGE. **(C)** HCT116 cells were treated as in (B) and protein lysates were resolved using standard SDS-PAGE. The arrowhead labels the shifted, phosphorylated form of SNM1B. Neg, Negative control

A

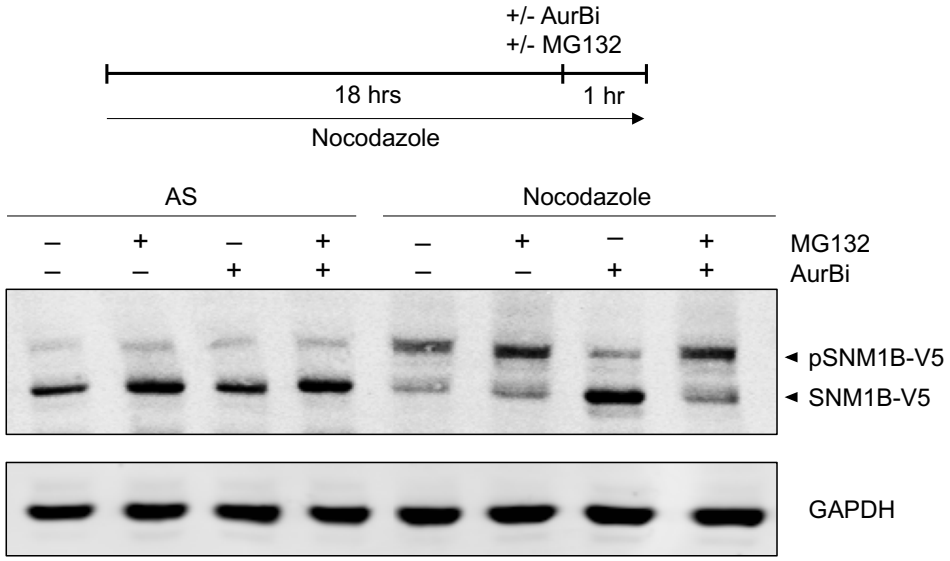
+/- AurBi
+/- MG132
18 hrs
1 hr
Nocodazole
AS
Nocodazole
– + – + – + – +
– – + + – – + +
MG132
AurBi
pSNM1B-V5
SNM1B-V5
GAPDH

B

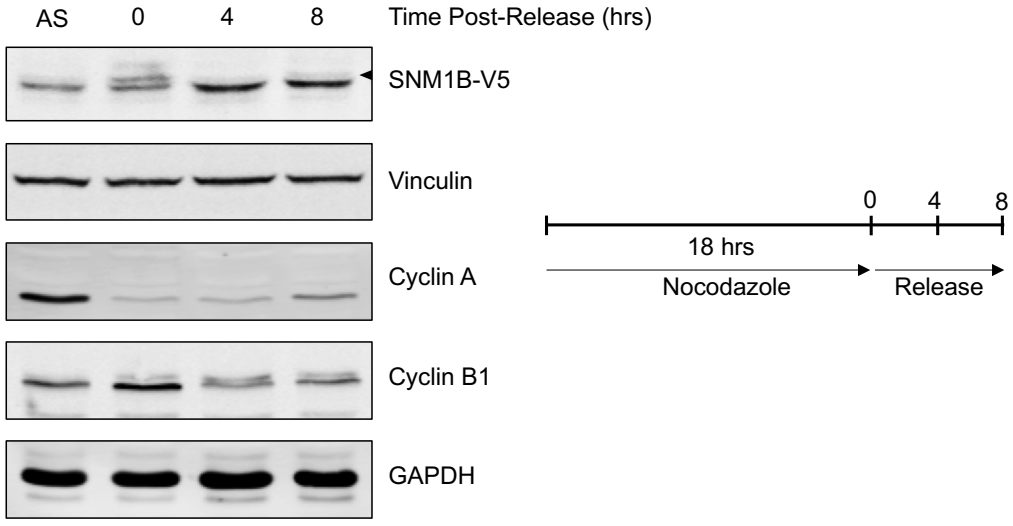
AS 0 4 8
Time Post-Release (hrs)
SNM1B-V5
Vinculin
Cyclin A
Cyclin B1
GAPDH
0 4 8
18 hrs
Nocodazole
Release

Figure 3.4 SNM1B phosphorylation decreases as cells progress out of mitosis
(A) WT SNM1B HCT116 cells were treated with 400ng/ml nocodazole for 18 hrs and the Aurora B kinase inhibitor (AurBi-5μM) was added in the presence or absence of 40μM MG132 for the final hour. Cells were harvested by mitotic shake-off and protein lysates were resolved using Phos-tag SDS-PAGE. **(B)** WT SNM1B HCT116 cells were treated with 100ng/ml nocodazole for 18 hrs and cells were harvested at the indicated timepoints after release. Cell extracts were examined via Western blot. Cyclins A and B1 were used as controls for cell cycle progression. Vinculin serves as a loading control for SNM1B-V5, whereas GAPDH was used as a loading control for the cyclins. The arrowhead labels the shifted, phosphorylated form of SNM1B. AS, Asynchronous

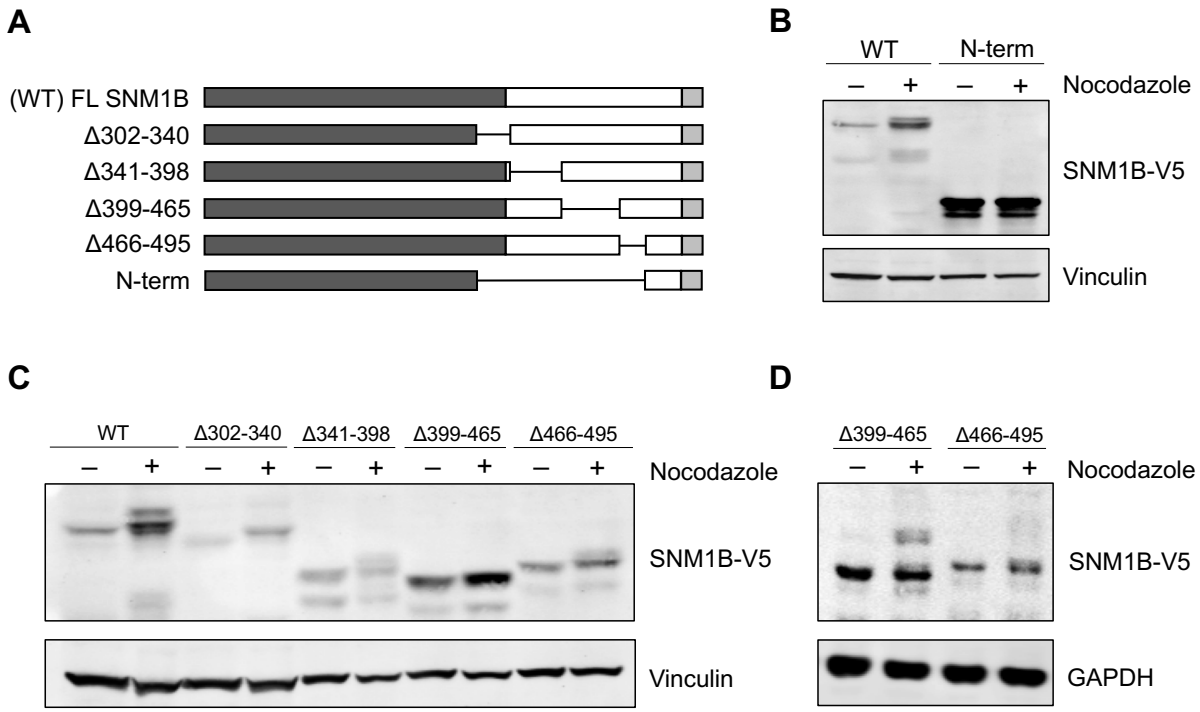
A
(WT) FL SNM1B
Δ302-340
Δ341-398
Δ399-465
Δ466-495
N-term
B
WT
N-term
– + – +
Nocodazole
SNM1B-V5
Vinculin
C
WT
Δ302-340
Δ341-398
Δ399-465
Δ466-495
– + – + – + – + – +
Nocodazole
SNM1B-V5
Vinculin
D
Δ399-465
Δ466-495
– + – +
Nocodazole
SNM1B-V5
GAPDH
E
S474
S481
S487
H. sapiens G P E A T G N Q S A W M G H G S P L S H S S K G T P L L A T
M. musculus G S P A R G N Q S D C V G C G S P P A H I S R A V P L T P –
R. norvegicus G S P T R G K Q S N G M G C G S P P T H I S R T T H L T P –
F
WT
3SA
– + – +
Nocodazole
SNM1B-V5
G
WT
S474A
S481A
SNM1B-V5

Figure 3.5 SNM1B is phosphorylated within its C-terminal domain on serine 481
(A) Schematic of SNM1B deletion mutants. The dark grey region represents the MBL/βCASP domain and the light grey region depicts the V5 epitope tag.
(B, C, D) HCT116 cells stably expressing WT or mutant SNM1B-V5 were treated with 400ng/ml nocodazole for 18 hrs and the phosphorylation status was examined using standard SDS-PAGE (B and C) or Phos-tag SDS-PAGE (D) followed by Western blotting. **(E)** Protein sequence alignments illustrating the three most conserved serine residues (grey boxes) within the 466-495aa region of SNM1B. These sites were mutated to alanines in combination to generate the 3SA SNM1B mutant. **(F)** HCT116 cells stably expressing WT or 3SA SNM1B-V5 were treated with 400ng/ml nocodazole for 18 hrs and protein extracts were examined via Western blot. The arrowhead labels the shifted, phosphorylated form of SNM1B. **(G)** Single point mutants were generated for the S474 and S481 residues and HCT116 cells were transfected with vectors expressing WT or mutant SNM1B-V5. Cells were treated with 400ng/ml nocodazole and the phosphorylation of mutant SNM1B-V5 was examined by immunoblotting.

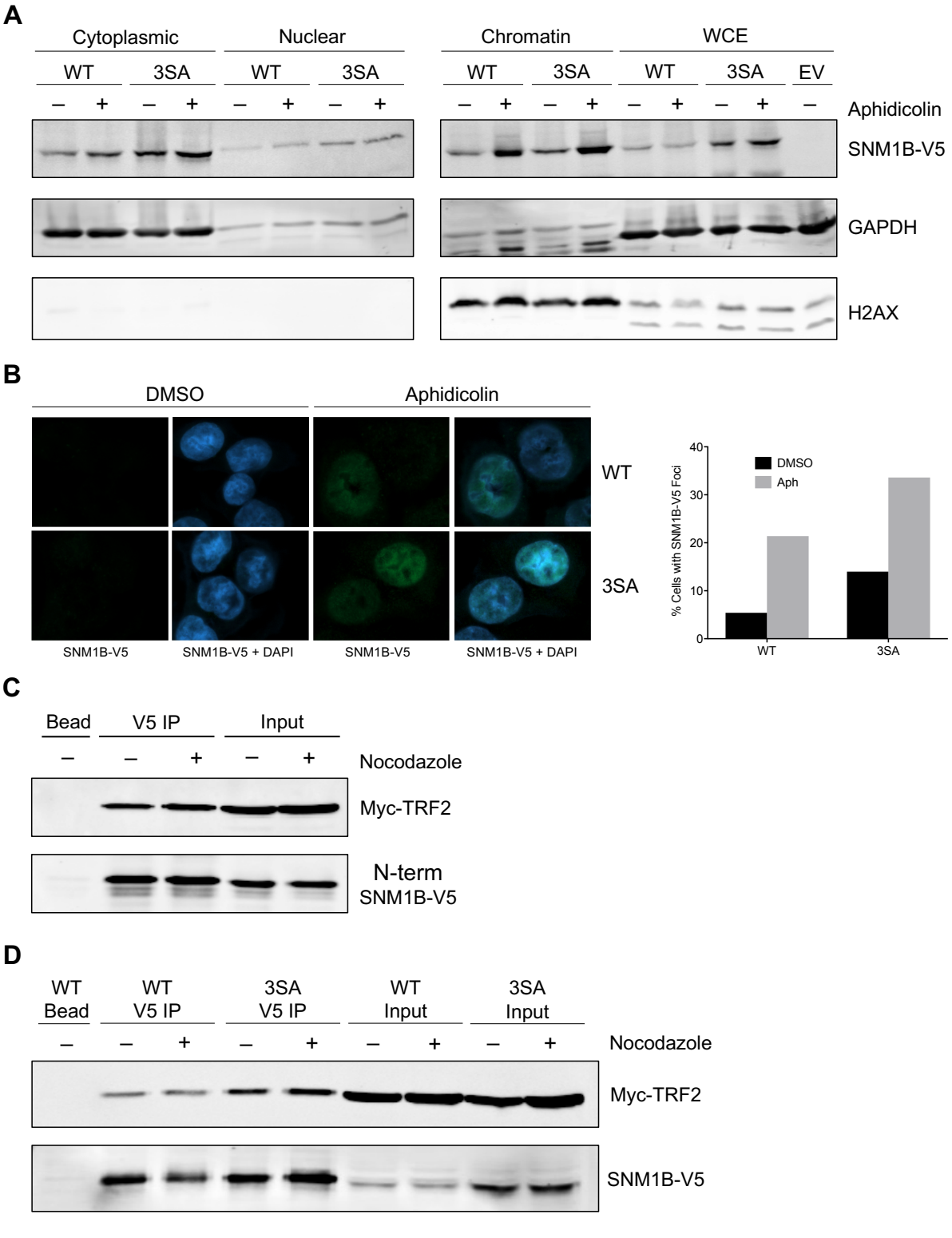
A
Cytoplasmic
Nuclear
Chromatin
WCE
WT
3SA
WT
3SA
WT
3SA
WT
3SA
EV
– + – + – + – + – + – + – + – + –
Aphidicolin
SNM1B-V5
GAPDH
H2AX
B
DMSO
Aphidicolin
WT
3SA
SNM1B-V5
SNM1B-V5 + DAPI
SNM1B-V5
SNM1B-V5 + DAPI
% Cells with SNM1B-V5 Foci
DMSO
Aph
0
10
20
30
40
WT
3SA
C
Bead
V5 IP
Input
– – + – +
Nocodazole
Myc-TRF2
N-term
SNM1B-V5
D
WT
Bead
WT
V5 IP
3SA
V5 IP
WT
Input
3SA
Input
– – + – + – + – +
Nocodazole
Myc-TRF2
SNM1B-V5

Figure 3.6 SNM1B phosphorylation is not required for its recruitment to stalled forks or for its interaction with TRF2

(A) WT and 3SA SNM1B HCT116 cells were treated with 1μM aphidicolin for 24 hrs and harvested for cellular fractionation. Immunoblotting was performed to assess protein levels within each fraction. GAPDH and H2AX were used as controls for cytoplasmic and chromatin fractions, respectively. **(B)** WT and 3SA SNM1B HCT116 cells were treated with 1μM aphidicolin for 24 hrs, fixed, and stained for the visualization of SNM1B-V5 foci. The percentage of cells positive for SNM1B-V5 foci was calculated and plotted in the bar graph. **(C and D)** HCT116 cells were co-transfected with vectors expressing the WT, 3SA, or N-terminus of SNM1B (N-term) and Myc-TRF2. Cells were treated with 400ng/ml nocodazole and harvested for co-immunoprecipitation using an anti-V5 antibody. A bead-only sample was used as a control (Bead). Aph, Aphidicolin

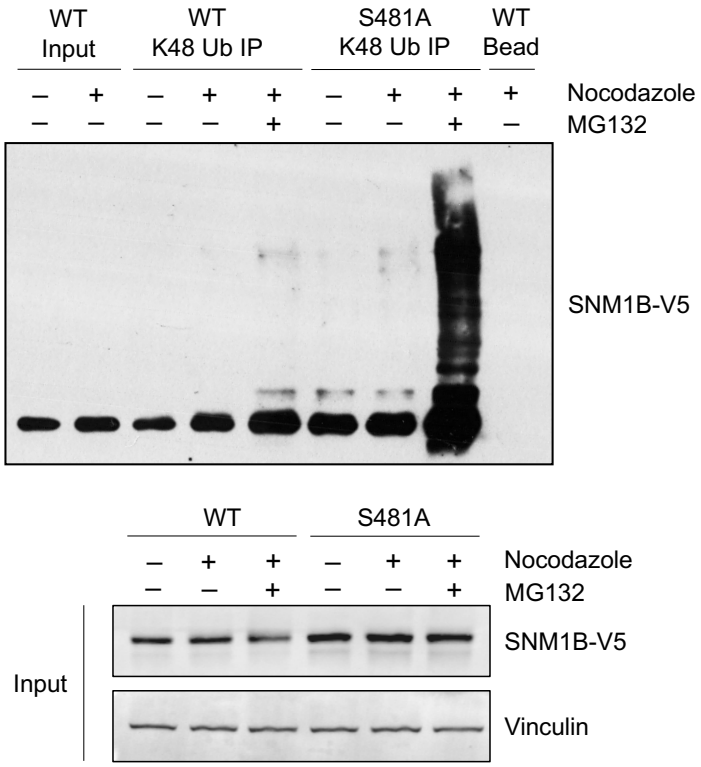

Figure 3.7 The S481A SNM1B mutant is polyubiquitinated in mitosis
HCT116 cells were transfected with plasmids expressing WT or S481A SNM1B and treated with 400ng/ml nocodazole for 18 hrs with or without the addition of 40μM MG132 for the last hour. Cells were harvested for co-immunoprecipitation using an antibody against K48-linked ubiquitin and a bead-only sample was used as a control (Bead).

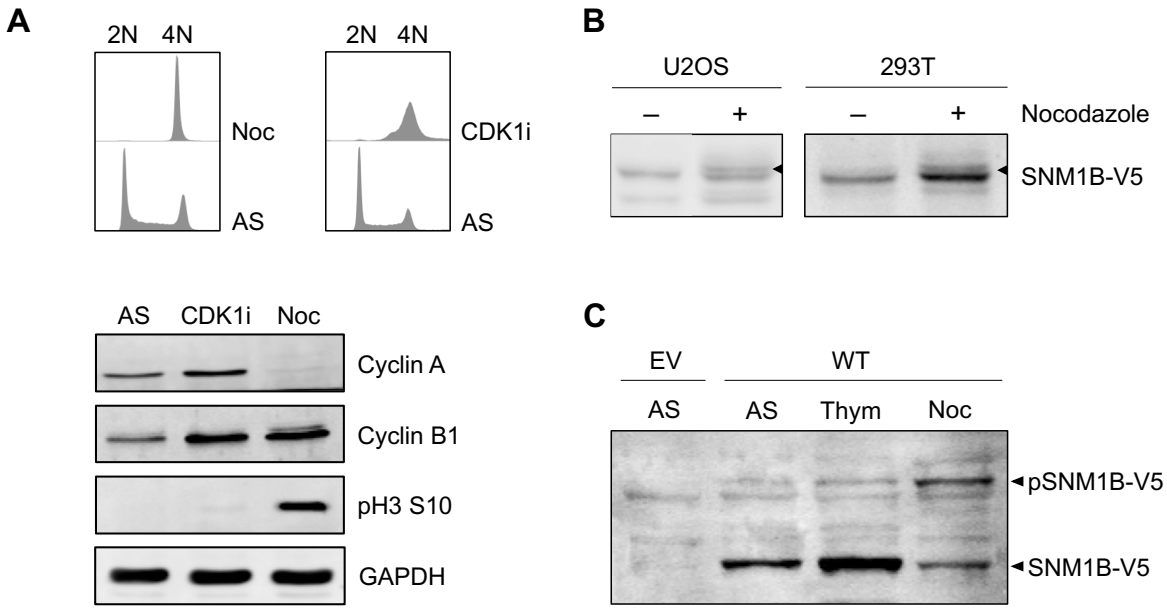

Figure 3.S1 Validation of cell synchronization and SNM1B phosphorylation
(A) Representative cell cycle profiles of WT SNM1B HCT116 cells treated with 400ng/ml nocodazole for 18 hrs or 9μM RO3306 (CDK1i) for 20 hrs. Western blots showing common markers for G2- or M-phase synchronization. **(B)** U2OS cells stably expressing WT SNM1B-V5 and 293T cells transfected with a vector expressing WT SNM1B-V5 were treated with 400ng/ml nocodazole for 18 hrs. SNM1B phosphorylation was examined via Western blot. The arrowhead labels the shifted, phosphorylated form of SNM1B. **(C)** WT SNM1B HCT116 cells synchronized by a double thymidine block or nocodazole were analyzed using Phos-tag SDS-PAGE. AS, Asynchronous, Noc, Nocodazole, Thym, Thymidine Block

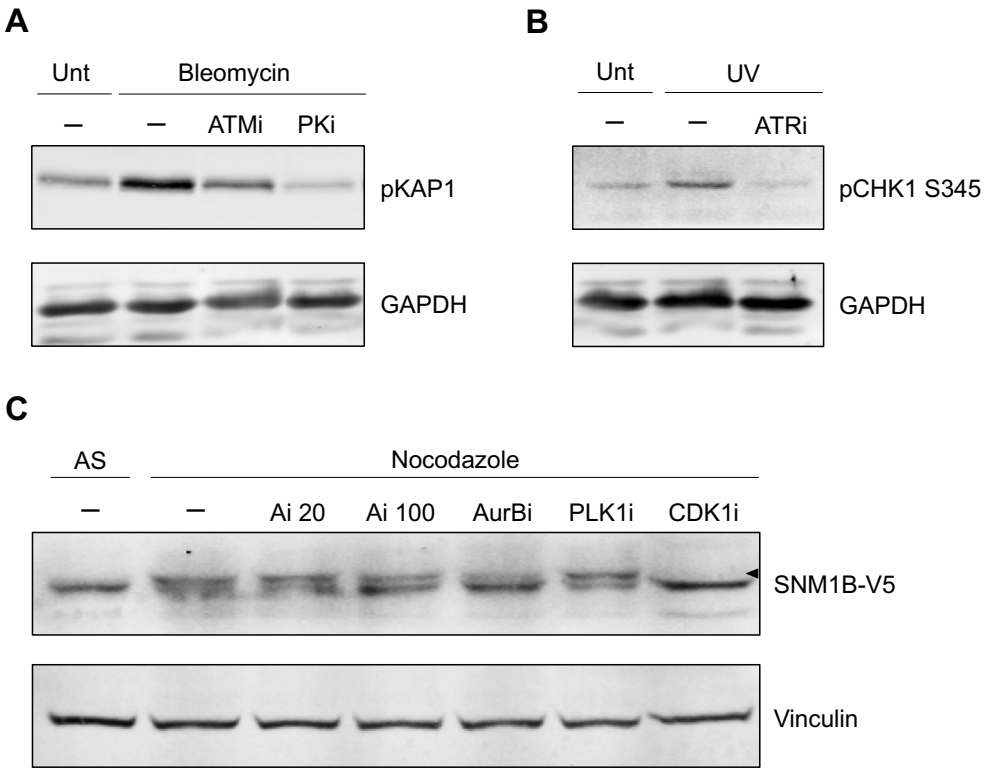

Figure 3.S2 Controls for protein kinase inhibition
(A) WT SNM1B HCT116 cells were pre-treated with ATM or DNA-PKcs kinase inhibitors for 1 hr and treated with 10µg/ml bleomycin for 30 min. Cells were harvested for pKAP1 analysis via Western blot. **(B)** WT SNM1B HCT116 cells were pre-treated with an ATR kinase inhibitor for 1 hr and exposed to 15 J/m^2 UV. Cells were allowed to recover for 30 minutes and then harvested for pCHK1 analysis via Western blot. **(C)** WT SNM1B HCT116 cells were treated with nocodazole for 18 hrs followed by treatment with mitotic kinase inhibitors for an additional 1 hr. SNM1B phosphorylation was examined by immunoblotting. The arrowhead labels the shifted, phosphorylated form of SNM1B. Ai, Aurora A (20nM, 100nM); AurBi, Aurora B (5µM); PLK1i, PLK1 (25nM); CDK1i, CDK1(9µM). The arrowhead labels the shifted, phosphorylated form of SNM1B. Unt, Untreated; AS, Asynchronous

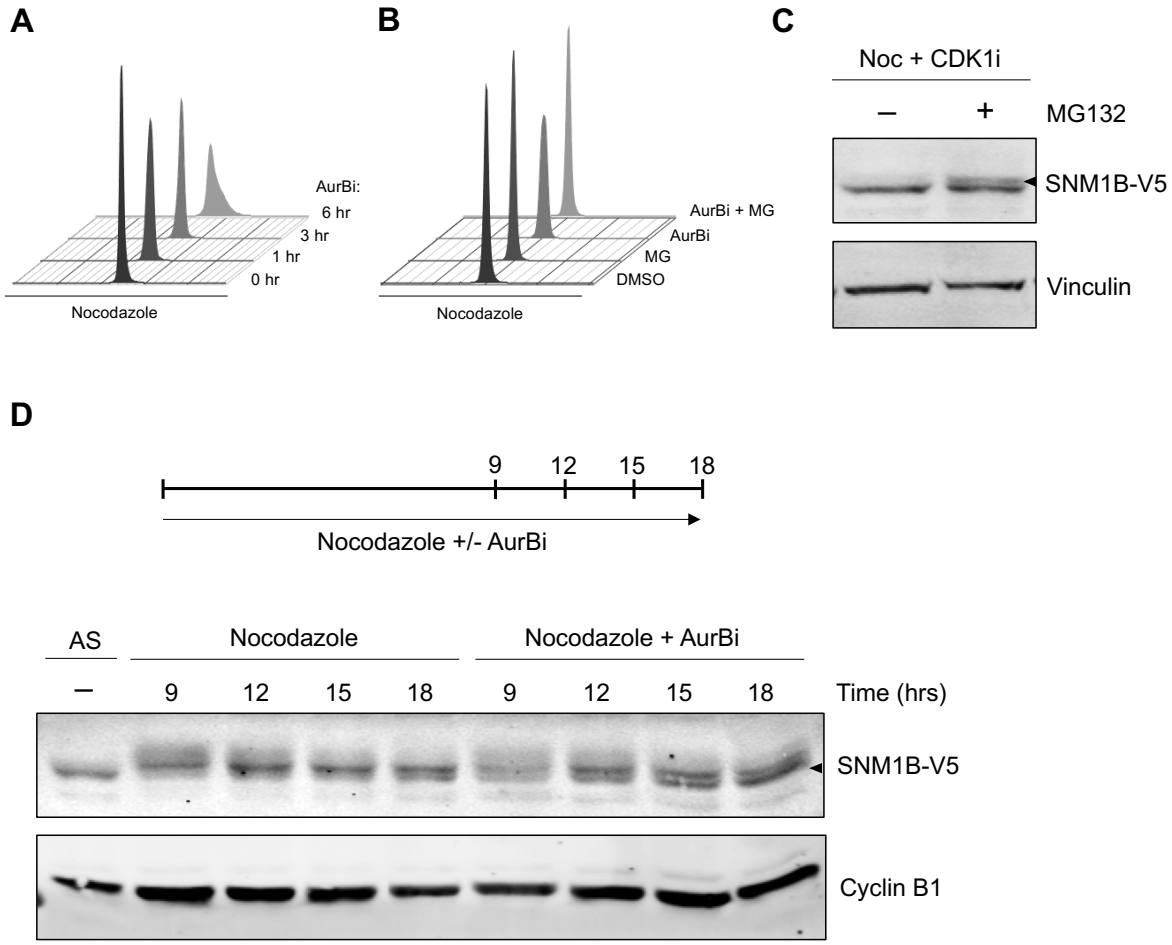

Figure 3.S3 Cell cycle analysis and SNM1B phosphorylation status in mitotic cells treated with Aurora B or CDK1 inhibitors

(A) WT SNM1B HCT116 cells were synchronized with 400ng/ml nocodazole and 5μM Aurora B kinase inhibitor was added for 1, 3, or 6 hrs. Cells were harvested for propidium iodide staining and the cell cycle profiles are shown. **(B)** WT SNM1B HCT116 cells were synchronized with 400ng/ml nocodazole, after which 5μM Aurora B kinase inhibitor or 40μM MG132 was added alone or in combination for 1 hr. Cells were harvested for propidium iodide staining and the cell cycle profiles are shown. **(C)** WT SNM1B HCT116 cells were synchronized with 400ng/ml nocodazole, after which 9μM RO3306 (CDK1i) or 40μM MG132 was added alone or in combination for 1 hr. Cells were harvested for Western blot analysis. **(D)** WT SNM1B HCT116 cells were treated with 400ng/ml nocodazole alone or in combination with 5μM Aurora B kinase inhibitor and harvested at the indicated timepoints. Protein lysates were analyzed by Western blot. AS, Asynchronous; Noc, Nocodazole; AurBi, Aurora B inhibitor; CDK1i, CDK1 inhibitor; MG, MG132

References

1. Branzei, D. & Foiani, M. Regulation of DNA repair throughout the cell cycle. *Nat. Rev. Mol. Cell Biol.* **9**, 297–308 (2008).
2. Hustedt, N. & Durocher, D. The control of DNA repair by the cell cycle. *Nat. Cell Biol.* **19**, 1–9 (2017).
3. Lenain, C. *et al.* The Apollo 5′ Exonuclease Functions Together with TRF2 to Protect Telomeres from DNA Repair. *Curr. Biol.* **16**, 1303–1310 (2006).
4. Mason, J. M. & Sekiguchi, J. M. Snm1B/Apollo functions in the Fanconi anemia pathway in response to DNA interstrand crosslinks. *Hum. Mol. Genet.* **20**, 2549–2559 (2011).
5. Mason, J. M. *et al.* The SNM1B/APOLLO DNA nuclease functions in resolution of replication stress and maintenance of common fragile site stability. *Hum. Mol. Genet.* **22**, 4901–4913 (2013).
6. Demuth, I., Digweed, M. & Concannon, P. Human SNM1B is required for normal cellular response to both DNA interstrand crosslink-inducing agents and ionizing radiation. *Oncogene* **23**, 8611–8618 (2004).
7. Ishiai, M. *et al.* DNA Cross-Link Repair Protein SNM1A Interacts with PIAS1 in Nuclear Focus Formation. *Mol. Cell. Biol.* **24**, 10733–10741 (2004).
8. Yu, X. & Baer, R. Nuclear Localization and Cell Cycle-specific Expression of CtIP, a Protein That Associates with the BRCA1 Tumor Suppressor. *J. Biol. Chem.* **275**, 18541–18549 (2000).
9. Chen, L., Nievera, C. J., Lee, A. Y.-L. & Wu, X. Cell Cycle-dependent Complex Formation of BRCA1·CtIP·MRN Is Important for DNA Double-strand Break Repair. *J. Biol. Chem.* **283**, 7713–7720 (2008).
10. Anand, R., Ranjha, L., Cannavo, E. & Cejka, P. Phosphorylated CtIP Functions as a Co-factor of the MRE11-RAD50-NBS1 Endonuclease in DNA End Resection. *Mol. Cell* **64**, 940–950 (2016).
11. Rozier, L. *et al.* The MRN-CtIP pathway is required for metaphase chromosome alignment. *Mol. Cell* **49**, 1097–1107 (2013).
12. Croteau, D. L., Popuri, V., Opresko, P. L. & Bohr, V. A. Human RecQ Helicases in DNA Repair, Recombination, and Replication. *Annu. Rev. Biochem.* **83**, 519–552 (2014).
13. Chan, K.-L., North, P. S. & Hickson, I. D. BLM is required for faithful chromosome segregation and its localization defines a class of ultrafine anaphase bridges. *EMBO J.* **26**, 3397–3409 (2007).
14. Böhm, S. & Bernstein, K. A. The role of post-translational modifications in fine-tuning BLM helicase function during DNA repair. *DNA Repair* **0**, 123–132 (2014).
15. Dutertre, S. *et al.* Cell cycle regulation of the endogenous wild type Bloom's syndrome DNA helicase. *Oncogene* **19**, 2731–2738 (2000).

16. Leng, M. *et al.* MPS1-dependent mitotic BLM phosphorylation is important for chromosome stability. *Proc. Natl. Acad. Sci.* **103**, 11485–11490 (2006).
17. Kharat, S. S. *et al.* Mitotic phosphorylation of Bloom helicase at Thr182 is required for its proteasomal degradation and maintenance of chromosomal stability. *Oncogene* **35**, 1025–1038 (2016).
18. Petsalaki, E., Dandoulaki, M., Morrice, N. & Zachos, G. Chk1 protects against chromatin bridges by constitutively phosphorylating BLM serine 502 to inhibit BLM degradation. *J Cell Sci* **127**, 3902–3908 (2014).
19. Liu, L. *et al.* SNM1B/Apollo interacts with Astrin and is required for the prophase cell cycle checkpoint. *Cell Cycle* **8**, 628–638 (2009).
20. Chin, C. F. & Yeong, F. M. Safeguarding Entry into Mitosis: the Antephase Checkpoint. *Mol. Cell. Biol.* **30**, 22–32 (2010).
21. Akhter, S. *et al.* Deficiency in SNM1 Abolishes an Early Mitotic Checkpoint Induced by Spindle Stress. *Mol. Cell. Biol.* **24**, 10448–10455 (2004).
22. Scolnick, D. M. & Halazonetis, T. D. *Chfr* defines a mitotic stress checkpoint that delays entry into metaphase. *Nature* **406**, 430–435 (2000).
23. Ogi, K. *et al.* Small interfering RNA-induced CHFR silencing sensitizes oral squamous cell cancer cells to microtubule inhibitors. *Cancer Biol. Ther.* **4**, 773–780 (2005).
24. Kim, S. *et al.* Fanconi anemia complementation group A (FANCA) localizes to centrosomes and functions in the maintenance of centrosome integrity. *Int. J. Biochem. Cell Biol.* **45**, 1953–1961 (2013).
25. Vassilev, L. T. *et al.* Selective small-molecule inhibitor reveals critical mitotic functions of human CDK1. *Proc. Natl. Acad. Sci. U. S. A.* **103**, 10660–10665 (2006).
26. Shiloh, Y. & Ziv, Y. The ATM protein kinase: regulating the cellular response to genotoxic stress, and more. *Nat. Rev. Mol. Cell Biol.* **14**, 197–210 (2013).
27. Davis, A. J., Chen, B. P. C. & Chen, D. J. DNA-PK: a dynamic enzyme in a versatile DSB repair pathway. *DNA Repair* **17**, 21–29 (2014).
28. Maréchal, A. & Zou, L. DNA Damage Sensing by the ATM and ATR Kinases. *Cold Spring Harb. Perspect. Biol.* **5**, (2013).
29. Kim, S.-T., Lim, D.-S., Canman, C. E. & Kastan, M. B. Substrate Specificities and Identification of Putative Substrates of ATM Kinase Family Members. *J. Biol. Chem.* **274**, 37538–37543 (1999).
30. Matsuoka, S. *et al.* ATM and ATR Substrate Analysis Reveals Extensive Protein Networks Responsive to DNA Damage. *Science* **316**, 1160–1166 (2007).
31. Huertas, P. & Jackson, S. P. Human CtIP Mediates Cell Cycle Control of DNA End Resection and Double Strand Break Repair. *J. Biol. Chem.* **284**, 9558–9565 (2009).

32. Peterson, S. E. *et al.* Cdk1 uncouples CtIP-dependent resection and Rad51 filament formation during M-phase double-strand break repair. *J. Cell Biol.* **194**, 705–720 (2011).

33. Simoneau, A., Robellet, X., Ladouceur, A.-M. & D'Amours, D. Cdk1-dependent regulation of the Mre11 complex couples DNA repair pathways to cell cycle progression. *Cell Cycle* **13**, 1078–1090 (2014).

34. Tomimatsu, N. *et al.* Phosphorylation of EXO1 by CDKs 1 and 2 regulates DNA end resection and repair pathway choice. *Nat. Commun.* **5**, 3561 (2014).

35. Willems, E. *et al.* The functional diversity of Aurora kinases: a comprehensive review. *Cell Div.* **13**, (2018).

36. Petronczki, M., Lénárt, P. & Peters, J.-M. Polo on the Rise—from Mitotic Entry to Cytokinesis with Plk1. *Dev. Cell* **14**, 646–659 (2008).

37. Fry, A. M. The Nek2 protein kinase: a novel regulator of centrosome structure. *Oncogene* **21**, 6184–6194 (2002).

38. Benada, J., Burdová, K., Lidak, T., von Morgen, P. & Macurek, L. Polo-like kinase 1 inhibits DNA damage response during mitosis. *Cell Cycle* **14**, 219–231 (2015).

39. Li, Z. *et al.* Plk1 Phosphorylation of Mre11 Antagonizes the DNA Damage Response. *Cancer Res.* **77**, 3169–3180 (2017).

40. Kettenbach, A. N. *et al.* Quantitative Phosphoproteomics Identifies Substrates and Functional Modules of Aurora and Polo-Like Kinase Activities in Mitotic Cells. *Sci Signal* **4**, rs5–rs5 (2011).

41. Asteriti, I. A. *et al.* The Aurora-A inhibitor MLN8237 affects multiple mitotic processes and induces dose-dependent mitotic abnormalities and aneuploidy. *Oncotarget* **5**, 6229–6242 (2014).

42. Tsuda, Y. *et al.* Mitotic slippage and the subsequent cell fates after inhibition of Aurora B during tubulin-binding agent–induced mitotic arrest. *Sci. Rep.* **7**, 16762 (2017).

43. Kaestner, P., Stolz, A. & Bastians, H. Determinants for the efficiency of anticancer drugs targeting either Aurora-A or Aurora-B kinases in human colon carcinoma cells. *Mol. Cancer Ther.* **8**, 2046–2056 (2009).

44. Skoufias, D. A., Indorato, R.-L., Lacroix, F., Panopoulos, A. & Margolis, R. L. Mitosis persists in the absence of Cdk1 activity when proteolysis or protein phosphatase activity is suppressed. *J. Cell Biol.* **179**, 671–685 (2007).

45. King, R. W., Deshaies, R. J., Peters, J.-M. & Kirschner, M. W. How Proteolysis Drives the Cell Cycle. *Science* **274**, 1652–1659 (1996).

46. van Overbeek, M. & de Lange, T. Apollo, an Artemis-Related Nuclease, Interacts with TRF2 and Protects Human Telomeres in S Phase. *Curr. Biol.* **16**, 1295–1302 (2006).

47. Kee, Y., Kim, J. M. & D'Andrea, A. Regulated degradation of FANCM in the Fanconi anemia pathway during mitosis. *Genes Dev.* **23**, 555–560 (2009).

48. Rieder, C. L. & Maiato, H. Stuck in Division or Passing through: What Happens When Cells Cannot Satisfy the Spindle Assembly Checkpoint. *Dev. Cell* **7**, 637–651 (2004).

49. Weaver, B. A. A. & Cleveland, D. W. Decoding the links between mitosis, cancer, and chemotherapy: The mitotic checkpoint, adaptation, and cell death. *Cancer Cell* **8**, 7–12 (2005).

50. Balachandran, R. S. & Kipreos, E. T. Addressing a weakness of anticancer therapy with mitosis inhibitors: Mitotic slippage. *Mol. Cell. Oncol.* **4**, e1277293 (2017).

51. Gascoigne, K. E. & Taylor, S. S. Cancer Cells Display Profound Intra- and Interline Variation following Prolonged Exposure to Antimitotic Drugs. *Cancer Cell* **14**, 111–122 (2008).

52. Akhter, S., Lam, Y. C., Chang, S. & Legerski, R. J. The telomeric protein SNM1B/Apollo is required for normal cell proliferation and embryonic development. *Aging Cell* **9**, 1047–1056 (2010).

53. Lam, Y. C. *et al.* SNMIB/Apollo protects leading-strand telomeres against NHEJ-mediated repair. *EMBO J.* **29**, 2230–2241 (2010).

54. Touzot, F. *et al.* Function of Apollo (SNM1B) at telomere highlighted by a splice variant identified in a patient with Hoyeraal–Hreidarsson syndrome. *Proc. Natl. Acad. Sci.* **107**, 10097–10102 (2010).

55. Ye, J. *et al.* TRF2 and Apollo Cooperate with Topoisomerase 2α to Protect Human Telomeres from Replicative Damage. *Cell* **142**, 230–242 (2010).

56. Hayashi, M. T., Cesare, A. J., Fitzpatrick, J. A. J., Lazzerini-Denchi, E. & Karlseder, J. A Telomere Dependent DNA Damage Checkpoint Induced by Prolonged Mitotic Arrest. *Nat. Struct. Mol. Biol.* **19**, 387–394 (2012).

57. de Lange, T. T-loops and the origin of telomeres. *Nat. Rev. Mol. Cell Biol.* **5**, 323–329 (2004).

58. Lange, T. de. Shelterin: the protein complex that shapes and safeguards human telomeres. *Genes Dev.* **19**, 2100–2110 (2005).

59. Hayashi, M. T., Cesare, A. J., Rivera, T. & Karlseder, J. Cell death during crisis is mediated by mitotic telomere deprotection. *Nature* **522**, 492–496 (2015).

60. Hauf, S. *et al.* The small molecule Hesperadin reveals a role for Aurora B in correcting kinetochore–microtubule attachment and in maintaining the spindle assembly checkpoint. *J. Cell Biol.* **161**, 281–294 (2003).

61. Potapova, T. A. *et al.* The reversibility of mitotic exit in vertebrate cells. *Nature* **440**, 954–958 (2006).

62. Wysong, D. R., Chakravarty, A., Hoar, K. & Ecsedy, J. A. The inhibition of Aurora A abrogates the mitotic delay induced by microtubule perturbing agents. *Cell Cycle* **8**, 876–888 (2009).

63. Courtheoux, T. *et al.* Aurora A kinase activity is required to maintain an active spindle assembly checkpoint during prometaphase. *J Cell Sci* **131**, jcs191353 (2018).

64. Songyang, Z. *et al.* A structural basis for substrate specificities of protein Ser/Thr kinases: primary sequence preference of casein kinases I and II, NIMA, phosphorylase kinase, calmodulin-dependent kinase II, CDK5, and Erk1. *Mol. Cell. Biol.* **16**, 6486–6493 (1996).

65. Blom, N., Gammeltoft, S. & Brunak, S. Sequence and structure-based prediction of eukaryotic protein phosphorylation sites11Edited by F. E. Cohen. *J. Mol. Biol.* **294**, 1351–1362 (1999).

66. Bacus, S. S. *et al.* Taxol-induced apoptosis depends on MAP kinase pathways (ERK and p38) and is independent of p53. *Oncogene* **20**, 147–155 (2001).

67. Deacon, K., Mistry, P., Chernoff, J., Blank, J. L. & Patel, R. p38 Mitogen-Activated Protein Kinase Mediates Cell Death and p21-Activated Kinase Mediates Cell Survival during Chemotherapeutic Drug-induced Mitotic Arrest. *Mol. Biol. Cell* **14**, 2071–2087 (2003).

68. Zhang, H. *et al.* Nocodazole-induced p53-dependent c-Jun N-terminal Kinase Activation Reduces Apoptosis in Human Colon Carcinoma HCT116 Cells. *J. Biol. Chem.* **277**, 43648–43658 (2002).

69. Dhavan, R. & Tsai, L.-H. A decade of CDK5. *Nat. Rev. Mol. Cell Biol.* **2**, 749–759 (2001).

70. Stringer, J. R. & Counter, C. M. Snm1B Interacts with PSF2. *PLOS ONE* **7**, e49626 (2012).

71. Anders, M., Mattow, J., Digweed, M. & Demuth, I. Evidence for hSNM1B/Apollo functioning in the HSP70 mediated DNA damage response. *Cell Cycle* **8**, 1725–1732 (2009).

72. Gruber, J., Harborth, J., Schnabel, J., Weber, K. & Hatzfeld, M. The mitotic-spindle-associated protein astrin is essential for progression through mitosis. *J. Cell Sci.* **115**, 4053–4059 (2002).

73. Freibaum, B. D. & Counter, C. M. The Protein hSnm1B Is Stabilized When Bound to the Telomere-binding Protein TRF2. *J. Biol. Chem.* **283**, 23671–23676 (2008).

74. Kinoshita, E. & Kinoshita-Kikuta, E. Improved Phos-tag SDS-PAGE under neutral pH conditions for advanced protein phosphorylation profiling. *PROTEOMICS* **11**, 319–323 (2011).

Chapter 4

Discussion

Complete replication of the genome and accurate chromosomal segregation are essential for the transmission of genetic information to daughter cells. However, during DNA synthesis, the replication machinery can encounter a number of obstacles that impede its progression and cause the fork to stall [1]. If stalled forks are not properly restarted, they can collapse, resulting in the formation of DNA double-strand breaks (DSBs). These breaks, when mis-repaired, can lead to increased genome instability in the form of chromosomal gaps, breaks, deletions, amplifications, and rearrangements [2,3]. Genome instability can also occur if the replicated DNA is aberrantly segregated during mitosis. Therefore, the cell has evolved intricate mechanisms to ensure accurate cell division and efficient resolution of stalled replication forks. Understanding the details of these molecular pathways is critical for addressing the association between genomic integrity and disease.

The resolution of stalled replication forks requires the nucleolytic processing of DNA intermediate structures. One DNA nuclease that has been implicated in these processing events is SNM1B [4]. SNM1B has known functions in DNA interstrand crosslink (ICL) repair and is important for the recruitment of key DNA repair proteins to stalled replication forks [5,6]. Herein, we have expanded on the current knowledge of the role of SNM1B in the resolution of replication stress and highlight potential mechanisms for its regulation. We found that SNM1B is required for normal replication fork progression and that it participates in the late-stage processing events of recombination-mediated collapsed fork repair. We also discovered that SNM1B is

phosphorylated during G2-phase and mitosis and that this modification may promote SNM1B protein stability. In this chapter, I will discuss the implications of these findings and propose future directions to better understand the role of SNM1B and its regulation in DNA repair processes.

Several DNA repair factors have been implicated in the resolution of stalled replication forks, but the coordinated actions of these proteins in this process are not well understood. To elucidate the order of events that may occur at sites of replication stress, we examined foci formation of various DNA repair proteins relative to one another over time. We found that RPA and MRE11 are recruited early to aphidicolin-stalled forks, followed by SNM1B and FANCD2. These data support previous findings that SNM1B is not required for the proper localization of RPA and MRE11 to stalled forks, but that it is necessary for the efficient localization of FANCD2 [6]. This is also consistent with the discovery that SNM1B is dispensable for the early ATR-dependent signaling events in response to aphidicolin [6]. Since MRE11 localizes to stalled forks prior to SNM1B, we asked whether it may be important for recruiting SNM1B to sites of replication stress. We found that the exonuclease activity of MRE11 is not necessary for the association of SNM1B with chromatin after exposure to aphidicolin. This is in contrast to the repair factors FANCD2, CtIP, and BRCA1, which all require the nucleolytic function of MRE11 for their efficient localization to chromatin after fork stalling [7]. MRE11 has also been described to regulate foci formation and stability of FANCD2 [8]. Seeing as FANCD2 preferentially binds to ssDNA substrates, these studies proposed that MRE11 processes DNA intermediates to generate ssDNA for FANCD2 localization [8]. It is possible that SNM1B may be independently recruited to stalled forks to process the opposing nascent DNA strand to recruit factors such as FANCD2 and BRCA1. SNM1B has been reported to bind to both MRE11 and FANCD2, so these factors may also rely on physical interactions to localize to stalled forks [9]. Future studies could expand on the functional importance of these interactions during the resolution of replication stress.

The generation of ssDNA is a common phenomenon observed at stalled forks induced by various forms of genotoxic stress, either through polymerase-helicase uncoupling or through processing of DNA intermediate structures [10]. DNA nucleases

play a crucial role in these processing events, but unregulated nucleolytic activity can lead to excessive DNA degradation and genome instability. MRE11 is one of the nucleases associated with this excessive end resection, but other enzymes such as EXO1 and FAN1, have also been linked to uncontrolled DNA processing at stalled forks [11–15]. This excessive degradation is prevented by members of the FA/BRCA network, specifically BRCA1, BRCA2, RAD51, and FANCD2 [11–13,16]. Since SNM1B is important for the efficient localization of BRCA1 and FANCD2 to stalled forks, we examined the impact of SNM1B on ssDNA formation [6]. We found that SNM1B suppresses the formation of ssDNA in both untreated and aphidicolin-treated cells. This suggests that SNM1B may recruit proteins of the FA/BRCA network to stalled forks in order to stabilize and protect them from excessive degradation by other nucleases, such as MRE11 (Figure 4.1). Additional experiments utilizing the established DNA combing assay could be performed to assess whether the ssDNA in SNM1B-depleted cells is indeed a result of nascent DNA hyper-resection.

Nucleolytic digestion of annealed DNA strands at a regressed fork is one potential mechanism to initiate fork restart [17,18]. However, excessive degradation and the formation of ssDNA regions could make the fork more susceptible to breakage. We demonstrated that SNM1B is important for preventing the accumulation of DSBs, as assessed by γH2AX and 53BP1 colocalization, which are both key regulators of the DSB response. Although γH2AX is present at stalled forks prior to break formation, its increased colocalization with 53BP1 in SNM1B-deficient cells suggests that forks have begun to collapse [19]. Once a fork collapses, the DSB is resected to promote RAD51 filament formation and homologous recombination (HR). Our studies determined that SNM1B is required for efficient RAD51 foci formation following aphidicolin-induced replication stress. This finding implicates SNM1B in the later stages of fork repair, potentially after fork collapse, to promote RAD51 loading and HR. Similar to its role in the resection of leading-strand telomeres, the 5’ to 3’ nuclease activity of SNM1B could contribute to the generation of 3’ overhangs at DSBs after fork collapse (Figure 4.1). This would allow for the proper assembly of HR proteins and facilitate strand invasion of the homologous template.

Several lines of evidence have implicated SNM1B in the efficient repair of DSBs. Previous studies have shown that SNM1B rapidly localizes to sites of IR-induced damage and is involved in homology-directed repair of I-SceI-induced breaks [5,20]. To gain insight into the role of SNM1B in the response to replication-associated DSBs, we analyzed recombination products in SNM1B-deficient cells after site-specific fork stalling. We revealed that SNM1B promotes HR-mediated repair after fork collapse and that it is specifically involved in regulating conservative short-tract gene conversion (STGC), which is the primary HR product generated from processing bidirectionally stalled forks. Similar results have been reported for the Fanconi anemia (FA) and HR proteins BRCA1, BRCA2, CtIP, RAD51, FANCM, FANCA, FANCD2, and FANCP/SLX4 [21,22]. However, only some of these factors, such as BRCA1, BRCA2, and RAD51 have been implicated in suppressing error-prone long-tract gene conversion (LTGC) [21]. In comparison, SNM1B depletion results in a decrease in LTGC products compared to controls and does not significantly increase the absolute frequency of LTGC at collapsed forks.

LTGC is an aberrant HR outcome which entails a replicative mechanism that copies several kilobases from the sister chromatid [23–25]. Therefore, LTGC could be caused by a termination failure of HR, potentially when the second non-invading strand is missing (one-ended DSB) or not properly coordinated with the invading strand [25]. Interestingly, increased spatial separation between converging forks at a replication barrier impairs the coordination of DSB ends, thereby favoring LTGC [26]. Since the loss of SNM1B does not significantly bias HR towards LTGC, SNM1B may not be essential for the termination events during recombination or for the coordination of the invading and non-invading DNA ends. These processes may rely more on the combinatorial actions of BRCA1, BRCA2, and RAD51. It is possible that the nuclease activity of SNM1B is required for initiating the DNA resection of the invading strand that promotes HR. This would explain the decrease observed for both STGC and LTGC products after SNM1B knockdown, since neither form of gene conversion could efficiently occur without proper initiation of recombination. Interestingly, a detailed examination of stalled forks at a site-specific interstrand crosslink (ICL) revealed that one of the two converging forks undergoes reversal and that the nascent lagging strand is extensively

resected [27,28]. If a similar DNA intermediate formed in our system, SNM1B could facilitate the 5' to 3' end resection of the regressed lagging strand to generate the overhang for strand invasion. Overall, the coordination of SNM1B and the aforementioned members of the FA/BRCA network may facilitate this fork regression, stabilization, and efficient processing of DNA intermediates to regulate HR-mediated repair.

In addition to the replicative recombination products described above, small microhomology-mediated tandem duplications (TDs) have also been observed in *BRCA1*-mutant cells [22]. These rearrangements are associated with *BRCA1*-linked cancers and are often enriched at loci that disrupt tumor suppressor genes [29,30]. At site-specific stalled forks, TDs are predicted to arise from an aberrant replication restart-bypass mechanism or by microhomology-mediated template switching [22]. These processes are analogous to the mechanisms proposed for CNV formation, which frequently overlap with common fragile sites (CFSs) [31,32]. Since SNM1B is important for CFS stability, it may be involved in preventing TD formation at stalled replication forks [6]. Because nonrecurrent CNVs and TDs both contain breakpoint microhomologies, we could sequence the rearrangement breakpoints in SNM1B-depleted cells after Tus-induced fork stalling. It would also be interesting to examine the combined effects of SNM1B and BRCA1 on TDs, as co-depletion of BRCA1 and other repair factors that promote CFS stability, such as BLM and FANCM, independently suppress TD formation [22]. These studies would provide further insight into the mechanistic roles of SNM1B in replication fork repair and its impact on genome instability.

Most of what is currently known about SNM1B is on its functions in telomere maintenance and in the DNA damage response during S-phase [4]. However, the regulatory mechanisms of SNM1B and its nucleolytic activity have not been well characterized. In this thesis, I examined the cellular regulation of SNM1B to gain a better understanding of how it is controlled during cell cycle-specific repair processes. I have shown that SNM1B protein levels remain relatively unaltered throughout the cell cycle, but increase in S-phase in response to replication stress induced by aphidicolin or a double thymidine block. These findings indicate that SNM1B is not cell cycle regulated in unperturbed conditions, but that the protein becomes stabilized after

replication fork stalling (Figure 4.1). The stability of SNM1B may be partly controlled by protein interactions. Previous studies have revealed that TRF2 binding increases the stability of SNM1B by preventing its polyubiquitination and subsequent degradation [33,34]. Since TRF2 can rapidly localize to photo-induced DSBs in non-telomeric DNA, TRF2 may help stabilize SNM1B in response to DNA damage and replication stress, as well as at telomeres [20,35]. PSF2, a member of the GINS complex that is required for DNA replication, may also support SNM1B stability. PSF2 has been shown to interact with SNM1B, and its overexpression promotes SNM1B chromatin association [36]. Interestingly, we observed increased SNM1B chromatin association after aphidicolin treatment, therefore it is possible that PSF2 facilitates SNM1B localization and stabilization after fork stalling. PSF2 binds to SNM1B within the same region as TRF2, which suggests that PSF2 may stabilize SNM1B during DNA replication, whereas TRF2 might be responsible for SNM1B stabilization at telomeres.

In addition to changes in protein stability, the regulation of DNA repair pathways also relies heavily on post-translational modifications (PTMs). Besides polyubiquitination, no PTMs of SNM1B have been fully described or functionally studied. In this thesis, I have defined a novel phosphorylation event on SNM1B that occurs primarily during G2-phase and mitosis (Figure 4.1). Phosphorylated SNM1B is reduced as cells exit mitosis, suggesting tight control of this regulatory event throughout the cell cycle. I identified the specific residue (S481) that is phosphorylated on SNM1B and generated a non-phosphorylatable point mutant (S481A) to investigate its functional importance. I found that the phosphorylation of SNM1B is dispensable for its chromatin association and foci formation at stalled forks and for its interaction with TRF2. However, SNM1B phosphorylation may be important for repair events outside of S-phase.

SNM1B may extend its roles in replication repair into mitosis, and the phosphorylation event could be essential for these mitotic functions. At loci that are difficult to replicate, such as CFSs and telomeres, the completion of DNA synthesis can be delayed. Although late replication was assumed to occur during G2-phase, experimental evidence suggests that replication can extend into early mitosis. These under-replicated regions trigger a non-canonical form of mitotic DNA synthesis called

MiDAS [37]. This pathway is a form of HR-based DNA repair that acts as a salvage mechanism to prevent lethal chromosome mis-segregation.

MiDAS has been described to resemble break-induced replication (BIR) in yeast, which entails repair of one-ended DSBs through strand invasion and conservative DNA synthesis [38–40]. This process is initiated by the cleavage of stalled forks by SLX4 and MUS81-EME1, which promotes POLD3-dependent replication. Interestingly, MiDAS was shown to be independent of RAD51 filament formation and instead requires RAD52, suggesting that breaks may be repaired through a microhomology-mediated BIR mechanism [38].

MiDAS is reported to occur at both CFSs and telomeres, as both loci can be under-replicated as cells enter mitosis [41]. SNM1B functions in the generation of 3' overhangs at telomeres and is important for maintaining fragile site stability, thereby associating SNM1B with these genomic regions [6,42–44]. We have shown that SNM1B is involved in DSB repair during replication stress, however the role of SNM1B in HR-mediated repair during MiDAS is unknown. Since SNM1B promotes RAD51 filament formation at collapsed forks, it would be interesting to determine if its phosphorylation is important for the switch from a canonical RAD51-dependent HR pathway in S- and G2-phase to the RAD52-mediated MiDAS pathway in mitosis. SNM1B has also been reported to physically interact with SLX4, MUS81, and MRE11, which are all proteins required for MiDAS, either at CFSs or at telomeres [9,37,45–47]. Therefore, SNM1B phosphorylation may alter its interactions with other proteins functioning at these sites or direct its localization to or from these genomic regions. To determine whether SNM1B plays a role in MiDAS, EdU labeling of nascent DNA in aphidicolin-treated mitotic cells could be examined after SNM1B knockdown. The colocalization of SNM1B and the EdU signal could also be analyzed to see if SNM1B is recruited to MiDAS loci. Additionally, the role of SNM1B phosphorylation in this process could be examined by performing similar studies with the S481A SNM1B mutant.

If under-replicated regions persist or if intermediate DNA structures are unresolved, this can lead to mitotic aberrations such as chromosome breaks, lagging chromatin, and anaphase bridges [48,49]. Anaphase bridges, which can be classified as either chromatin bridges or ultra-fine bridges (UFBs), are the result of intertwined sister

chromatids that fail to separate. Unlike chromatin bridges, which are bulky structures that can be visualized using conventional DNA dyes, UFBs are stretched DNA linkages that are dechromatinized and can only be detected by the proteins bound to them [50,51]. The two main factors that coat UFBs are BLM and the Polo-like kinase 1 interacting checkpoint helicase (PICH) [52,53]. There are at least three major types of UFBs that are classified by their anchorage points or the chromosomal loci from which they originate. These include UFBs that form at the centromere (C-UFBs), at common fragile sites (FS-UFBs), or at telomeres (T-UFBs). C-UFBs arise during mitosis in almost all unperturbed cells and are thought to occur from unresolved double-stranded DNA (dsDNA) catenanes, whereas FS-USBs and T-USBs contain a more aberrant DNA structure resulting from under-replicated DNA [52,54–57]. A fourth type of UFB has been more recently described as a consequence of unresolved recombination intermediates (HR-UFBs) and are distinct from replication-associated UFBs [58,59].

All types of UFBs are associated with PICH and BLM, which are thought to regulate DNA tension or condensation and resolve complex DNA intermediate structures in HR-based repair, respectively. The ssDNA-binding protein, RPA, also localizes to a subset of UFBs in a dependent but non-overlapping pattern with BLM, suggesting that BLM may potentially unwind structures to generate ssDNA [57,60]. FANCD2 and FANCI are present at the anchorage points of FS-UFBs and may help to stabilize the bridges or recruit factors that are required for their resolution [54,57]. Loss of the repair factors that localize to UFBs, such as FANCD2 and BLM, leads to defects in chromosome segregation in the form of increased and persistent anaphase bridges, binucleation, and micronucleation [52,54,61].

Previous studies have revealed that SNM1B depletion results in increased aneuploidy, binucleation, and anaphase bridges [62,63]. This suggests that SNM1B is important for accurate mitotic segregation, potentially through functions at UFBs. SNM1B has roles at both telomeres and CFSs, thereby associating it with two loci that commonly form UFBs under conditions of replication stress. It would be interesting to determine if SNM1B can be visualized along UFBs with PICH or BLM or if it localizes at the anchorage sites like FANCD2. This could reveal potential roles of SNM1B in stabilizing or processing DNA structures at UFBs. If SNM1B were to facilitate the

resolution of UFBs, its phosphorylation during mitosis may be important for this process. Studies have shown that a constitutively phosphorylated form of BLM localizes to anaphase bridges and prevents its degradation via cullin 3-mediated polyubiquitination [64]. This stabilization of BLM suppresses bridge formation in mitotic cells [64]. SNM1B may be regulated in a similar manner, as the S481A mutant is polyubiquitinated during mitosis. Phosphorylation might stabilize SNM1B by preventing its degradation by the proteasome, and this could allow it to aid in the resolution of UFBs.

Another role that phosphorylated SNM1B may play during mitosis is in centrosome maintenance. The centrosome is the primary center for microtubule organization and spindle assembly in animal cells. Centrosomes duplicate once in S-phase before they migrate to opposite poles of the cell during mitosis, where they orchestrate sister chromatid segregation by nucleating the spindle apparatus [65]. Considering this is a vital function in cell division, centrosome maturation must be highly regulated to prevent genome instability.

Several studies have shown that DDR proteins localize to centrosomes in various stages of the cell cycle to promote signaling and preserve centrosome integrity [66]. All three members of the PIKK family, in addition to effector kinases CHK1 and CHK2, have been visualized at the centrosome and are suspected to link the kinetics of microtubule formation to the DNA damage response [67]. BRCA1 and BRCA2 also localize to centrosomes and loss of these proteins lead to centrosome amplification [67–69]. BRCA1 was specifically shown to be involved in the ubiquitination of γ-tubulin, which is required for nucleating the polymerization of microtubules [68,70,71]. In addition, other members of the FA pathway localize to centrosomes or the mitotic spindle to maintain normal centrosome numbers and spindle assembly checkpoint (SAC) activation [72–74]. One FA protein, FANCA, has been shown to be phosphorylated by the kinase NEK2, which is involved in bipolar spindle formation and centrosome separation. Disruption of FANCA phosphorylation leads to supernumerary centrosomes, aberrant mitotic arrest, and sensitivity to nocodazole [73]. This indicates that FANCA, along with other DDR proteins, is important for maintaining centrosomal integrity.

Like its FA pathway counterparts, SNM1B has been reported to localize to the centrosome [75]. Mass spectrometry studies and a yeast two-hybrid assay have also

identified the microtubule component, β-tubulin, and the centrosomal protein, Cep146, as putative SNM1B binding partners [36,76]. Additionally, SNM1B was shown to physically interact with the spindle-associated protein, astrin [75]. Astrin localizes to the centrosome and the spindle apparatus during mitosis, and the loss of this protein results in supernumerary centrosomes and the formation of multipolar spindles. Although astrin is not required for SNM1B recruitment to the centrosome, the two proteins may act together to maintain appropriate centrosome numbers [75]. This same study revealed that knockdown of SNM1B results in increased phospho-histone H3 levels compared to controls, which is a similar phenotype to that observed for the FANCA phospho-mutant [73,75]. Phosphorylation of this histone variant is a common marker for mitotic index. Therefore, it would be interesting to examine whether the S481A SNM1B mutant can localize to centrosomes or alter phospho-histone H3 levels. Like FANCA, we also determined that SNM1B depletion leads to decreased survival in response to microtubule inhibition. It is possible that the loss of SNM1B could disrupt centrosome integrity, and upon added microtubule stress, result in cell death. To examine this further, we could assess centrosome number in SNM1B knockdown cells and in cells expressing the S481A mutant to see if chromosome segregation is affected.

SNM1B has been shown to function in an early mitotic prophase checkpoint, also known as the antephase checkpoint [75]. The prophase checkpoint delays commitment to mitosis by preventing or reversing chromatin condensation when cells encounter various stresses, such as microtubule inhibition [77]. The first protein to be identified as a component of this checkpoint pathway was the ubiquitin ligase, checkpoint with FHA and ring finger domains (CHFR) [78]. CHFR is a potential tumor suppressor that is mutated or down-regulated by promoter hypermethylation in many cancers [79]. CHFR-deficient cells exhibit increased sensitivity to microtubule inhibitors and a failure to arrest in prophase under conditions of spindle stress [80]. Endogenous and ectopically expressed CHFR is phosphorylated during mitosis, and although this event is not well characterized, it has been hypothesized in one study to regulate the stability of CHFR [81–83].

Similar to the phenotypes observed for CHFR-deficient cells, depletion of SNM1B also results in hypersensitivity to the microtubule inhibitor, nocodazole. Additionally,

previous studies have shown that SNM1B and its metallo-β-lactamase/βCASP family member, SNM1A, are both important for delaying cell cycle progression into mitosis when conditions are unfavorable for division [75,84]. These findings provide evidence for a functional role of SNM1B in the prophase checkpoint. It is possible that SNM1B phosphorylation may be a significant event in the checkpoint signaling pathway, potentially by promoting its stability similar to CHFR. In support of this hypothesis, the S481A SNM1B mutant displays increased K48 polyubiquitination in MG132-treated mitotic cells compared to the WT control. It is unlikely that CHFR is the ubiquitin ligase responsible for the polyubiquitination of SNM1B, as CHFR is not expressed in the primary cell line used in this study (HCT116). Because CHFR is down regulated in various cancer cell lines, future studies examining the role of SNM1B in mitotic progression would need to be performed in cells that are not already deficient in the prophase checkpoint.

Based on the findings that the S481A SNM1B mutant is polyubiquitinated in mitosis, the phosphorylation of SNM1B may be essential for maintaining SNM1B protein stability. We asked whether SNM1B phosphorylation disrupts its interaction with TRF2, as TRF2 binding has been previously shown to prevent polyubiquitination of SNM1B [34]. We determined that the phosphorylation event does not disrupt this well-established interaction, therefore it may promote stability via an alternative mechanism. This could involve a stabilizing interaction with another protein or an alteration of its local chemical properties and protein structure.

In this thesis, I have identified a major phosphorylation site on SNM1B, but there is evidence that SNM1B may acquire additional modifications. After nocodazole treatment, there is often more than one band shift observed in the Western blot and another slow-migrating band is frequently present in the chromatin fraction of cells expressing WT SNM1B (Figure 2.S2 and Figure 3.1B). Although I focused my studies on the major, most reproducible SNM1B modification, future efforts could address the possibility of other SNM1B PTMs. These additional PTMs could be identified through tandem affinity purification (TAP) and mass spectrometry using a tagged SNM1B construct that I have previously generated.

Since SNM1B is expressed at low levels and is undetectable by commercially available antibodies, all of our findings were based on the characterization of ectopically expressed V5-tagged SNM1B. Therefore, it would be beneficial to assess whether endogenous SNM1B is regulated in a similar manner. This could be achieved by tagging SNM1B at its native locus using modern genome editing systems, such as CRISPR/Cas9 [85]. This would ensure that the phenotypes we observe are reproducible when SNM1B is expressed at physiological levels.

In conclusion, this work provides mechanistic insight into the cell cycle-specific functions and regulation of the SNM1B nuclease. We demonstrate that SNM1B promotes the recovery of stalled replication forks and facilitates the HR-mediated repair of DSBs. We also uncover how SNM1B may be regulated during these repair processes through the discovery of a novel protein modification. Overall, my thesis research has defined novel roles for SNM1B in resolving stalled replication forks; and thus, provides new insights into the molecular events that prevent the accumulation of replication-associated DNA damage.

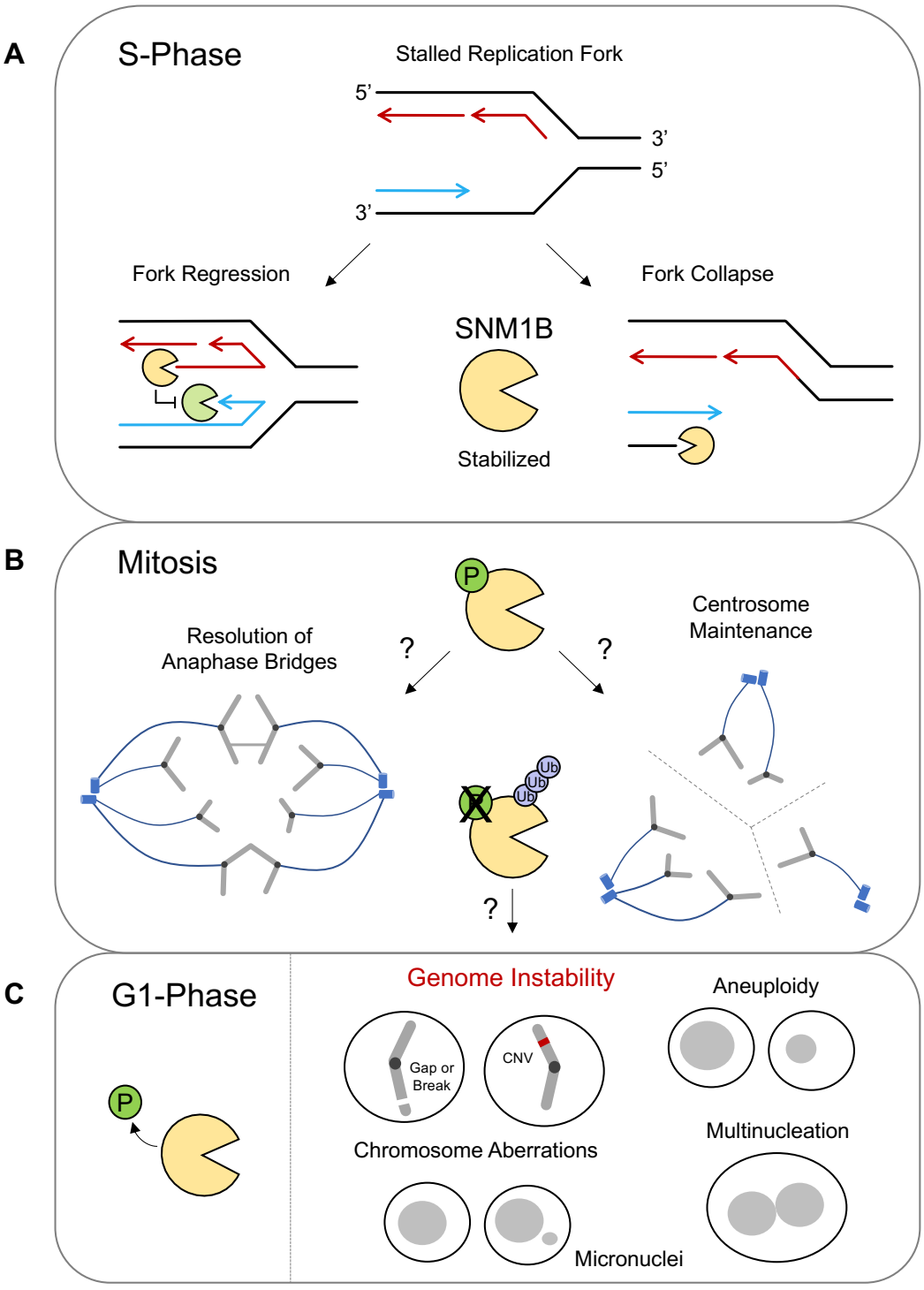
A
S-Phase
Stalled Replication Fork
5'
3'
5'
3'
Fork Regression
Fork Collapse
SNM1B
Stabilized
B
Mitosis
P
?
?
Resolution of
Anaphase Bridges
Centrosome
Maintenance
Ub
Ub
Ub
?
C
G1-Phase
P
Genome Instability
Gap or
Break
CNV
Chromosome Aberrations
Aneuploidy
Multinucleation
Micronuclei

Figure 4.1 Proposed model for cell cycle-specific functions and regulation of SNM1B

(A) In response to replication stress, SNM1B becomes stabilized and localizes to stalled forks. At a reversed fork, SNM1B may resect the lagging strand of the regressed arm using its 5' to 3' exonuclease activity. This recruits members of the FA/BRCA network to facilitate fork protection and prevent excessive DNA degradation by other nucleases. After fork collapse, SNM1B may initiate DNA end resection of DSBs to generate the 3' overhangs required for homologous recombination. **(B)** During mitosis, SNM1B becomes phosphorylated to maintain protein stability, as a non-phosphorylatable mutant is polyubiquitinated. We hypothesize that phosphorylated SNM1B may also be involved in centrosome maintenance or in the resolution of anaphase bridges. **(C)** Defects in these processes or mis-regulation of SNM1B stability could result in genome instability in the next G1-phase, where SNM1B is no longer phosphorylated under normal conditions.

References

1. Zeman, M. K. & Cimprich, K. A. Causes and consequences of replication stress. *Nat. Cell Biol.* **16**, 2–9 (2014).
2. Budzowska, M. & Kanaar, R. Mechanisms of Dealing with DNA Damage-Induced Replication Problems. *Cell Biochem. Biophys.* **53**, 17–31 (2009).
3. Petermann, E. & Helleday, T. Pathways of mammalian replication fork restart. *Nat. Rev. Mol. Cell Biol.* **11**, 683–687 (2010).
4. Schmiester, M., Demuth, I., Schmiester, M. & Demuth, I. SNM1B/Apollo in the DNA damage response and telomere maintenance. *Oncotarget* **8**, 48398–48409 (2017).
5. Mason, J. M. & Sekiguchi, J. M. Snm1B/Apollo functions in the Fanconi anemia pathway in response to DNA interstrand crosslinks. *Hum. Mol. Genet.* **20**, 2549–2559 (2011).
6. Mason, J. M. *et al.* The SNM1B/APOLLO DNA nuclease functions in resolution of replication stress and maintenance of common fragile site stability. *Hum. Mol. Genet.* **22**, 4901–4913 (2013).
7. Yeo, J. E., Lee, E. H., Hendrickson, E. A. & Sobeck, A. CtIP mediates replication fork recovery in a FANCD2-regulated manner. *Hum. Mol. Genet.* **23**, 3695–3705 (2014).
8. Roques, C. *et al.* MRE11–RAD50–NBS1 is a critical regulator of FANCD2 stability and function during DNA double-strand break repair. *EMBO J.* **28**, 2400–2413 (2009).
9. Bae, J.-B. *et al.* Snm1B/Apollo mediates replication fork collapse and S Phase checkpoint activation in response to DNA interstrand cross-links. *Oncogene* **27**, 5045–5056 (2008).
10. Zellweger, R. *et al.* Rad51-mediated replication fork reversal is a global response to genotoxic treatments in human cells. *J Cell Biol* **208**, 563–579 (2015).
11. Schlacher, K. *et al.* Double-Strand Break Repair-Independent Role for BRCA2 in Blocking Stalled Replication Fork Degradation by MRE11. *Cell* **145**, 529–542 (2011).
12. Schlacher, K., Wu, H. & Jasin, M. A Distinct Replication Fork Protection Pathway Connects Fanconi Anemia Tumor Suppressors to RAD51-BRCA1/2. *Cancer Cell* **22**, 106–116 (2012).
13. Ying, S., Hamdy, F. C. & Helleday, T. Mre11-Dependent Degradation of Stalled DNA Replication Forks Is Prevented by BRCA2 and PARP1. *Cancer Res.* **72**, 2814–2821 (2012).
14. Lemaçon, D. *et al.* MRE11 and EXO1 nucleases degrade reversed forks and elicit MUS81-dependent fork rescue in BRCA2-deficient cells. *Nat. Commun.* **8**, 860 (2017).

15. Chaudhury, I., Stroik, D. R. & Sobeck, A. FANCD2-Controlled Chromatin Access of the Fanconi-Associated Nuclease FAN1 Is Crucial for the Recovery of Stalled Replication Forks. *Mol. Cell. Biol.* **34**, 3939–3954 (2014).
16. Hashimoto, Y., Ray Chaudhuri, A., Lopes, M. & Costanzo, V. Rad51 protects nascent DNA from Mre11-dependent degradation and promotes continuous DNA synthesis. *Nat. Struct. Mol. Biol.* **17**, 1305–1311 (2010).
17. Neelsen, K. J. & Lopes, M. Replication fork reversal in eukaryotes: from dead end to dynamic response. *Nat. Rev. Mol. Cell Biol.* **16**, 207–220 (2015).
18. Meng, X. & Zhao, X. Replication fork regression and its regulation. *FEMS Yeast Res.* **17**, (2017).
19. Sirbu, B. M. *et al.* Analysis of protein dynamics at active, stalled, and collapsed replication forks. *Genes Dev.* **25**, 1320–1327 (2011).
20. Demuth, I. *et al.* Endogenous hSNM1B/Apollo interacts with TRF2 and stimulates ATM in response to ionizing radiation. *DNA Repair* **7**, 1192–1201 (2008).
21. Willis, N. A. *et al.* BRCA1 controls homologous recombination at Tus/Ter-stalled mammalian replication forks. *Nature* **510**, 556–559 (2014).
22. Willis, N. A. *et al.* Mechanism of tandem duplication formation in *BRCA1*-mutant cells. *Nature* **551**, 590–595 (2017).
23. Johnson, R. D. & Jasin, M. Sister chromatid gene conversion is a prominent double-strand break repair pathway in mammalian cells. *EMBO J.* **19**, 3398–3407 (2000).
24. Puget, N., Knowlton, M. & Scully, R. Molecular analysis of sister chromatid recombination in mammalian cells. *DNA Repair* **4**, 149–161 (2005).
25. Chandramouly, G. *et al.* BRCA1 and CtIP suppress long tract gene conversion between sister chromatids. *Nat. Commun.* **4**, 2404 (2013).
26. Willis, N. A. & Scully, R. Spatial separation of replisome arrest sites influences homologous recombination quality at a Tus/Ter-mediated replication fork barrier. *Cell Cycle* **15**, 1812–1820 (2016).
27. Amunugama, R. *et al.* Replication Fork Reversal during DNA Interstrand Crosslink Repair Requires CMG Unloading. *Cell Rep.* **23**, 3419–3428 (2018).
28. Räschle, M. *et al.* Mechanism of Replication-Coupled DNA Interstrand Crosslink Repair. *Cell* **134**, 969–980 (2008).
29. Menghi, F. *et al.* The tandem duplicator phenotype as a distinct genomic configuration in cancer. *Proc. Natl. Acad. Sci.* **113**, E2373–E2382 (2016).
30. Nik-Zainal, S. *et al.* Landscape of somatic mutations in 560 breast cancer whole-genome sequences. *Nature* **534**, 47–54 (2016).
31. Arlt, M. F., Wilson, T. E. & Glover, T. W. Replication stress and mechanisms of CNV formation. *Curr. Opin. Genet. Dev.* **22**, 204–210 (2012).

32. Wilson, T. E. *et al.* Large transcription units unify copy number variants and common fragile sites arising under replication stress. *Genome Res.* **25**, 189–200 (2015).

33. Freibaum, B. D. & Counter, C. M. hSnm1B Is a Novel Telomere-associated Protein. *J. Biol. Chem.* **281**, 15033–15036 (2006).

34. Freibaum, B. D. & Counter, C. M. The Protein hSnm1B Is Stabilized When Bound to the Telomere-binding Protein TRF2. *J. Biol. Chem.* **283**, 23671–23676 (2008).

35. Bradshaw, P. S., Stavropoulos, D. J. & Meyn, M. S. Human telomeric protein TRF2 associates with genomic double-strand breaks as an early response to DNA damage. *Nat. Genet.* **37**, 193–197 (2005).

36. Stringer, J. R. & Counter, C. M. Snm1B Interacts with PSF2. *PLOS ONE* **7**, e49626 (2012).

37. Minocherhomji, S. *et al.* Replication stress activates DNA repair synthesis in mitosis. *Nature* **528**, 286–290 (2015).

38. Bhowmick, R., Minocherhomji, S. & Hickson, I. D. RAD52 Facilitates Mitotic DNA Synthesis Following Replication Stress. *Mol. Cell* **64**, 1117–1126 (2016).

39. Donnianni, R. A. & Symington, L. S. Break-induced replication occurs by conservative DNA synthesis. *Proc. Natl. Acad. Sci.* **110**, 13475–13480 (2013).

40. Saini, N. *et al.* Migrating bubble during break-induced replication drives conservative DNA synthesis. *Nature* **502**, 389–392 (2013).

41. Özer, Ö. & Hickson, I. D. Pathways for maintenance of telomeres and common fragile sites during DNA replication stress. *Open Biol.* **8**, (2018).

42. Lam, Y. C. *et al.* SNMIB/Apollo protects leading-strand telomeres against NHEJ-mediated repair. *EMBO J.* **29**, 2230–2241 (2010).

43. Wu, P., van Overbeek, M., Rooney, S. & de Lange, T. Apollo Contributes to G Overhang Maintenance and Protects Leading-End Telomeres. *Mol. Cell* **39**, 606–617 (2010).

44. Wu, P., Takai, H. & de Lange, T. Telomeric 3′ Overhangs Derive from Resection by Exo1 and Apollo and Fill-In by POT1b-Associated CST. *Cell* **150**, 39–52 (2012).

45. Özer, Ö., Bhowmick, R., Liu, Y. & Hickson, I. D. Human cancer cells utilize mitotic DNA synthesis to resist replication stress at telomeres regardless of their telomere maintenance mechanism. *Oncotarget* **9**, 15836–15846 (2018).

46. Min, J., Wright, W. E. & Shay, J. W. Alternative Lengthening of Telomeres Mediated by Mitotic DNA Synthesis Engages Break-Induced Replication Processes. *Mol. Cell. Biol.* **37**, (2017).

47. Salewsky, B., Schmiester, M., Schindler, D., Digweed, M. & Demuth, I. The nuclease hSNM1B/Apollo is linked to the Fanconi anemia pathway via its interaction with FANCP/SLX4. *Hum. Mol. Genet.* **21**, 4948–4956 (2012).

48. Gelot, C., Magdalou, I. & Lopez, B. S. Replication Stress in Mammalian Cells and Its Consequences for Mitosis. *Genes* **6**, 267–298 (2015).

49. Fragkos, M. & Naim, V. Rescue from replication stress during mitosis. *Cell Cycle* **16**, 613–633 (2017).

50. Liu, Y., Nielsen, C. F., Yao, Q. & Hickson, I. D. The origins and processing of ultra fine anaphase DNA bridges. *Curr. Opin. Genet. Dev.* **26**, 1–5 (2014).

51. Sarlós, K., Biebricher, A., Petermann, E. J. G., Wuite, G. J. L. & Hickson, I. D. Knotty Problems during Mitosis: Mechanistic Insight into the Processing of Ultrafine DNA Bridges in Anaphase. *Cold Spring Harb. Symp. Quant. Biol.* **82**, 187–195 (2017).

52. Chan, K.-L., North, P. S. & Hickson, I. D. BLM is required for faithful chromosome segregation and its localization defines a class of ultrafine anaphase bridges. *EMBO J.* **26**, 3397–3409 (2007).

53. Baumann, C., Körner, R., Hofmann, K. & Nigg, E. A. PICH, a Centromere-Associated SNF2 Family ATPase, Is Regulated by Plk1 and Required for the Spindle Checkpoint. *Cell* **128**, 101–114 (2007).

54. Naim, V. & Rosselli, F. The FANC pathway and BLM collaborate during mitosis to prevent micro-nucleation and chromosome abnormalities. *Nat. Cell Biol.* **11**, 761–768 (2009).

55. Chan, K. L. & Hickson, I. D. On the origins of ultra-fine anaphase bridges. *Cell Cycle* **8**, 3065–3066 (2009).

56. Barefield, C. & Karlseder, J. The BLM helicase contributes to telomere maintenance through processing of late-replicating intermediate structures. *Nucleic Acids Res.* **40**, 7358–7367 (2012).

57. Chan, K. L., Palmai-Pallag, T., Ying, S. & Hickson, I. D. Replication stress induces sister-chromatid bridging at fragile site loci in mitosis. *Nat. Cell Biol.* **11**, 753–760 (2009).

58. Chan, Y. W., Fugger, K. & West, S. C. Unresolved recombination intermediates lead to ultra-fine anaphase bridges, chromosome breaks and aberrations. *Nat. Cell Biol.* **20**, 92 (2018).

59. Chan, Y. W. & West, S. C. A new class of ultrafine anaphase bridges generated by homologous recombination. *Cell Cycle* **17**, 2101–2109 (2018).

60. Hengeveld, R. C. C. *et al.* Rif1 Is Required for Resolution of Ultrafine DNA Bridges in Anaphase to Ensure Genomic Stability. *Dev. Cell* **34**, 466–474 (2015).

61. Vinciguerra, P., Godinho, S. A., Parmar, K., Pellman, D. & D'Andrea, A. D. Cytokinesis failure occurs in Fanconi anemia pathway–deficient murine and human bone marrow hematopoietic cells. *J. Clin. Invest.* **120**, 3834–3842 (2010).

62. Akhter, S., Lam, Y. C., Chang, S. & Legerski, R. J. The telomeric protein SNM1B/Apollo is required for normal cell proliferation and embryonic development. *Aging Cell* **9**, 1047–1056 (2010).

63. Ye, J. *et al.* TRF2 and Apollo Cooperate with Topoisomerase 2α to Protect Human Telomeres from Replicative Damage. *Cell* **142**, 230–242 (2010).

64. Petsalaki, E., Dandoulaki, M., Morrice, N. & Zachos, G. Chk1 protects against chromatin bridges by constitutively phosphorylating BLM serine 502 to inhibit BLM degradation. *J Cell Sci* **127**, 3902–3908 (2014).

65. Fu, J., Hagan, I. M. & Glover, D. M. The Centrosome and Its Duplication Cycle. *Cold Spring Harb. Perspect. Biol.* **7**, (2015).

66. Mullee, L. I. & Morrison, C. G. Centrosomes in the DNA damage response—the hub outside the centre. *Chromosome Res.* **24**, 35–51 (2016).

67. Zhang, S., Hemmerich, P. & Grosse, F. Centrosomal localization of DNA damage checkpoint proteins. *J. Cell. Biochem.* **101**, 451–465 (2007).

68. Starita, L. M. *et al.* BRCA1-Dependent Ubiquitination of γ-Tubulin Regulates Centrosome Number. *Mol. Cell. Biol.* **24**, 8457–8466 (2004).

69. Tutt, A. *et al.* Absence of Brca2 causes genome instability by chromosome breakage and loss associated with centrosome amplification. *Curr. Biol.* **9**, 1107-S1 (1999).

70. Sankaran, S., Starita, L. M., Simons, A. M. & Parvin, J. D. Identification of Domains of BRCA1 Critical for the Ubiquitin-Dependent Inhibition of Centrosome Function. *Cancer Res.* **66**, 4100–4107 (2006).

71. Parvin, J. D. & Sankaran, S. The BRCA1 E3 Ubiquitin Ligase Controls Centrosome Dynamics. *Cell Cycle* **5**, 1946–1950 (2006).

72. Nalepa, G. *et al.* Fanconi anemia signaling network regulates the spindle assembly checkpoint. *J. Clin. Invest.* **123**, 3839–3847 (2013).

73. Kim, S. *et al.* Fanconi anemia complementation group A (FANCA) localizes to centrosomes and functions in the maintenance of centrosome integrity. *Int. J. Biochem. Cell Biol.* **45**, 1953–1961 (2013).

74. Zou, J. *et al.* FancJ regulates interstrand crosslinker induced centrosome amplification through the activation of polo-like kinase 1. *Biol. Open* **2**, 1022–1031 (2013).

75. Liu, L. *et al.* SNM1B/Apollo interacts with Astrin and is required for the prophase cell cycle checkpoint. *Cell Cycle* **8**, 628–638 (2009).

76. Anders, M., Mattow, J., Digweed, M. & Demuth, I. Evidence for hSNM1B/Apollo functioning in the HSP70 mediated DNA damage response. *Cell Cycle* **8**, 1725–1732 (2009).

77. Chin, C. F. & Yeong, F. M. Safeguarding Entry into Mitosis: the Antephase Checkpoint. *Mol. Cell. Biol.* **30**, 22–32 (2010).

78. Scolnick, D. M. & Halazonetis, T. D. *Chfr* defines a mitotic stress checkpoint that delays entry into metaphase. *Nature* **406**, 430–435 (2000).

79. Sanbhnani, S. & Yeong, F. M. CHFR: a key checkpoint component implicated in a wide range of cancers. *Cell. Mol. Life Sci.* **69**, 1669–1687 (2012).

80. Ogi, K. *et al.* Small interfering RNA-induced CHFR silencing sensitizes oral squamous cell cancer cells to microtubule inhibitors. *Cancer Biol. Ther.* **4**, 773–780 (2005).

81. Bothos, J., Summers, M. K., Venere, M., Scolnick, D. M. & Halazonetis, T. D. The Chfr mitotic checkpoint protein functions with Ubc13-Mms2 to form Lys63-linked polyubiquitin chains. *Oncogene* **22**, 7101–7107 (2003).

82. Shtivelman, E. Promotion of Mitosis by Activated Protein Kinase B After DNA Damage Involves Polo-Like Kinase 1 and Checkpoint Protein CHFR11Institutional funds from the Cancer Research Institute, University of California San Francisco. *Mol. Cancer Res.* **1**, 959–969 (2003).

83. Burgess, A. *et al.* Chfr interacts and colocalizes with TCTP to the mitotic spindle. *Oncogene* **27**, 5554–5566 (2008).

84. Akhter, S. *et al.* Deficiency in SNM1 Abolishes an Early Mitotic Checkpoint Induced by Spindle Stress. *Mol. Cell. Biol.* **24**, 10448–10455 (2004).

85. Ratz, M., Testa, I., Hell, S. W. & Jakobs, S. CRISPR/Cas9-mediated endogenous protein tagging for RESOLFT super-resolution microscopy of living human cells. *Sci. Rep.* **5**, 9592 (2015).